Doctoral Dissertation

Study on Vacuum Insulation Panels with Slim-thickness and Light-weight and Their Application Method for Retrofitting Insulation to Existing Buildings

(既存建築の断熱改修に寄与する薄型･軽量の真空断熱材とその適用方法に関する研究)

Supervisor: Takao Katsura

2018.2.14

Graduate School of Engineering, Hokkaido University

Division of Human Environmental Systems

Environmental System Research Laboratory

Zhang YANG

学 位 論 文 内 容 の 要 旨

博士の専攻分野の名称　　博士（工学）　　氏 名 楊　樟

学 位 論 文 題 名

Study on Vacuum Insulation Panels with Slim-thickness and Light-weight and Their Application Method for Retrofitting Insulation to Existing Buildings

(既存建築の断熱改修に寄与する薄型･軽量の真空断熱材とその適用方法に関する研究)

Retrofitting the insulation in older buildings would reduce the energy required for heating, resulting in cost and energy savings. Usually, insulation performance is poor in older buildings. This study aimed at retrofitting insulation to existing buildings by applying vacuum insulation panels (VIPs). As a state-of-art thermal insulation, a VIP has almost 10 times insulation performance than conventional thermal insulations. However, conventional VIPs also have issues, such as: expensive production cost, lack of airtightness, complex construction, low durability and big thermal bridge. In order to develop new type VIP and retrofit insulation to existing buildings, the authors divided the study into retrofit insulation in windows with developed transparency VIP and retrofit insulation to walls with developed filling type VIP. The details present in each Chapters:

Chapter 1 is the introduction, background of this study is presented. Applying VIPs to retrofit insulation to existing buildings is good for energy conversation. And objective and proposal are established in this Chapter.

Chapter 2 presents the historic development of VIPs. In general, VIPs are divided into two types: filling VIPs and vacuum layer VIPs, determined by the way in which the vacuum layer is generated. The filling VIPs include a gas barrier envelope and a core material. This core material is usually a glass wool, polyester fiber, silica powder, or any other porous material. The filling type VIPs are often used in new buildings to improve the insulation performance of the walls. Vacuum glazing which a representative of transparency evacuated product consists of an outer pane of low-emissivity glass and an inner pane of clear float, with a vacuum in between rather than air or another gas.

Chapter 3, from this Chapter, the authors are developing slim and light-weight vacuum insulation panels (VIPs) by producing vacuum layers with spacers and plastic plates aimed to retrofit insulation to windows. The developed VIPs have the advantages of a low cost and easy installation in existing buildings. In addition, one of the developed VIPs is slim and translucent so that it can be easily used for windows. In this view, the authors propose a vacuum layer type

slim translucent VIP and focus on a reasonable design method. Next, the authors introduce the design process in which the structural design is obtained with element mechanical analysis and a three-dimensional analysis is conducted for the VIP element. In the study, a heat transfer model is used to predict the insulation performance through numerical analysis. Subsequently, the authors perform an experiment to measure the thermal conductivity to validate the performance prediction. Finally, case studies are performed to confirm how the different design conditions affect the insulation performance. The optimum design of the vacuum layer type slim and translucent VIP will have sufficient structural strength to hold and maintain the vacuum layer. The thermal conductivity is approximately 0.007 $W/(m \cdot K)$ that can effectively improve the insulation performance in applications.

Chapter 4, to ensure the performance of our proposal, the authors proposed a frame structural VIP so that the total material area is reduced and the possibilities of gas generation should be also reduced. Then, the authors propose a frame structural slim translucent VIP and focus on a reasonable design method. The same process as Chapter 3, after design and validation, the thermal conductivity is approximately 0.0049 $W/(m \cdot K)$ that can effectively improve the insulation performance in applications.

Chapter 5, the authors give 5 different proposal to test and validate the VIP performance, of course these 5 models are totally transparent design. In this Chapter, the authors analyzed the experimental result and the outgassing and desorption issue should be the largest effect to VIP production. Additionally, the mesh and frame structural VIPs can achieve a relatively better insulation performance, however, the local thermal bridge is big effect and the transparency is not good due to the concentrated web. Finally, the authors summarized the properties of those transparent VIP models, and the reasonable suggestion can be proposed to improve the performance further.

Chapter 6, proposal of an overlapped VIP combination to retrofit insulation to walls. Slim and multiple layered VIPs can be applied to reduce the effect of the thermal bridge, for improving the architectural insulation performance. In this Chapter, a calibration hot-box apparatus is setup to evaluate the “U” values and the apparent thermal conductivity of a multilayered combination of VIPs. Then, a calculation model is generated for analyzing the insulation performance of full-scale VIPs, which is solved using Finite Element Analysis (FEA). As per the experimental results, the apparent thermal conductivity in a triple layer application should be 1.083 times that of the original; numerical results demonstrate that for a large VIP application with a triple layer, the apparent thermal conductivity is 1.004 times the original.

Chapter 7, summary of this study, discussed the design method and every proposal has been validated and the objective is reached with various achievements. Finally, the outlook and perspective are given in the end.

Acknowledgment

First of all, I would like to express my gratitude to all those who helped me during the writing of this thesis. My deepest gratitude goes first and foremost to Dr. Takao Katsura, my supervisor, for his constant encouragement and guidance. He has walked me through all the stages of the writing of this thesis. Without his consistent and illuminating instruction, this thesis could not have reached its present form.

Second, I would like to express my gratitude to all teachers who helped to review my doctoral dissertation, they are: Dr. Katsunori Nagano, Dr. Takao Katsura, Dr. Yasuhiro Hamada and Dr. Tarou Mori. I real appreciate their kindly help to review and effectively comments.

Then, I am also greatly indebted to the professors and teachers at the Graduated School of Engineering who gives useful and meaningful lectures that have instructed and helped me a lot in the past three years. I am also deeply indebted to Mr. Masahiro Aihara, Mr. Makoto Nakamura and prof. Katsunori Nagano who ever kindly support me in experiment and sample production. Thanks Mr. Tomoaki Murakami who ever start the preface of this topic with experimental testing, his results indicated a lot and saved lots of my time.

Next, I would like to express my heartfelt gratitude to Dr. En Li associate professor in Xi'an University of Architecture and Technology, Dr. Yongtao Bai associate professor in Xi'an Jiaotong University, who led me into the world of academic. He led me and teach me very effective logical considerations for academic topic and show me his opinions to revise my thinking. Then, I would like to express my gratitude to my dear friends I made in Hokkaido University in Sapporo city, Mr. Shuai Yin and Mr. Jiuzhou Tian, who shared all my happiness and sadness time in past three years and our conversation always interesting and brilliant will go on inspiring me.

Last my thanks would go to my beloved family for their loving considerations and great confidence in me all through these years. I also owe my sincere gratitude to my friends and my fellow classmates who gave me their help and time in listening to me and helping me work out my problems during the difficult course of the thesis.

Nomenclature

A	Measurement area	$[m^2]$
a	Span between spacers	[mm]
C	Thermal conductance	$[W/(m^2 \cdot K)]$
D	Stiffness	[N/m]
d	Thickness	[m]
d_p	Thickness of acrylic plate	[mm]
d_m	Molecular diameter	[nm]
E	Young's modulus	[Pa]
E	Emission coefficient	[-]
G_r	Grashof number	[-]
g	Acceleration due to gravity	$[m/s^2]$
K	Absolute temperature	[K]
k	Boltzmann constant	[J/K]
L_v	Thickness of vacuum layer	[m]
l	Mean free path of air	[m]
M	Molecular mass	$[g/mol]$
P	Pressure	[Pa]
P_b	Pressure ratio	[-]
P_0	Atmospheric pressure	[Pa]
P_r	Prandtl number	[-]
Q	Average electric power	$[W]$
Q_0	Heat from the heater, without heat loss	$[W]$
R	Thermal resistance	$[(m^2 \cdot K)/W]$
T	Temperature	$[K]$
ΔT	Temperature difference between hot and cold plates	$[K]$
U	Overall heat transfer coefficient	$[W/(m^2 \cdot K)]$
U_0	Overall heat transfer coefficient for polystyrene foam	$[W/(m^2 \cdot K)]$
v	Kinematic viscosity	$[m^2/s]$

Greek symbols

α	Convection heat transfer rate	$[W/(m^2 \cdot K)]$
α_{ti}, α_{to}	Overall heat transfer coefficients of the low and high temperature sides	$[W/(m^2 \cdot K)]$
β	Coefficient of volume expansion	[-]

β_0	Accommodation coefficient	[-]
γ	Specific heat ratio	[-]
θ	Average temperature	[℃]
θ_n	Ambient temperature	[℃]
σ	Stefan–Boltzmann constant	$[W/(m^2 \cdot K^4)]$
λ	Thermal conductivity	$[W/(m \cdot K)]$
ε	Emissivity	[-]
μ	Poisson ratio	[-]
δ	Coefficient when rectangular flat plate is functioned by uniform load	[-]
$\bar{\omega}_{max}$	Maximum deflection	[mm]

Subscripts

a	Average
C	Cold/ Calibrated
c	Conduction/Chamber
m	Mean
H	Hot
h	High temperature
l	Low temperature
P	Plate
r	Radiation/ Surface of the Baffle plate
s	Specimen surface
1, 2	Surface 1 or 2
VIP	Vacuum insulation panel
v	Vacuum layer
$va1,\ va2,\ va3$	Gaps in GHP apparatus
Foam	Polystyrene foam

Contents

Chapter 1
Introduction

1.1 Research background

The future is uncertain, both short and long term. Nowadays, the energy demand and consumption are increased growth along with the World's changing which consist of the population growth and development needs. Figure 1-1 shows the schematic diagram of the energy demand [1]. Furthermore, according to IEA data from 1990 to 2008, the average energy use per person increased 10% while world population increased 27%. Regional energy use also grew from 1990 to 2008: Middle East increased by 170%, China by 146%, India by 91%, Africa by 70%, Latin America by 66%, the USA by 20%, the EU-27 block by 7%, and world overall grew by 39%. The energy consumption growth in the G20 slowed down to 2% in 2011, after the strong increase of 2010.

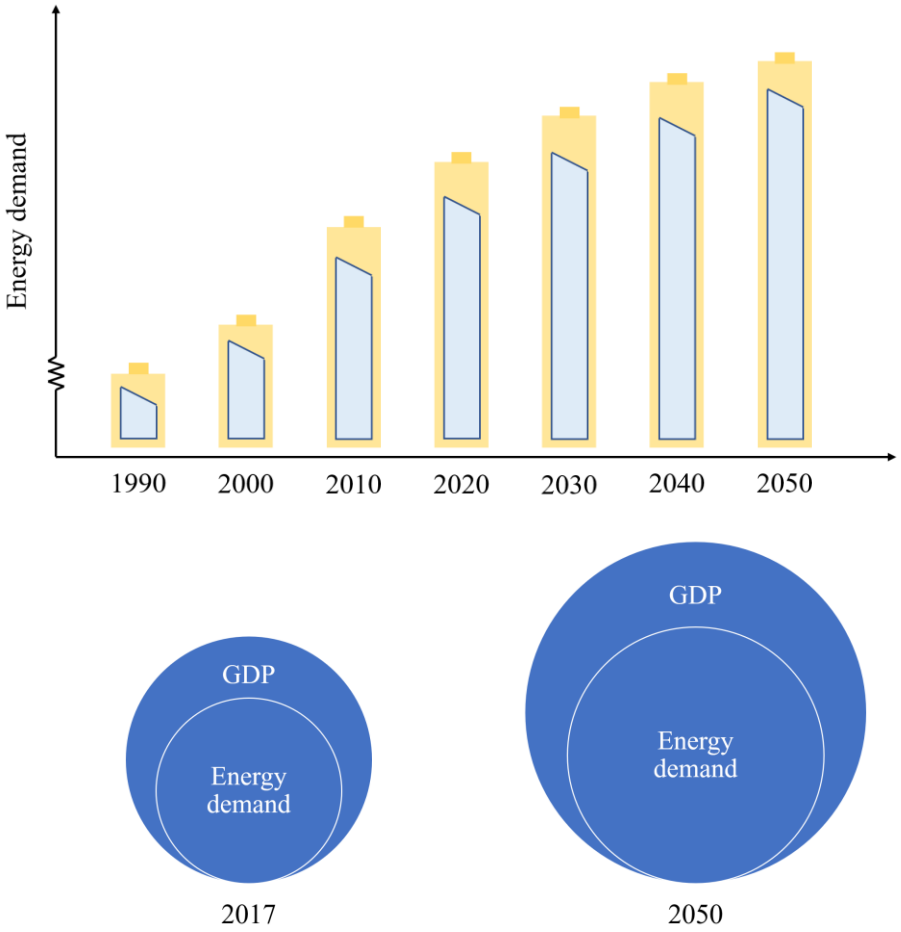

Figure 1-1 Schematic diagram of energy demand trend

Figure 1-2 shows world primary energy consumption in quadrillion Btu from 1980 to 2010 by region according to the U.S. Energy Information Administration [2]. Here, Btu is British thermal unit, 1 Btu can be converted into 2.931×10^{-4} GWh.

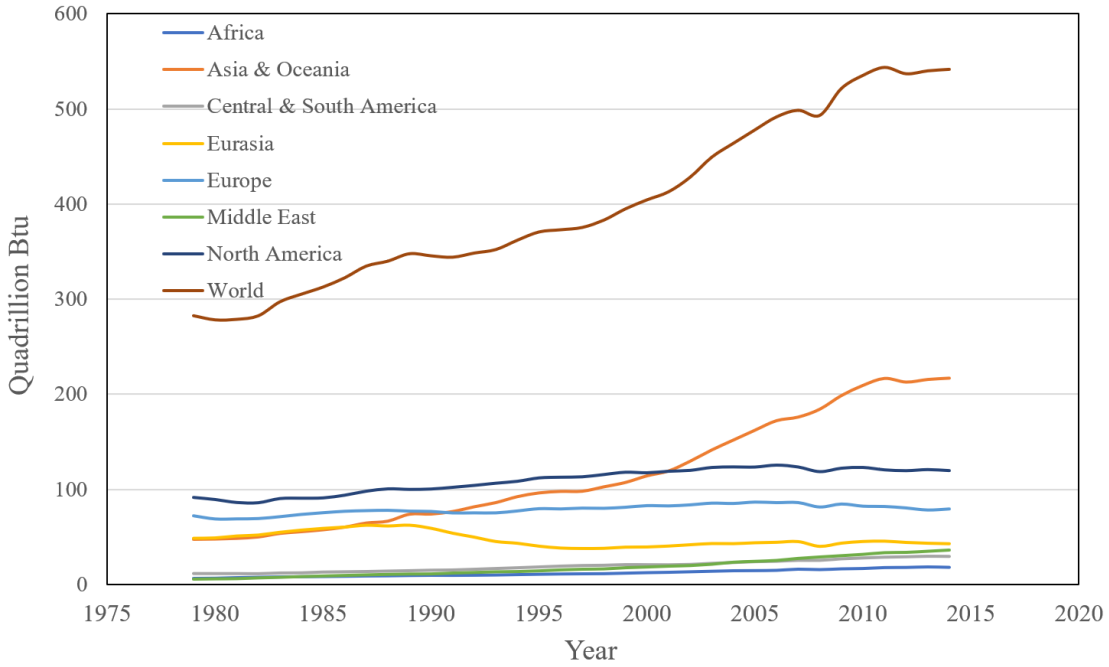

Figure 1-2 World primary energy consumption in quadrillion Btu from 1980 to 2010 by region

Energy demand is driven by economic growth, changes in individual sectors' contributions to this growth, technology developments and investor and consumer decisions. These decisions are in turn influenced by market signals, lifestyle and other broad societal trends, and policy. Superior equipment is often more expensive so that only a portion of technical replacement possibilities makes economic sense to investors, and replacement decisions are normally bound by equipment lifetimes. History shows that energy consumption is becoming more efficient, but also suggests that it is not easy to politically push the pace of improvements. Research on the impacts of existing energy efficiency policies is inconclusive. There are examples of energy intensities declining as a direct result of policy intervention.

Globally, energy demand has grown in a fairly stable relationship to GDP. IEA data suggests a ratio of global primary energy demand growth to global GDP growth of 0.70 for the 1972-2014 period. Dividing the world into the OECD countries on the one hand and all other countries on the other, and focusing on the shorter, more recent 1990-2014 period, shows a ratio of 0.32 for the former countries and a ratio of 0.62 for the latter. As

economies mature, they become more service and high-tech industry based and require less energy to sustain growth. OECD area primary energy consumption seems to have levelled out. IEA data suggest that between 2009 and 2014 a 1.8% per year increase in GDP generated a mere 0.1%/y increase in energy demand. Outside the OECD area, however, a 5.5%/y growth in GDP drove a 3.8%/y growth in energy use. The non-OECD share of world energy demand increased from 48% in 1990 to 62% in 2015, and continues to increase. Figure 1- 3 illustrate the yearly World primary energy demand (a) and the trend growth with GDP increasing (b) [3]. In the Figures, unit mtoe in Y axis is tonne of oil equivalent, and 1 mtoe can be converted into 11630 GWh from IEA source.

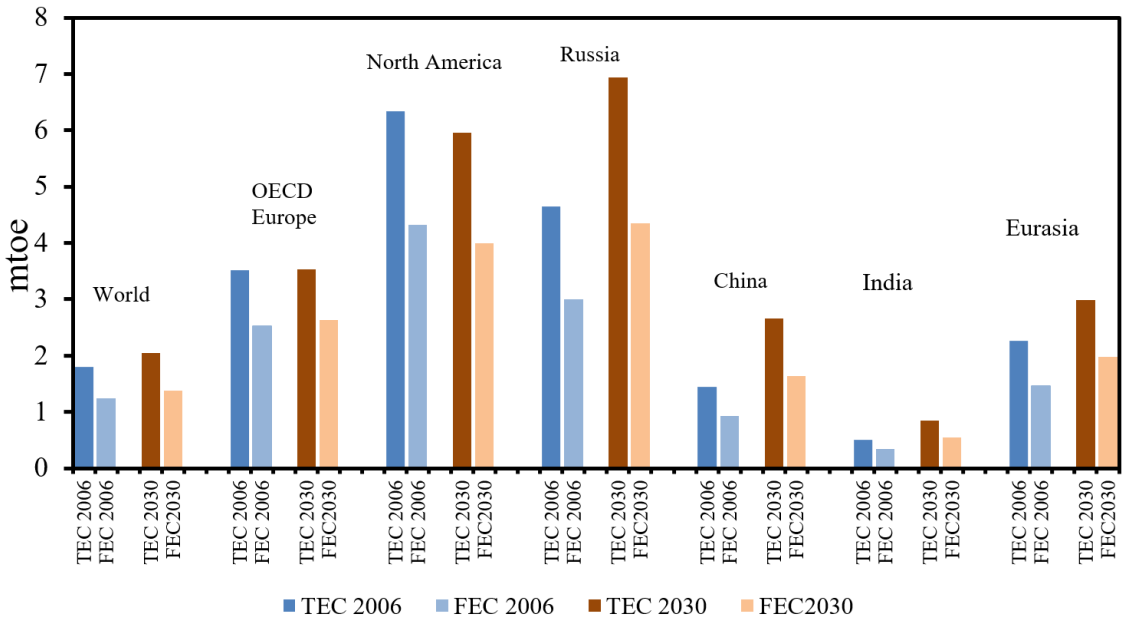

Figure 1-3 (a) Yearly growth of the World primary demand

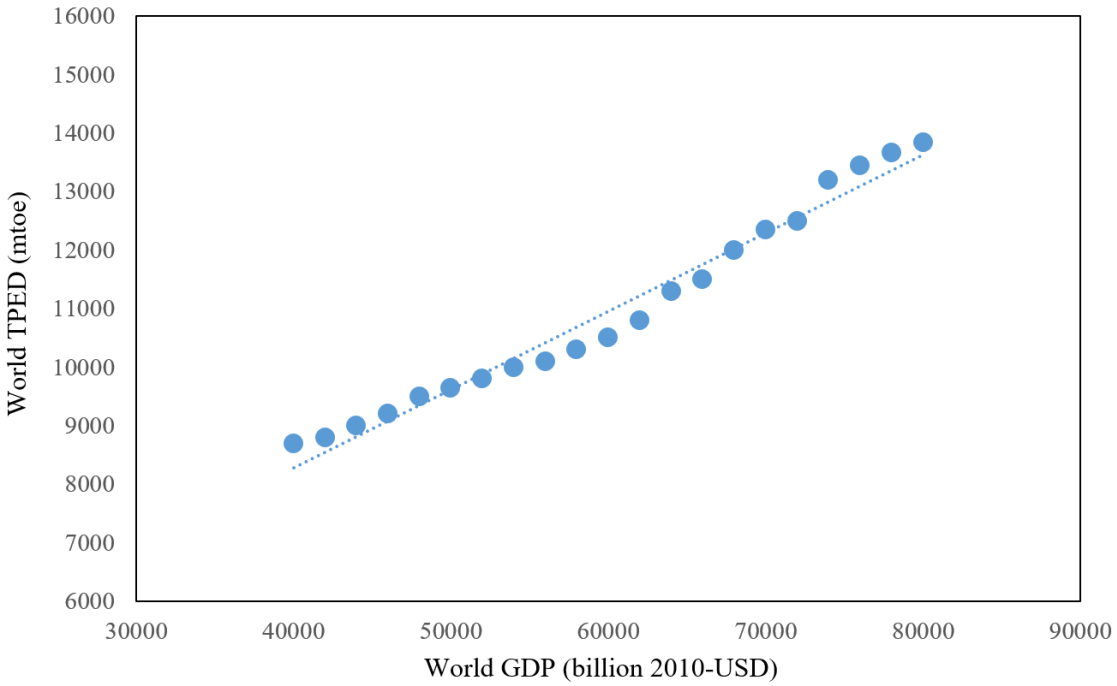

Figure 1-3 (b) The World primary energy demand trend with GDP

No doubt that the environmental load and energy nowadays are two of the biggest problems all over the world. The Climate change; which was noticed from the 50th of 19th century; and the oil crises at 1973 are examples of this problem. For the human being's future, the sustainable development is considered to be one of the most important common topics in the world. Up to now, for this common target, some agreements and necessary procedures with world-wide cooperation are in progress, and the technical researches about the new energy and environmental load controlling draw more attentions.

Generally, the aim and the result of social development are to improve common people's living quality. However, this improvement always indicates energy requirement increasing. Fig.1-4 shows the schematic diagram of society development and the corresponding environmental load [4].

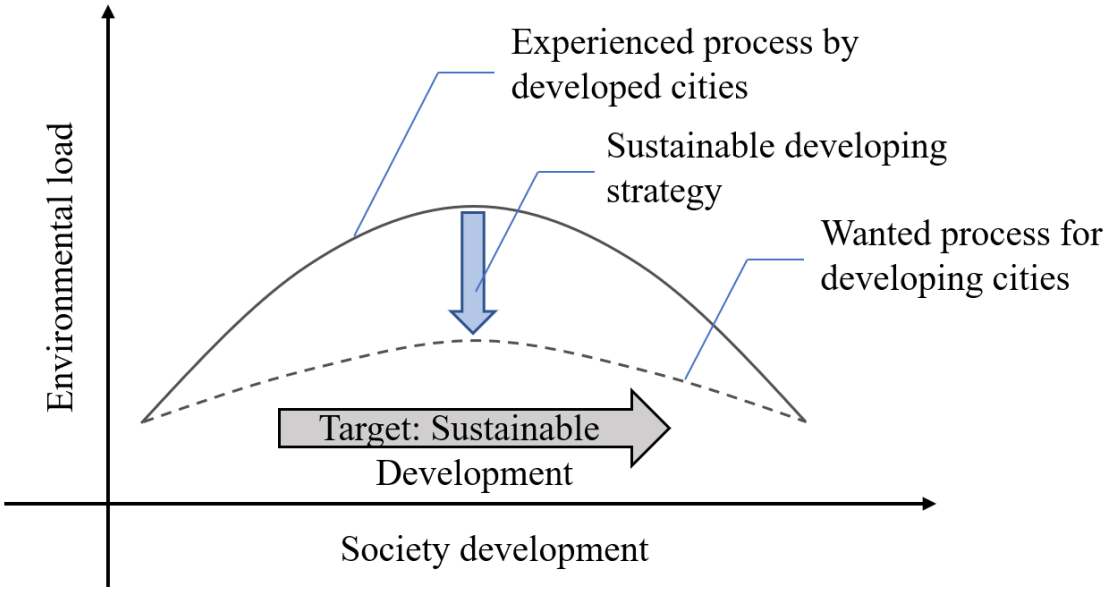

Figure 1-4 Schematic diagram of society development and the corresponding environmental load

According to the experience of developed countries, the environmental load growth is always the result of the developing process. Afterward, the World paid attention to this issue and invented more developed technology to control it. Environmental load in most of the developed countries were under controlled and then got reduced gradually. Therefore, developed countries have experienced the environmental load procedure of low-high-low. In Figure 1-4, the black solid curve shows this procedure.

As for the developing countries, because of the technical and financial limitations, the environmental controlling was not handled as well as the developed countries did. With the increasing of the environmental problems, it is easy to assume that if the developing countries following the track of developed ones, global environment will face more serious damage. Therefore, solving the contradictions between social development and environmental issues for the developing areas is a meaningful topic as well as an urgent target. In Figure 1-4, the dash line shows the targeted development procedure of developing countries, this curve is flatter than the black solid one, which means the developing areas should not track the old way of developed countries and should have a developing procedure with few environmental loads increasing.

A vacuum insulation panel (VIP) is a form of thermal insulation consisting of a gas-tight enclosure surrounding a rigid core, from which the air has been evacuated. It is used in building construction to provide better insulation performance than conventional insulation materials. VIPs consist of: 1) Membrane walls, used to prevent air from

entering the panel; 2) A panel of a rigid, highly-porous material, such as fumed silica, aerogel, perlite or glass fiber, to support the membrane walls against atmospheric pressure once the air is evacuated; 3) Chemicals (known as getters) to collect gases leaked through the membrane or off-gassed from the membrane materials. These are added to VIPs with glass-fiber or foam cores, because cores with bigger pore size require a higher vacuum (less than about 100 Pa) during the planned service life. Heat transfer occurs by three modes: convection, conduction and radiation. Creating a vacuum practically eliminates convection, since this relies on the presence of gas molecules able to transfer heat energy by bulk movement. A small decrease in pressure has no effect on the thermal conductivity of a gas, because the reduction in energy-carrying molecules is offset by a reduction in collisions between molecules. However, at sufficiently low pressure, the distance between collisions exceeds the size of the vessel, and then the conductivity does reduce with pressure. Since the core material of a VIP is similar in thermal characteristics to materials used in conventional insulation, VIPs therefore achieve a much lower thermal conductivity (k-value) than conventional insulation, or in other words a higher thermal resistance per unit of thickness. Typically, commercially available VIPs achieve a thermal conductivity of 0.004 $W/(m \cdot K)$ across the centre of the panel, or an overall value of 0.006~0.008 $W/(m \cdot K)$ after allowing for thermal bridging (heat conduction across the panel edges) and the inevitable gradual loss of vacuum over time [5]. The thermal resistance of VIPs per unit thickness compares very favourably to conventional insulation [6]. For instance, standard mineral wool has a thermal conductivity of 0.0044 $W/(m \cdot K)$ [7], and rigid polyurethane foam panels about 0.0024 $W/(m \cdot K)$. This means that VIPs have about one-fifth the thermal conductivity of conventional insulation, and therefore about five times the thermal resistance (R-value) per unit thickness. Based on a typical k-value of 0.007 $W/(m \cdot K)$, the R-value of a typical 25 mm-thick VIP would be 3.5 $(m^2 \cdot K)/W$. To provide the same R-value, 154 mm of rockwool or 84 mm of rigid polyurethane foam panel would be required. However, thermal resistance per unit price is much less than conventional materials. VIPs are more difficult to manufacture than polyurethane foams or mineral wools, and strict quality control of manufacture of the membranes and sealing joins is important if a panel is to maintain its vacuum over a long period of time. Air will gradually enter the panel, and as the pressure of the panel normalizes with its surrounding air its R-value deteriorates. Conventional insulation does not depend on the evacuation of air for its thermal performance, and is therefore not susceptible to this form of deterioration. However, materials like polyurethane foam are susceptible to water absorption and performance degradation as well. In addition, VIP products cannot be cut to fit as with conventional insulation, as this would destroy the

vacuum, and VIPs in non-standard sizes must be made to order, which also increases the cost. So far this high cost has generally kept VIPs out of traditional housing situations, However, their very low thermal conductivity makes them useful in situations where either strict insulation requirements or space constraints make traditional insulation impractical. VIP performance is also temperature dependent — with increasing temperature, convective and radiative transfer increase. Furthermore, typical panels cannot operate much above 100 °C due to the adhesive used to seal the thin envelope.

1.2 Research objective and significances

According to the previous background, it clear that we are focusing on reducing the environmental load, especially, in the buildings. Of late, various energy saving techniques are being employed in new buildings; however, these techniques are difficult to apply to existing buildings. Especially in Japan, the window's thermal insulation performance in an existing building is generally poor and it is important to improve this insulation performance. Applying a high insulation glass such as low-e triple glass or vacuum glazing can improve the insulation performance but there are some issues in the application to existing buildings, which are high cost and difficulty to construction. The authors developed a new model of a VIP that is thin and translucent and can be easily installed in buildings including even the windows, as illustrated in Figure 1-5. This VIP model consisted of two plates with a low-e film coating achieved using a gas barrier film, whereas the vacuum layer was supported by plastic spacers core any other core structures.

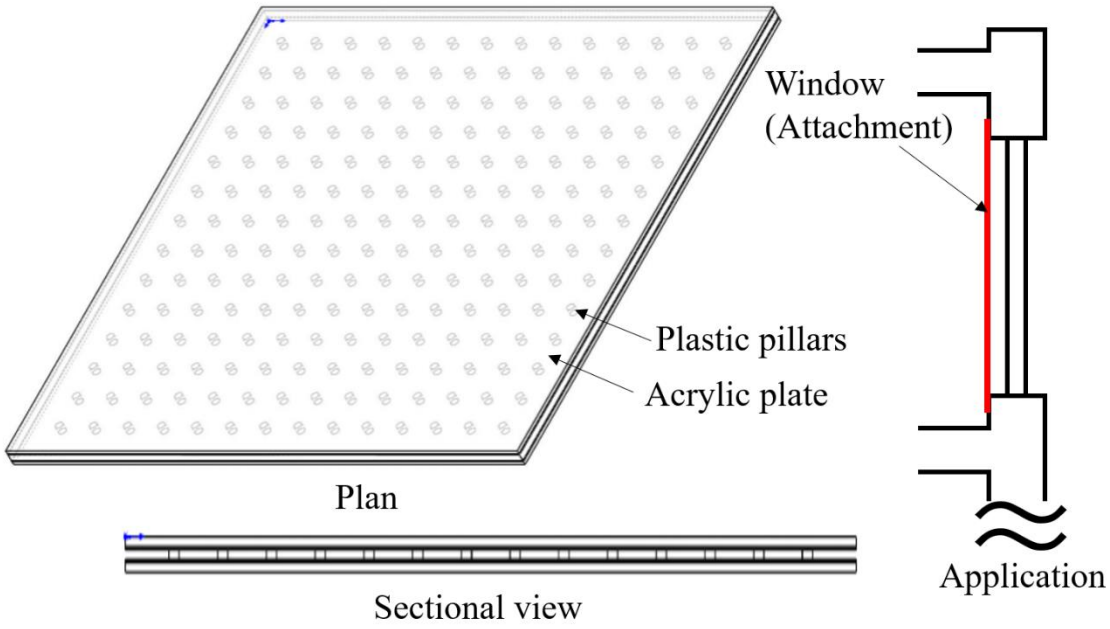

Figure 1-5 Concept diagram of the VIP application to buildings

1.2.1 Research objective

The authors are developing a slim and translucent vacuum insulation panels (VIPs) by producing vacuum layers with spacers. The developed VIPs have the advantages of low cost and can be set easily on the window due to its light weight. Therefore, the VIPs have the large potential to simplify the retrofitting insulation and improve drastically the thermal insulation performance of existing buildings. Furthermore, to have a reasonable design for this translucent vacuum layer type VIP, both the structure can hold the vacuum layer and the heat transmittance should be small enough to get a good insulation performance. The authors tested lots of core material and possibilities of core structures, then, an appropriate development is proposed.

The thermal bridge, previously known as the cold bridge, has a significant negative impact on the architectural performance. Slim and multiple layered vacuum insulation panels (VIPs) can be applied to reduce the effect of the thermal bridge, for improving the architectural insulation performance. The authors proposed an overlapped combination method to install the VIPs to the surface of building envelop directly. This application method can simplify the construction and reduce the effect of thermal bridge efficiently. Also, the high cost performance and simple construction can reduce the effect of degradation, which is the biggest issue of VIPs.

In this study, Sapporo city will be taken as an example to carry on the testing of the

VIP applications, the experiment is set up as the application method to against the serious cold in winter.

The purpose of this research is shown as following:

(1) Develop a vacuum insulation panel with transparent materials which consist of two steps: a) design a reasonable structure to hold the vacuum layer; b) estimate the heat transmittance to evaluate the insulation performance.
(2) Trial manufacture and experimental measurement to validate the insulation performance of VIPs with different core material or core structures to improve the insulation performance again.
(3) Experimental measurement to evaluate the application performance and reduction of thermal bridge effect.
(4) Actual test the insulation performance and improvement with a field experiment.

1.2.2 Research significances

The significances of this research have the following aspects.

(1) The proposed VIP has the vacuum layer which hold by the core structure, the thickness will be easy to smaller than 5 mm, and the light-weight provide a simple construction.
(2) The proposed VIP have very good insulation performance. The apparent thermal conductivity should be reach to 0.005~0.008 $W/(m \cdot K)$, and the overall heat transfer coefficient can be lower than 2 $W/(m^2 \cdot K)$.
(3) The proposed VIP is made of transparent materials, thus, the completed production will also a certain extent transparency or just called translucent. Therefore, we can apply the product to the windows with attachment installation.
(4) Materials for manufacturing are all cheap, thus, the VIPs will have a good cost performance. Degradation is the biggest effect to evacuated products, the good cost performance means we can replace the deteriorated VIP to a new one directly.
(5) The proposed VIP overlapped combination application method can quite reduce the effect of thermal bridge, the apparent thermal conductivity shows 1.004 time of original thermal conductivity of a applied VIP.
(6) The heating load can be reduced to half of original by applying the VIPs, it can be just 30~36% of original if the windows is applied the translucent VIPs too.
(7) In an actual field experiment, the environmental load reduction can be achieved as good as our prediction.

1.3 Flow of doctoral dissertation

Reconsideration of the development history and what should be studied further, the authors proposed to develop a new type with slim thickness, light weight, cost efficiency and translucent to retrofit insulation to windows in existing buildings. The specific way to implement can be divided as retrofitting insulations to windows and to walls, respectively. And the detailed process and considerations will present in following Chapters, the flow of my doctoral dissertation is shown as Figure 1-5.

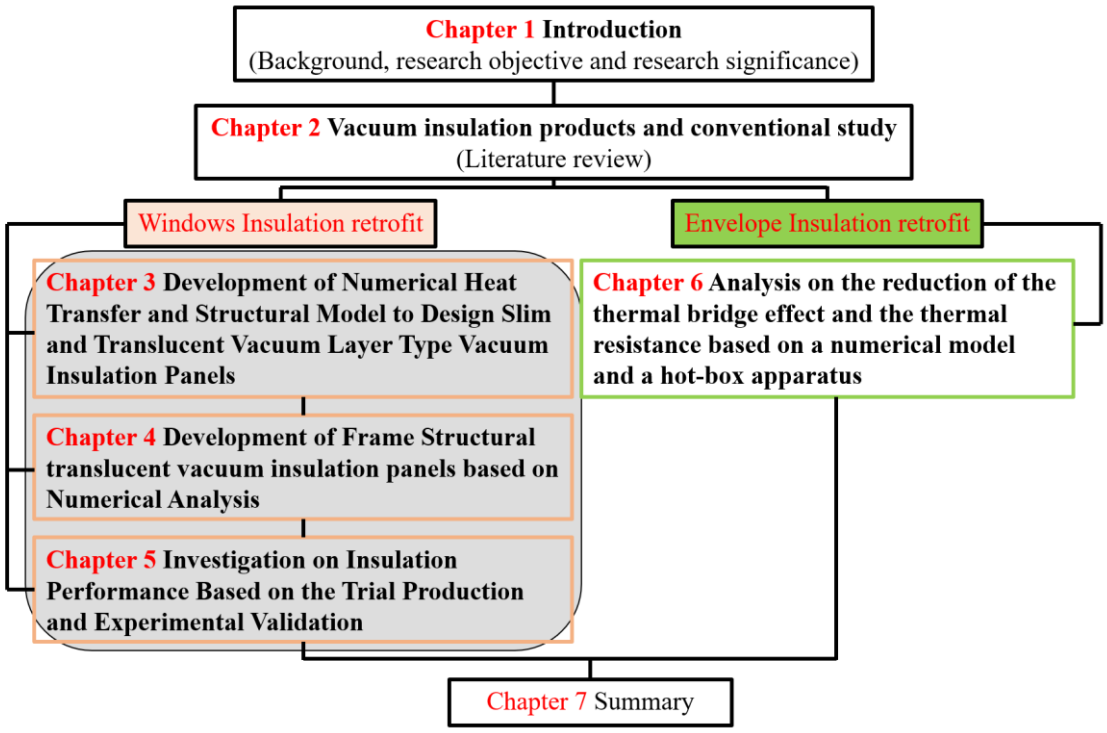

Figure 1-5 Flow of doctoral dissertation

Reference:

[1] The 2017 edition of Energy Perspectives, analysts at Statoil, June 8 2017.

[2] Martin Kraus - own, data source: U.S. Energy Information Administration (http://www.eia.gov/countries/data.cfm)

[3] World Energy Statistics 2017, 2017 Edition, IEA source.

[4] En Li, Passive Design Strategy on Residential Buildings for Sustainable Development of Lhasa, Doctoral thesis in Xi'an University of Architecture and Technology.

[5] Vacuum insulation in the building sector: systems and applications, Annex 39: High performance thermal insulation (HiPTI), The IEA Energy in Buildings and Communities (EBC, formerly known as ECBCS) Programme, 2005, retrieved 2011-10-10

[6] Fricke, J; Heinemann, U; Ebert, HP (2008-03-14), "Vacuum insulation panels—From research to market", Vacuum, 82 (7): 680–690, Bibcode:2008 Vacuum. 82. 680 F, doi:10.1016/j.vacuum.2007.10.014

[7] Rockwool roll, Rockwool, retrieved 2011-10-10

Chapter 2
Vacuum insulation products and conventional study

2.1 Introduction

Most insulation materials have been developed before 1950 but the extensive use of thermal insulation started only after the oil crisis in 1973. Since the oil crisis, the thermal insulation of buildings became the key element to prevent heat losses and to improve energy efficiency. For a long time for regions with an extended annual heating period, 10 cm of standard insulation such as expanded or extruded polystyrene, foamed polyurethane (PU), fiber-glass, etc., were considered as good insulation. But energy specialists calculated that the economically optimized thickness should be 30-50 cm depending on the specific climatic conditions. Today, many existing building regulations and standards demand U-value that is approximately equal to 0.2 $W/(m^2 \cdot K)$ for roofs and walls, which means about 20 cm thick insulation layers. Many architects have a problem with such regulations. They want to create spaces, not insulated bunkers. The problem of thick insulation layers is especially critical in the case of renovated buildings where there are severe limitations on space and also many other technical constraints.

Various sources indicate that buildings have big energy saving potential, especially, for the existing buildings which insulation performance is poor. Currently, there are a lot of effective technologies are applied to new buildings to reduce energy consumption such as: smart energy management, renewable energy system, heat recovery ventilation and high insulation technique, etc. However, these new techniques are difficult to install to existing buildings, thus, insulation retrofit to existing buildings is a effective way to contribute to energy conservation. A vacuum insulated panel (VIP) is a form of thermal insulation consisting of a gas-tight enclosure surrounding a rigid core, from which the air has been evacuated. It is used in building construction to provide better insulation performance than conventional insulation materials. As a modern state-of-the-art thermal insulation, VIPs have a thermal resistance that is approximately 10 times higher than that of equally thick conventional polystyrene boards, and the insulation performance if applied VIPs has been investigated in some studies (Taesub Lim 2017; Alfonso Capozzoli 2015; Seung-Yeong Song 2014) [1-3].

In general, VIPs can be divided as filling type and vacuum layer type through the generation form of vacuum layer. Filling type VIPs contained a gas barrier envelope and “core material”, usually, core material is selected as glass wool, polyester fiber, silica powder or any other porous materials. The filling type VIPs are well used in some new buildings to improve the insulation performance to walls. Vacuum glazing by R.E. Collins [4-10], a well investigated study which maintained a vacuum layer by using spacers. A

vacuum glazing consists of an outer pane of low-emissivity glass and an inner pane of clear float, with a vacuum rather than air or another gas in between. Then, the durability of spacers is investigated and the material selection for spacers is discussed. R. E. Collins and Simko (1998) give a details description of the high insulation performance technique for vacuum glazing [11]. According to their study, a Japanese company (Nippon Sheet Glass Co., 2005) developed a double layer vacuum glazing as a commercial product with "U" value in 1.5 $W/(m^2 \cdot K)$ [12]. Ulster studies the edge thermal conduction and sealing method to vacuum glazing (Griffiths et al., 1998) [13]. The Fraunhofer Institute for Solar Energy Systems developed a hermetic glazing edge seal for vacuum glazing based on a sputtered metallic layer and a soldering technique (Wittwer, 2005; Baechli, 1991; Baechli, 1992; Sager-Hintermann and Baechli, 2002) [14-17]. There studies above well investigate vacuum glazing and achieved good insulation performance to new constructions. However, the weight of vacuum glazing is so heavy that it's not good enough to insulation retrofit to existing buildings due to the additional construction cost. So far, activities in the field of vacuum glazing have mainly focused on glazing with a single evacuated cavity. However, so-called hybrid insulating glazing units—triple glazing featuring both an evacuated and a gas-filled cavity—have been proposed and manufactured with the aim of cutting thermal transmittance (Asano et al., 1999). Units of this kind with thermal transmittances between 0.7 and 0.9 are now commercially available (Nippon Sheet Glass Co., 2005). Following publication of the review article by Collins and Simko (1998), several additional patent applications have been filed in relation to vacuum glazing in recent years. These, for example, cover manufacturing or processing methods (Veerasamy, 2000; Demars, 1999; Poix et al., 2001; Zhao and Zhao, 2002; Futagami et al., 2003) and techniques for applying a dry carbon lubricant between the pillars and glass surfaces in order to reduce scratching or cracking of the glass during temperature-induced relative movement (Collins and Tang, 2000). Very recently, a triple vacuum glazing employing thin wires in the cavities to support glass sheets was patented (Wuethrich, 2005). Collins and Simko (1998) suggested baking the glazing during the evacuation process at temperatures between 100 and 250 ℃ in order to remove gases from the internal surfaces. More recent work by Ng et al. (2003, 2005), and Minaai et al. (2005) has shown that higher temperatures (>350 ℃) during manufacture are needed to prevent a pressure increase when the glazing is exposed to sunlight. Despite the painstaking and promising efforts in the field of vacuum glazing, the thermal transmittances achieved by this glazing type still fail to meet the requirements of today's advanced low-energy buildings. This study therefore sets out to investigate the theoretical potential of glazing with two evacuated cavities and support pillar arrays. As units with a

second evacuated cavity can significantly improve on the thermal transmittance performance achieved by present triple glazing with inert gas filled cavities, the triple vacuum glazing concept holds considerable potential for low-energy building applications. The progress made in recent years in the fields of low-emittance coatings, materials and process technology has brightened the prospects of such an endeavour. This study uses analytical and numerical methods to identify suitable parameter sets for triple vacuum glazing, taking into account also the mechanical stresses due to atmospheric pressure [18]. By summarizing articles above, the significances are shown as follows (Table 2-1~Table 2-5).

2.2 Energy in buildings

The effect of a major adoption of the VIP (Vacuum Insulation Panel) technology by the construction industry on environment is expected to be absolutely huge. The official numbers for the EU given below show that using VIP in buildings could account for most of the very challenging target of 8% reduction in emission of greenhouse gases (Kyoto Protocol).

The total final energy consumption in the EU in 1997 was about 930 Mtoe (Million tons oil equivalent). A simplified breakdown of this demand shows the importance of buildings in this context: 40.7% of total energy demand is used in the residential and commercial sectors, most of it for building-related energy services (Table 1) [19]. It should also be pointed out that approximately 10% of the consumed energy in buildings comes from renewable energy sources. Space heating is by far the largest energy end-use of households in EU Member States (57%), followed by water heating (25%). Electrical appliances and lighting make up 11% of the sector's total energy consumption. For the commercial sector the importance of space heating is somewhat lower (52%), while energy consumption for lighting, office equipment and "other" (water heating, cooking and cooling) are 14%, 16% and 18%, respectively.

Table 2-1 Accumulation of articles (Insulation retrofit)

Authors	Title	Journal & volume	Year	Method	Film	Thickness
Pär Johansson, Stig Geving, Carl-Eric Hagentoft	Interior insulation retrofit of a historical brick wall using vacuum insulation panels: Hygrothermal numerical simulations	Building and Environment 79 (2014) 31-45	2014	Investigate the hygrothermal performance of a brick wall with wooden beam ends after it was insulated on the interior with VIPs.	Not focus	20 mm
Pär Johansson, Carl-Eric Hagentoft	Retrofitting of a listed brick and wood building using vacuuminsulation panels on the exterior of the facade: Measurementsand simulations	Energy and Buildings 73 (2014) 92–104	2014	The goal is to improve the thermal transmittance and moisture per-formance of the wall and the thermal comfort for the occupants.	Multi-layered polymer laminates with thin aluminum layers	20 mm
David Tetlowa, Lia De Simon, Soon Yee Liew	Cellulosic-crystals as a fumed-silica substitute in vacuum insulated panel technology used in building construction and retrofit applications	Energy and Buildings 156 (2017) 187–196	2017	Nano-cellulose technology VIP retrofit as application	PET+PE+Al+PP	Not focus
Abdullahi Ahmeda, Monica Mateo-Garcia	Methodology for Evaluating Innovative Technologies for Low- Energy Retrofitting of Public Buildings	Energy Procedia 112 (2017) 166 – 175	2017	Evaluation of the process of low-energy retrofit and the selection and evaluation of low-energy technologies for retrofit.	Not focus	Not focus
Amanda L. Webb	Energy retrofits in historic and traditional buildings: A review of problems and methods	Renewable and Sustainable Energy Reviews 77 (2017) 748–759	2017	While energy consumption and conservation are the dominant criteria, a number of others are also important, including the needs of the building fabric, occupants, and collections, as well as economics, embodied energy, and climate change.	Not focus	Not focus
M. Harrestrup, S. Svendsen	Full-scale test of an old heritage multi-storey building undergoing energy retrofitting with focus on internal insulation and moisture	Building and Environment 85 (2015) 123e133	2015	A solution where the insulation was stopped 200 mm above the floor was investigated, increased the heat flows through the wall compared to a fully insulated wall	Not focus	Not focus

Table 2-1 Energy consumption of buildings in Europe

Residential Sector	[%]	Commercial	[%]
Space Heating	57	Space Heating	52
Water Heating	25	Water Heating	9
Electric Appliance	11	Lighting	14
Cooking	7	Office Equipment	16
		Cooking	5
		Cooling	4

From these numbers it can be derived that more than 25% of EU energy consumption and also CO_2 emissions are caused by heat transfer processes in buildings, which directly depend on insulation standards. It has to be kept in mind that these heat transfer processes not only do occur in the building envelope but also in boilers, refrigerators and freezers and cold storage rooms.

2.3 Potential impact of VIP for building insulation

In 1995, there were roughly 150 million dwellings in the EU-15; 32% of this stock was built prior to 1945, 40% between 1945 and 1975 and 28% between 1975 and 1995. The ratio, housing starts vs. housing stocks, varies between 1 to 2%. Therefore the reduction in CO_2 emissions by using VIP technology depends largely on how well the new technology is adopted in retrofitting the old building stock, which to a large extent (around 50%) is not insulated at all. This success depends not only on the technical solutions but also on regulations and energy prices. However, it can be assumed that the energy consumption of the dominating old buildings can be reduced by a factor of three. This means that the EU CO_2 emissions would be reduced by about 8%, which is the reduction the EU agreed on in the Kyoto Protocol. Since VIP-based systems are thinner and their recycling economically attractive, the resource intensity will be lower than for conventional solutions. Additional important impacts are reduction in adverse environmental effects of transporting fuel (sea and land) to and inside Europe and also reduction in the rate at which the global energy reservoirs is depleted. Furthermore, if one takes into account that use of the VIP technology is not limited to Europe only, the numbers can be much more impressive.

2.4 Vacuum insulation today

Currently VIP have only limited use, mainly in top models home refrigerators/freezers and cold shipping boxes. Japan controls more than 50% of the small global VIP market with several million panels per year. The VIP market in Japan is fast growing. The common core materials are fumed and precipitated silica, open-cell PU and several types of fiber-glass. Both metallized-film and aluminum foil laminates are being used to seal the vacuum.

For buildings, most of the VIP activity is still in the R&D phase with some demonstration projects. Germany and Switzerland are the only countries where a market in its early stage has been established. Fumed silica boards are being used almost exclusively. Fumed silica is the best core material due to the small size of the pores and the low heat conductivity of the powder.

2.5 Physics

The physics of heat transfer through conventional insulation materials is well known. A short description of the most important phenomena is given below. In conventional insulation materials like mineral wool, glass wool or organic foams the total heat transfer is dominated by the contribution of the (non-convective) gas within the hollow spaces or pores.

Thus, a large potential for improvement of the insulation properties can be realized by reducing or even completely eliminating the gas conductivity. The gas conductivity in a porous medium is determined by the number of gas molecules as transfer medium as well as by the number of "walls" on the way from the hot to the cold side. At a high pressure, when the mean free path of the gas molecules is much smaller than the size of the pores, collision between the gas particles is the limiting mechanism for an efficient heat transfer. Here an increase in the gas pressure with an increase in the number of gas particles is correlated with a decrease in the mean free path. As the two effects, number of gas particles and frequency of collisions, compensate each other the thermal conductivity of a gas is nearly independent on the gas pressure, at higher pressures.

Table 2-2 Accumulation of articles (filling type VIPs)

Authors	Title	Journal & volume	Year	Core material	Film	Thickness
Yuying Liang, Huijun Wua, Gongsheng Huang, Jianming Yanga and Yunfei Ding	Prediction and Optimization of Thermal Conductivity of Vacuum Insulation Panels with Aerogel Composite Cores	Procedia Engineering 205 (2017) 2855–2862	2017	Fiber felt/silica aerogel composite cores	Not focus	6 mm
Yuying Liang, Huijun Wu, Gongsheng Huang, Jianming Yang, Huan Wang	Thermal performance and service life of vacuum insulation panelswith aerogel composite cores	Energy and Buildings 154 (2017) 606–617	2017	Glass fiber	Barrier envelope (MF)	6 mm
Q.R. Zheng, Z.W. Zhu, J. Chen, W.S. Yu	Preparation of carbon based getter for glass fiber core vacuum insulation panels (VIPs) used on marine reefer containers	Vacuum 146 (2017) 111-119	2017	Glass fiber	Not focus	10 mm
Xiaobo Di, Yimin Gao, Chonggao Bao, Shengqiang Ma	Thermal insulation property and service life of vacuum insulationpanels with glass fiber chopped strand as core materials	Energy and Buildings 73 (2014) 176–183	2014	Glass fiber	A three-fold aluminum-coated polymer laminate as barrier envelope	10-25 mm
H. Singh, M. Geisler, F. Menzel	Experimental investigations into thermal transport phenomena invacuum insulation panels (VIPs) using fumed silica cores	Energy and Buildings 107 (2015) 76–83	2015	Fumed silica cores	Not focus	20 mm
Xiangyu Li, Huisu Chen , Huiqiang Li, Lin Liu, Zeyu Lu, Tao Zhang, Wen Hui Duan	Integration of form-stable paraffin/nanosilica phase change material composites into vacuum insulation panels for thermal energy storage	Applied Energy 159 (2015) 601–609	2015	Form-stable paraffin/nanosilica phase change material	Not focus	10 mm

Haeyong Jung, InseokYeo, Tae-HoSong	Al-foil-bonded enveloping and double enveloping for application to vacuum insulationpanels	Energy and Buildings 84 (2014) 595–606	2014	Glass fiber	Al-foil-bonded enveloping, PET*3+Al+PE	15 mm
I. Mandilaras, I. Atsonios, G. Zannis, M. Founti	Thermal performance of a building envelope incorporating ETICS withvacuum insulation panels and EPS	Energy and Buildings 85 (2014) 654–665	2014	Fumed silica cores	Not focus	20 mm
Haeyong Jung, Choong Hyo Jang, In Seok Yeo, Tae-Ho Song	Investigation of gas permeation through Al-metallized film for vacuum insulation panels	International Journal of Heat and Mass Transfer 56 (2013) 436–446	2013	Fumed silica cores	12 μm (PET) film. 12 μm PET film coated with a 33 nm aluminum layer	20 mm
Bongsu Choi, Inseok Yeo, Jaehyug Lee, Won Kyeong Kang, Tae-Ho Song	Pillar-supported vacuum insulation panel with multi-layered filler material	International Journal of Heat and Mass Transfer 102 (2016) 902–910	2016	Glass wool	Not focus	15 mm
K. Ghazi Wakili, T. Stahl, S. Brunner	Effective thermal conductivity of a staggered double layer of vacuum insulation panels	Energy and Buildings 43 (2011) 1241–1246	2011	Glass wool, fumed silica cores	PET+Al+PE	30 mm
Choonghyo Jang, Haeyong Jung, Jaehyug Lee, Tae-Ho Song	Radiative heat transfer analysis in pure scattering layers to be used in vacuum insulation panels	Applied Energy 112 (2013) 703–709	2013	Silica powder, glass fiber	Not focus	10 mm
Inseok Yeo, Haeyong Jung, Tae-Ho Song	Gas permeation characteristics through heat-sealed flanges of vacuum insulation panels	Vacuum 104 (2014) 70-76	2014	Silica powder, glass fiber	PET+LDPE+Al+LDPE +LLDPE	20 mm

Oliver Miesbauer, Esra Kucukpinara, Sandra Kiese, Yoash Carmi, Klaus Noller	Studies on the barrier performance and adhesion strength of novelbarrier films for vacuum insulation panels	Energy and Buildings 85 (2014) 597–603	2014	Glass fiber	Hybrid polymeric+Al+PET	15 mm
Jae-Sung Kwon, Choong Hyo Jang, Haeyong Jung, Tae-Ho Song	Effective thermal conductivity of various filling materials for vacuum insulation panels	International Journal of Heat and Mass Transfer 52 (2009) 5525–5532	2009	Silica powder, glass fiber	Not focus	15 mm
Fred Edmond Boafo, Jun-Tae Kima, Zhaofeng Chen	Configured cavity-core matrix for vacuum insulation panel: Concept,preparation and thermophysical properties	Energy and Buildings 97 (2015) 98–106	2015	Glass fiber	Not focus	20 mm
Jae-Sung Kwon, Choong Hyo Jang, Haeyong Jung, Tae-Ho Song	Vacuum maintenance in vacuum insulation panels exemplified with a staggered beam VIP	Energy and Buildings 42 (2010) 590–597	2010	Glass fiber	Not focus	20 mm
Glenn De Meersmana, Nathan Van Den Bossche, Arnold Janssens	Long term durability of Vacuum Insulation Panels: determination of the Sd-value of MF-2 foils	Energy Procedia 78 (2015) 1574 – 1580	2015	Fumed silica cores	PET (1, 2, 3)+Al+PE	20 mm
Choonghyo Jang, Jongmin Kim, Tae-Ho Song	Combined heat transfer of radiation and conduction in stacked radiation shields for vacuum insulation panels	Energy and Buildings 43 (2011) 3343–3352	2011	Stacked radiation shields	Not focus	15 mm
Chengdong Li, Binbin Li, Ning Pan, Zhaofeng Chen,Muhammad Umar Saeed, Tengzhou Xu	Thermo-physical properties of polyester fiber reinforced fumedsilica/hollow glass microsphere composite core and resulted vacuuminsulation panel	Energy and Buildings 125 (2016) 298–309	2016	Polyester fiber reinforced fumed silica	PET+Al+PE+PET	20 mm

At atmospheric gas pressure the above behavior holds for most conventional insulation materials. Also, gaseous conductivity is determined by the thermal conductivity of the non-convective gas. Reducing the gas pressure by "evacuation", the gaseous conductivity remains almost unaffected until the mean free path attains values that are in the order of the size of the (largest) pores or higher. An extraordinary material in this regard is pressed powder boards made of fumed silica with the largest pores in the same order of magnitude as the mean free path of air molecules at atmospheric pressure (about 70 nm). For this material even at atmospheric pressure gaseous conductivity already is affected by the fine structure. It may be considered as "partially evacuated" and thus seems to be a favorite material for "evacuated" insulations.

Current VIP-technology uses especially this material with the least requirements to the quality of the vacuum, that has to be achieved and maintained in combination with special high barrier films and foils, which fulfil the requirements for long term applications as in buildings (Figure 2-1).

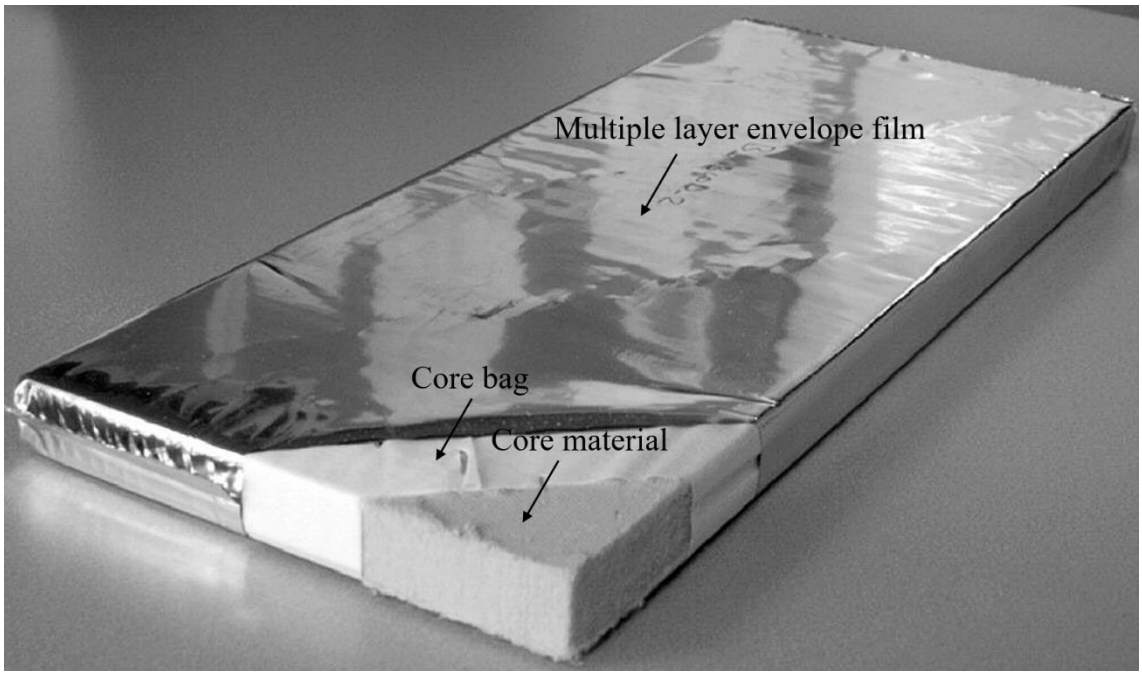

Figure 2-1 Components of a VIP. The core-bag provides mechanical stability for handling and protects the welding area from being polluted by core-powder [19]

2.6 Core material

The core material suitable for VIP production has to fulfil different requirements: very small pore diameter, open cell structure, resistance to compression (atmospheric pressure)

and almost impermeable to infrared radiation.

Pore diameter

To reduce the gas conductivity in normal insulation materials the pressure has to be very low (Figure 2) which is difficult to maintain by an envelope mainly made of organic materials. That is why for VIP a combination of a nano-structured core material and pressure reduction is used.

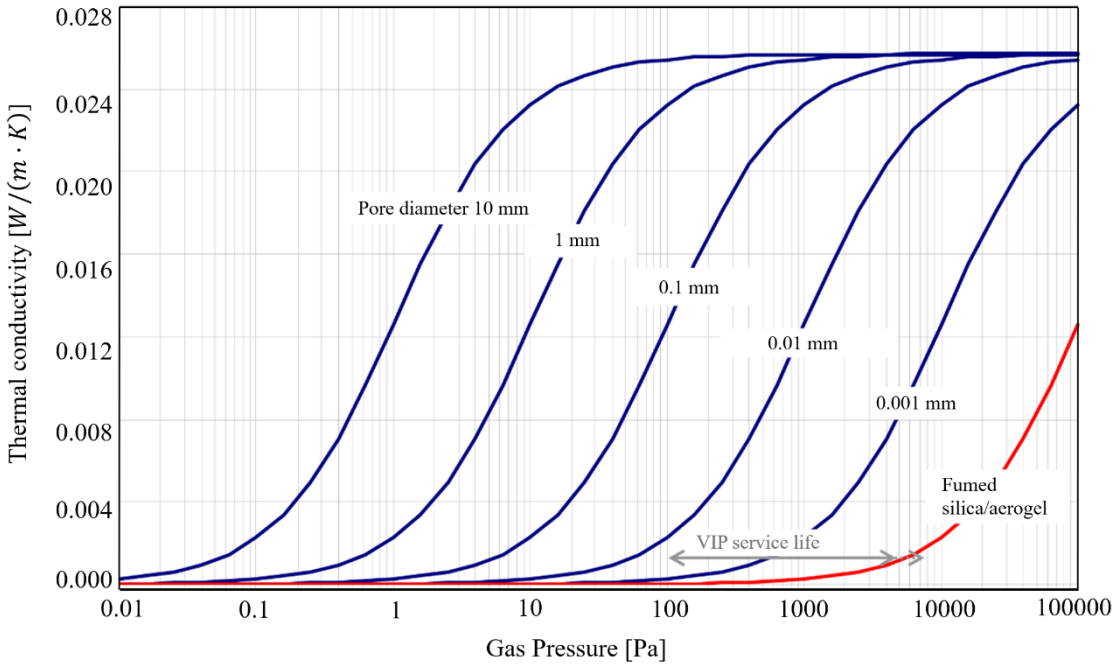

Figure 2-2 The small pore size of fumed silica or aerogels do reduce gas conductivity even at ambient pressure [20]

Today produced VIP (fumed silica core) start with in internal pressure in the range of 100 to 300 Pa. The VIP's end of service life is reached when the gas conductivity is starting to rise (5000-100000 Pa).

Cell structure

To be able to evacuate the core material it has to be 100% open-celled, so that the gas (air) can be quickly removed out of the material.

Stability

The internal pressure of a VIP is only few mbar. Consequently, the pressure load on the panel is close to 1 bar or 10 tons/m^2. The core material therefore has to be stable enough

so that the pores do not collapse when evacuated.

Radiation

Besides gas conductivity, radiation has also to be reduced to reach very low conductivity values. This is done by adding opacifiers to the core material.

Heat conductivity

Today different organic and inorganic insulation materials with open-cell structure are available for the use as core for VIP-production. Corresponding to the pore size distribution, the solid conductivity and the radiation properties of a material, a specific heat conductivity results, depending on the gas pressure (Figure 3). The figure shows clearly the advantages of fumed silica: low conductivity up to a pressure of more than 50 mbar and a conductivity at ambient pressure of half that of a conventional insulation material.

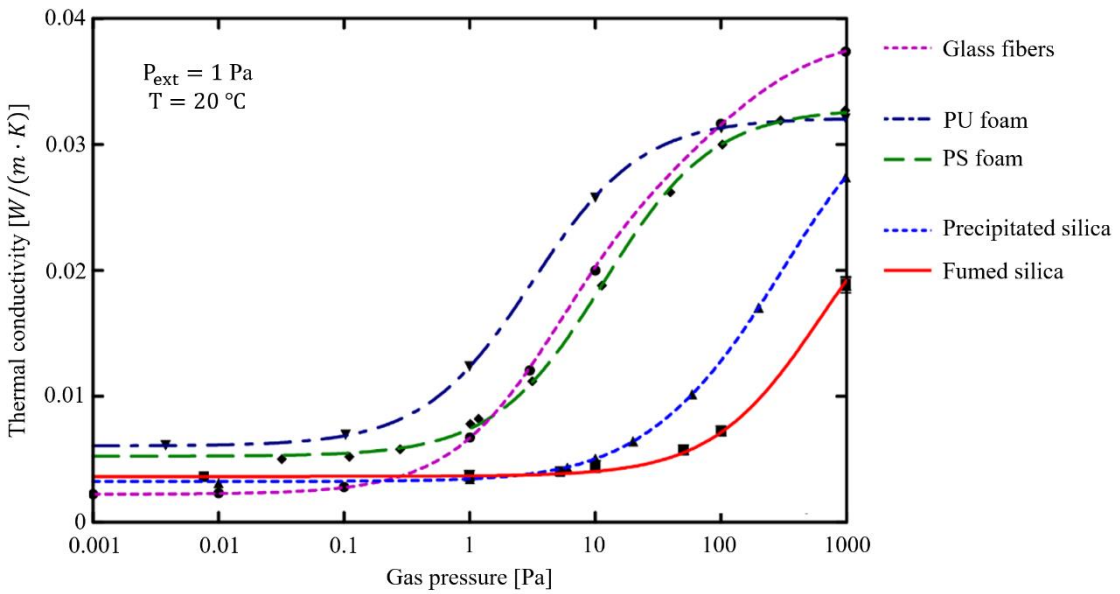

Figure 2-3 The heat conductivity of fumed silica starts to rise only above a gas pressure of more than 5000 Pa [21]

Most models of conventional VIPs include a core material with a low-thermal conductivity coating of a gas barrier film (in particular, aluminum foil), and they are always used in refrigerators and thermoses. In the current good building practices, windows are considerably less well-insulating than other parts of a structural envelope. The necessity to reduce energy consumption requires the use of smaller windows than

may be architecturally or aesthetically desirable that in turn reduces the potential for solar gain in cold climates. Therefore, the study of vacuum insulation technology that is applied to buildings is being performed since the 1990s. A representative study of the vacuum insulation technology is the study of vacuum glazing by R. E. Collins. In the corresponding research, pillars are used between two pieces of glasses to form a vacuum layer, and a low-e film is employed to reduce the thermal emissivity that is approximately 0.9 for glass. Then, the durability of the pillars is investigated and their influence is discussed [22-28]. The cost to produce the vacuum glazing is compared with a model in which argon is filled in a pair glass with a low-e film, and the result shows a 25% increase in the cost.

The study of the application of VIPs to buildings as panels and sheets is gaining prominence worldwide. An aluminum vapor deposited Polyethylene terephthalate (PET) film is used as a core material for analysis which called core material of metallic multilayer and fiber overlapping; however, it is yet to be manufactured. Analysis of the heat transfer model of nanoporous silica vacuum insulation material is proposed by Bouquerel. Kwon examined the powder, foam, and fiber type models, followed by the heat transfer model of the core material with a staggered beam. Finally, the fiber type model of the staggered beam core material was found to be effective. In addition, Johansson proposed a short-term in-situ performance measurement method for VIPs, and its accuracy is being verified [29-33].

In general, porous materials are used as the core materials, such as fumed silica, glass fiber, polymer foam and staggered beam structure.

Glass fiber core material

It is comprised of an evacuated open porous load bearing core material which is enveloped in high gas barrier envelope to maintain vacuum. In addition, adsorbent is essential to absorb residual gases released from core material and permeated by gas barrier multilayer foil film and heat seal layer, as shown in Figure 4 [34-35].

Silica aerogel core material

Silica aerogel have a efficiency performance for insulating as a thermal conductivity reach to 0.01 $W/(m \cdot K)$, in laboratory, silica aerogel is inserted to a gas barrier coating and sealed as a vacuum insulation panel.

2.7 Vacuum glazing

While very similar to a double-paned, gas-filled window, vacuum glazing has one unique difference; there's no air between the two panes of glass. Instead, the window is designed with a small hole that allows the oxygen to be removed from between the two pieces of glass and then sealed. By doing so, the conduction and convection processes that normally occur are significantly reduced. The concept originated in 1913 but was not technologically feasible until the late 1980s. By the early 21st Century Nippon Sheet Glass Group made the first commercially available models, which have been implemented in Japan's architectural designs for homes and businesses for over 10 years. Each of Pilkington SPACIA's products utilizes low-e glass and coatings which produce energy performance ratings similar, if not better, than conventional double-glazed windows with low-e coatings but with a significantly thinner frame profile. Ranging from 9mm to 21mm, Pilkington's SPACIA products are useful for older homes that need refurbishment or for newer homes as their lightweight and thin frames will not sacrifice aesthetics for insulation capabilities.

The concept diagram of vacuum glazing structural is shown as Figure 5 [36].

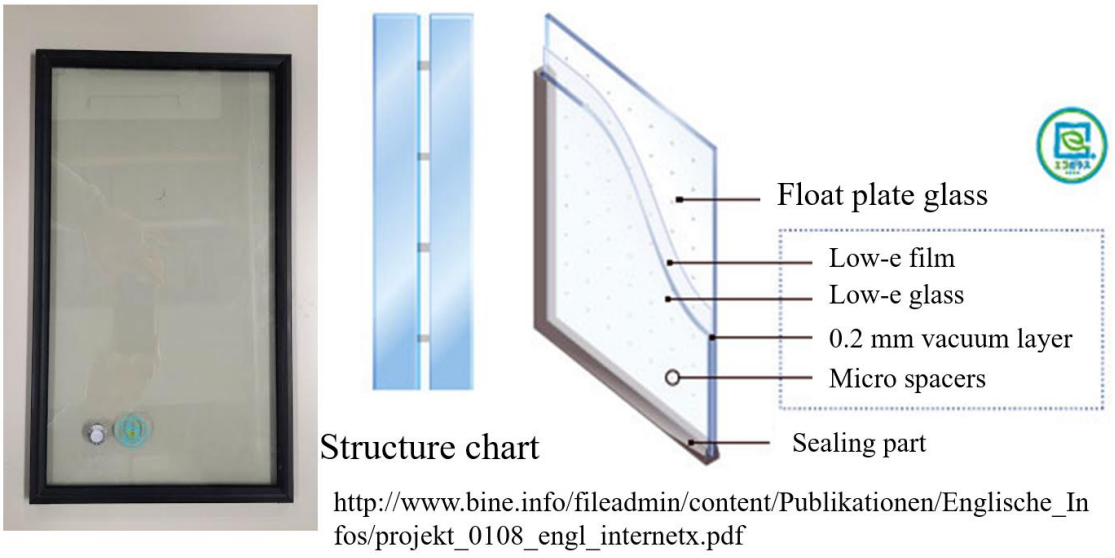

Figure 2-4 Concept diagram of structure for vacuum glazing

Table 2-3 Accumulation of articles (Vacuum glazing)

Authors	Title	Journal & volume	Year	Pillars radii	Thickness
H. Manz, S. Brunner, L. Wullschleger	Triple vacuum glazing: Heat transfer and basic mechanical design constraints	Solar Energy 80 (2006) 1632–1642	2006	＜0.25 mm	4mm, 6 mm
Yueping Fang, Philip C. Eames, Brian Norton	Effect of glass thickness on the thermal performance of evacuated glazing	Solar Energy 81 (2007) 395–404	2007	0.18 mm	6 mm
Yueping Fang, Trevor Hyde, Neil Hewitt, Philip C. Eames, Brian Norton	Thermal performance analysis of an electrochromic vacuum glazing with low emittance coatings	Solar Energy 84 (2010) 516–525	2010	0.18 mm	4 mm
P. W. GRIFFITHS, M. DI LEO, P. CARTWRIGHT, P. C. EAMES, P. YIANOULIS, G. LEFTHERIOTIS and B. NORTON	FABRICATION OF EVACUATED GLAZING AT LOW TEMPERATURE	Solar Energy Vol. 63, No. 4, pp. 243–249, 1998	1998	17.5 mm	4mm, 6 mm
Yueping Fang, Trevor J. Hyde, Neil Hewitt	Predicted thermal performance of triple vacuum glazing	Solar Energy 84 (2010) 2132–2139	2010	0.15 mm	4 mm
Saim Memon, Farukh Farukh, Philip C. Eames, Vadim V. Silberschmidt	A new low-temperature hermetic composite edge seal for the fabrication of triple vacuum glazing	Vacuum 120 (2015) 73-82	2015	0.15 mm	10 mm
Yueping Fang, Trevor J. Hyde, Farid Arya, Neil Hewitt, Ruzhu Wang, Yanjun Dai	Enhancing the thermal performance of triple vacuum glazing withlow-emittance coatings	Energy and Buildings 97 (2015) 186–195	2015	0.15 mm	6 mm
YuepingFang, TrevorHyde, NeilHewitt, PhilipC.Eames, BrianNorton	Comparison of vacuum glazing thermal performance predicted using two-and three dimensional models and their experimental validation	Solar Energy Materials & Solar Cells93 (2009)1492–1498	2009	0.15 mm	4mm, 6 mm
R. E. COLLINS, G. M. TURNER, A. C. FISCHER-CRIPPS, J.Z. TANG, T. M. SIMKO, C. J. DEY, D. A. CLUGSTON, Q.-C. ZHANG, J. D. GARRISON	Vacuum Glazing- A New Component for Insulating Windows	Building and Enaironmenf, Vol. 30. No. 4. pp. 459-492. 1995	1995	＜0.15 mm	＜6 mm

Vacuum glazing by R.E. Collins, a well investigated study which maintained a vacuum layer by using spacers. A vacuum glazing consists of an outer pane of low-emissivity glass and an inner pane of clear float, with a vacuum rather than air or another gas in between. Then, the durability of spacers is investigated and the material selection for spacers is discussed. R. E. Collins and Simko (1998) give a details description of the high insulation performance technique for vacuum glazing. According to their study, a Japanese company (Nippon Sheet Glass Co., 2005) developed a double layer vacuum glazing as a commercial product with "U" value in 1.5 $W/(m^2 \cdot K)$. Ulster studies the edge thermal conduction and sealing method to vacuum glazing (Griffiths et al., 1998). The Fraunhofer Institute for Solar Energy Systems developed a hermetic glazing edge seal for vacuum glazing based on a sputtered metallic layer and a soldering technique (Wittwer, 2005; Baechli, 1991; Baechli, 1992; Sager-Hintermann and Baechli, 2002). There studies above well investigate vacuum glazing and achieved good insulation performance to new constructions. However, the weight of vacuum glazing is so heavy that it's not good enough to insulation retrofit to existing buildings due to the additional construction cost.

So far, activities in the field of vacuum glazing have mainly focused on glazing with a single evacuated cavity. However, so-called hybrid insulating glazing units—triple glazing featuring both an evacuated and a gas-filled cavity—have been proposed and manufactured with the aim of cutting thermal transmittance (Asano et al., 1999). Units of this kind with thermal transmittances between 0.7 and 0.9 are now commercially available (Nippon Sheet Glass Co., 2005). Following publication of the review article by Collins and Simko (1998), several additional patent applications have been filed in relation to vacuum glazing in recent years. These, for example, cover manufacturing or processing methods (Veerasamy, 2000; Demars, 1999; Poix et al., 2001; Zhao and Zhao, 2002; Futagami et al., 2003) and techniques for applying a dry carbon lubricant between the pillars and glass surfaces in order to reduce scratching or cracking of the glass during temperature-induced relative movement (Collins and Tang, 2000). Very recently, a triple vacuum glazing employing thin wires in the cavities to support glass sheets was patented (Wuethrich, 2005). Collins and Simko (1998) suggested baking the glazing during the evacuation process at temperatures between 100 and 250 ℃ in order to remove gases from the internal surfaces. More recent work by Ng et al. (2003, 2005), and Minaai et al. (2005) has shown that higher temperatures (>350 ℃) during manufacture are needed to prevent a pressure increase when the glazing is exposed to sunlight. Despite the painstaking and promising efforts in the field of vacuum glazing, the thermal transmittances achieved by this glazing type still fail to meet the requirements of today's

advanced low-energy buildings. This study therefore sets out to investigate the theoretical potential of glazing with two evacuated cavities and support pillar arrays. As units with a second evacuated cavity can significantly improve on the thermal transmittance performance achieved by present triple glazing with inert gas filled cavities, the triple vacuum glazing concept holds considerable potential for low-energy building applications. The progress made in recent years in the fields of low-emittance coatings, materials and process technology has brightened the prospects of such an endeavour. This study uses analytical and numerical methods to identify suitable parameter sets for triple vacuum glazing, taking into account also the mechanical stresses due to atmospheric pressure.

2.8 Application of Vacuum insulation panels

Vacuum insulation panels (VIPs) are regarded as one of the most promising high performance thermal insulation solutions on the market today. Thermal performances three to six times better than still-air are achieved by applying a vacuum to an encapsulated micro-porous material, resulting in a great potential for combining the reduction of energy consumption in buildings with slim constructions. However, thermal bridging due to the panel envelope and degradation of thermal performance through time occurs with current technology. Furthermore, VIPs cannot be cut on site and the panels are fragile towards damaging. These effects have to be taken into account for building applications as they may diminish the overall usability and thermal performance. Vacuum Insulation Panels (VIPs) have already found application in some specialist applications where minimal energy consumption is important and space is at a premium. This paper investigates the feasibility of widespread application of VIPs in the cold chain by embedding them into the polyurethane (PU) foamed walls of traditional refrigerator and freezer cabinets. Although the largest application of the Vacuum insulation panels (VIPs) concerns the refrigeration industry (60%) and transport boxes (30%) and only a tiny amount is used in the building industry (10%), the number of scientific publications dealing with VIPs with regard to the latter dominate since more than a decade. The main topics addressed therein are the aging of the VIP as a whole as well as the role of the components, under different long term hygrothermal stress conditions. There is a clear expansion of VIP applications in buildings from primarily German speaking countries, toward Europe, and then to overseas. Recent years have witnessed an increasing confidence in this product among researchers and practitioners interested in energy efficient buildings worldwide [37-40].

Table 2-4 Accumulation of articles (Application)

Authors	Title	Journal & volume	Year	Method	Film	Thickness
Alfonso Capozzoli, Stefano Fantucci, Fabio Favoino and Marco Perino	Vacuum Insulation Panels: Analysis of the Thermal Performance of Both Single Panel and Multilayer Boards	Energies 2015, 8, 2528-2547	2015	Commericial product+wood joint combination	PE+Al(multilayerred)+PET	12-28 mm
S. Brunner, T. Stahl, K. Ghazi Wakili	An example of deteriorated vacuum insulation panels in a building façade	Energy and Buildings 54 (2012) 278–282	2012	The VIP panels (gray) are surrounded by an EPS hull which is 3 cm at the bottom and 1 cm on all the other sides.	0.1–20 microns coated aluminum	20-35 cm
P. Mukhopadhyaya, D. MacLean, J. Korn, D. van Reenen, S. Molleti	Building application and thermal performance of vacuum insulationpanels (VIPs) in Canadian subarctic climate	Energy and Buildings 85 (2014) 672–680	2014	On-site experiment, single layer between concrete and wall	Not focus	12 mm
Peyman Karami, Nadia Al-Ayish, Kjartan Gudmundsson	A comparative study of the environmental impact of Swedishresidential buildings with vacuum insulation panels	Energy and Buildings 109 (2015) 183–194	2015	Life cycle analysis in buildings with installing VIP (fumed silica core)	Not focus	Not focus
Francesco Isaia, Stefano Fantucci, Alfonso Capozzoli, Marco Perino	Vacuum Insulation Panels: thermal bridging effects and energy performance in real building applications	Energy Procedia 83 (2015) 269 – 278	2015	2D numerical analysis, discuss the VIP joint combination application performance	PET (12μm)*3+PE (50μm) + Sulfur dioxide core	15 cm
Alice Lorenzati, Stefano Fantucci, Alfonso Capozzoli, Marco Perino	Coupling VIPs and ABPs: assessment of overall thermal performance in building wall insulation	Energy Procedia 78 (2015) 2760 – 2765	2015	Show the influence of different joint material both considering the overall thermal performances and the economical aspects.	Not focus	Not focus

H. Sallée, D. Quenard, E. Valenti, M. Galan	VIP as thermal breaker for internal insulation system	Energy and Buildings 85 (2014) 631–637	2014	AVIP protected with PU foam and a finishing board. A mock-up has been built up in orderto investigate the efficiency of the thermal breaker for partition wall.	Not focus	53 mm
Jirí Zach, Vítezslav Novák	Study of the use of vacuum insulation as integrated thermal insulation in ceramic masonry blocks	Procedia Engineering 151 (2016) 206 – 213	2016	VIPs become integrated insulation, filling a block cavity with a VIP. Core (pyrogenic silica, defibred cotton)	Not focus	40 mm
Muhammad Abdul Mujeebu, Noman Ashraf, Abdulkarim H. Alsuwayigh	Effect of nano vacuum insulation panel and nanogel glazing on the energy performance of office building	Applied Energy 173 (2016) 141–151	2016	3D simulation model with solar incidence profile, analysis of energy performance	Not focus	50 mm
Taesub Lim, Jaewang Seok and Daeung Danny Kim	A Comparative Study of Energy Performance of Fumed Silica Vacuum Insulation Panels in an Apartment Building	Energies 2017, 10, 2000	2017	Fumes silica VIPs, eight combinations were compared to find the best energy efficient design conditions	Not focus	10, 17, 30 mm
Sihyun Park, Bo-Hye Choi, Jae-Han Lim and Seung-Yeong Song	Evaluation of Mechanically and Adhesively Fixed External Insulation Systems Using Vacuum Insulation Panels for High-Rise Apartment	Energies 2014, 7, 5764-5786	2014	Proposal comparisons and cost analysis, Core (fiberglass, fumed silica)	Metalized-film and aluminum-foil laminates	15-50 mm

2.9 Summary

The authors summarized article and discussed shown as Table 2-5, the studies of our development proposal will explain in the following content, and it's easy to understand that the authors developed vacuum insulation panels with thinner thickness, lighter weight, translucent and cost efficiency.

2.10 The present situation of research

Vacuum insulation panels were developed some time ago for use in appliances such as refrigerators and deep freezers. Their insulation performance is a factor of five to ten times better than that of conventional insulation. Used in buildings they enable thin, highly insulating constructions to be realized for walls, roof and floors.

The motivation for examining the applicability of high performance thermal insulation in buildings (i.e. evacuated insulation in the form of vacuum insulation panels) came from the difficulties involved in renovation — namely severe space limitations and therefore technical constraints, as well as from aesthetic considerations.

Investigations have been performed individually on the core materials and laminates designed for the envelope as well as manufactured VIP.

The introduction of such a novel insulation system in the building trade, however, is hampered by many open questions and risks. The work illustrates a wide selection of reports from practice, shows how the building trade deals with this new insulation system today, the experience gained and the constructions drawn there from. As well as presenting recommendations for the practical use of VIP, the report is also able to answer questions regarding the effective insulation values to be expected with today's VIP.

Table 2- 5 Discussion of conventional studies

	Conventional				Developed	
	Glass wool	Silica powder	Silica aerogel	Vacuum glazing	Pillars support	Frame
Thickness [mm]	15	20	6	8	6	4
Weight [kg/㎡]	6	45	0.05	16	6.8	2
Apparent thermal conductivity [mW/(m·K)]	4~5	4~5	2.5	1.2	7	5
Material cost	○	○	×	△	○	◎
Production difficulty	△	△	○	×	△	◎
Transparency	×	×	△	◎	◎	○

◎ Excellent, ○ Good, △ Adequate, × Not good

Reference:

[1] Nature Publishing Group. Architects of a low-energy future. Nature 2008, 452, 520–523

[2] Saari, A.; Kalamees, T.; Jokisalo, J.; Michelsson, R.; Alanne, K.; Kurnitski, J. Financial viability of energy-efficiency measures in a new detached house design in Finland. Appl. Energy 2012, 92, 76–83

[3] Lim, T.; Seok, J.; Kim, D.D. A Comparative Study of Energy Performance of Fumed Silica Vacuum Insulation Panels in an Apartment Building; Energies 2017, 10, 2000

[4] Capozzoli, A.; Fantucci, S.; Favoino, F.; Perino, M. Vacuum Insulation Panels: Analysis of the Thermal Performance of Both Single Panel and Multilayer Boards. Energies 2015, 8, 2528–2547

[5] Park, S.; Choi, B.-H.; Lim, J.-H.; Song, S.-Y. Evaluation of Mechanically and Adhesively Fixed External Insulation Systems Using Vacuum Insulation Panels for High-Rise Apartment Buildings. Energies 2014, 7, 5764–5786

[6] Collins, R.E.; Turner, G.M.; Fisher-Cripps, A.C. Vacuum Glazing—A New Component for Insulating Windows. Build. Environ. 1995, 30, 459–492.

[7] Fisher-Cripps, A.C.; Collins, R.E.; Turner, G.M.; Bezzel, E. Stress and Fracture Probability in Evacuated Glazing. Build. Environ. 1995, 30, 41–59.

[8] Garrison, J.D.; Collins, R.E. Manufacture and cost of Vacuum Glazing. Sol. Energy 1995, 55, 151–161.

[9] Turner, G.M.; Collins, R.E. Measurement of Heat flow through Vacuum Glazing at elevated Temperature. J. Heat Mass Transf. 1997, 40, 1437–1446.

[10] Lenzen, M.; Collins, R.E. Long-term Field Tests of Vacuum Glazing. Sol. Energy 1997, 61, 11–15.

[11] Collins, R.E.; Simko, T.M. Current Status of the Science and Technology of Vacuum Glazing. Sol. Energy 1998, 62, 189–213.

[12] Simko, T.M.; Fisher-Cripps, A.C.; Collins, R.E. Temperature-induced in Vacuum Glazing Modelling and Experimental Validation. Sol. Energy 1998, 63, 1–21.

[13] Collins, R.E., Simko, T.M., 1998. Current status of the science and technology of vacuum glazing. Solar Energy 62, 189–213.

[14] Nippon Sheet Glass Co., http://www.nsg-spacia.co.jp (retrieved 5/18/2005).

[15] Griffiths, P.W., Di Leo, M., Cartwright, P., Eames, P.C., Yianoulis, P., Leftheriotis, G., Norton, B., 1998. Fabrication of evacuated glazing at low temperature. Solar Energy 63, 243–249.

[16] Wittwer, V., Private communication. Fraunhofer Institute for Solar Energy Systems, Freiburg, Germany (2005-03-11).

[17] Baechli, E., 1991. Thermally insulating construction and/or lighting element. European Patent No. 0247098B1.

[18] Baechli, E., 1992. Gastight edge seal. European Patent No. 0434802B1.

[19] IEA source, Directive of the European Parliament and The Council on the energy performance of buildings.

[20] M. Knudsen: Die molekulare Wärmeleitung der Gase und der Akkommodationskoef fizient. Annalen der Physik IV. Folge 34, 593--656 (1911).

[21] Handbook of Vacuum Technology (1st Edition), Edited by Karl Jousten, (2008) pp. 51–81.

[22] Lim, T.; Seok, J.; Kim, D.D. A Comparative Study of Energy Performance of Fumed Silica Vacuum Insulation Panels in an Apartment Building; Energies 2017, 10, 2000
[23] Capozzoli, A.; Fantucci, S.; Favoino, F.; Perino, M. Vacuum Insulation Panels: Analysis of the Thermal Performance of Both Single Panel and Multilayer Boards. Energies 2015, 8, 2528–2547
[24] Park, S.; Choi, B.-H.; Lim, J.-H.; Song, S.-Y. Evaluation of Mechanically and Adhesively Fixed External Insulation Systems Using Vacuum Insulation Panels for High-Rise Apartment Buildings. Energies 2014, 7, 5764–5786
[25] Collins, R.E.; Turner, G.M.; Fisher-Cripps, A.C. Vacuum Glazing—A New Component for Insulating Windows. Build. Environ. 1995, 30, 459–492.
[26] Fisher-Cripps, A.C.; Collins, R.E.; Turner, G.M.; Bezzel, E. Stress and Fracture Probability in Evacuated Glazing. Build. Environ. 1995, 30, 41–59.
[27] Garrison, J.D.; Collins, R.E. Manufacture and cost of Vacuum Glazing. Sol. Energy 1995, 55, 151–161.
[28] Turner, G.M.; Collins, R.E. Measurement of Heat flow through Vacuum Glazing at elevated Temperature. J. Heat Mass Transf. 1997, 40, 1437–1446.
[29] Jongmin Kim, Choonghyo Jang, Tea-Ho Song: Combined heat transfer in multi-layer radiation shields for vacuum insulation panels: Theoretical/numerical analysis and experiment, Applied Energy, Volume 94, pp. 295–302 (2012)
[30] Jea-Sung Kwon, Choonghyo Jang, Heayong Jung, Tea-Ho Song: Vacuum maintenance in vacuum insulation panels exemplified with a staggered beam VIP, Energy and Buildings, Volume. 42, Issues 5, pp. 590–597 (2010)
[31] Mathias Bouquerel, Thierry Duforestel, Dominique Baillis, Gilles Rusaouen: Heat transfer modelling in vacuum insulation panels containing nanoporous silica-A review, Energy and Buildings, Volume 54, pp. 320–336 (2012)
[32] Jae-Sung Kwon, Choonghyo Jang, Haeyong Jung, Tae-Ho Song: Effective thermal conductivity of various filling materials for vacuum insulation panels, International Journal of Heat and Mass Transfer, Volume 52, Issues 23–24, pp. 5525–5532 (2009)
[33] Pär Johanssonn, Bijan Adl-Zarrabi, Carl-Eric Hagentoft, Using transient plane source sensor for determination of thermal properties of vacuum insulation panels, Frontiers of Architectural Research, Volume 1, Issues 4, pp. 334–340 (2012)
[34] H. Schwab, U. Heinemann, A. Beck, H.P. Ebert, J. Fricke, Dependence of thermal conductivity on water content in vacuum insulation panels with fumed silica kernels, Journal of Thermal Envelope and Building Science, 28 (2005), pp. 319-326
[35] X.B. Di, Y.G. Gao, C.G. Bao, Y.N. Hu, Z.G. Xie, Optimization of glass fiber based core materials for vacuum insulation panels with laminated aluminum foils as envelopes, Vacuum, 97 (2013), pp. 55-59
[36] IEA source, Directive of the European Parliament and The Council on the energy performance of buildings.
[37] Baechli, E., 1992. Gastight edge seal. European Patent No. 0434802B1.
[38] Sager-Hintermann, K., Baechli, E., 2002. Method and equipment for making heat-insulating construction and/or lighting elements. European Patent No. 1221526.
[39] H. Manz, S. Brunner, L. Wullschleger; Triple vacuum glazing: Heat transfer and basic mechanical design constraints; Solar Energy 80 (2006) 1632–1642

[40] SamuelBrunner, KarimGhazi Wakili, Thomas Stahl, BrunoBinder; Energy and Buildings, Volume 85, December 2014, Pages 592-596

Chapter 3
Design of translucent vacuum layer type vacuum insulation panels by pillars support

3.1 Introduction

The authors are developing slim and light-weight vacuum insulation panels (VIPs) by producing vacuum layers with spacers and plastic plates. The developed VIPs have the advantages of a low cost and easy installation in existing buildings. In addition, one of the developed VIPs is slim and translucent so that it can be easily used for windows. In this paper, first, the authors propose a vacuum layer type slim translucent VIP and focus on a reasonable design method. Next, the authors introduce the design process in which the structural design is obtained with element mechanical analysis and a three-dimensional analysis is conducted for the VIP element. In the study, a heat transfer model is used to predict the insulation performance through numerical analysis. Subsequently, the authors perform an experiment to measure the thermal conductivity to validate the performance prediction. Finally, case studies are performed to confirm how the different design conditions affect the insulation performance. The optimum design of the vacuum layer type slim and translucent VIP will have sufficient structural strength to hold and maintain the vacuum layer. The thermal conductivity is approximately 0.007 $W/(m \cdot K)$ that can effectively improve the insulation performance in applications.

The guarded hot plate (GHP) method is considered because it is a satisfactory method for measuring very low thermal conductivities [1]. In particular, a vacuum GHP (VGHP) apparatus is manufactured to eliminate the residual gas conduction. A VGHP can maintain a high vacuum level (below 10−4 Pa), leading to effective measurement of thermal conductivities.

The authors developed a new model of a VIP that is thin and translucent and can be easily installed in buildings including even the windows, as illustrated in Figure 3-1. This VIP model consisted of two plates with a low-e film coating achieved using a gas barrier film, whereas the vacuum layer was supported by plastic spacers. In this paper, the heat transfer calculation model for the above VIP is described and the calculation conditions are summarized to divide how strong the condition affect the insulation performance of VIPs. The calculated results are summarized and compared with each other. Subsequently, in the study, an experiment is conducted to measure the heat flux of the VIP samples and the results are compared with the calculated results. Finally, the insulation performance of the proposed VIP is discussed. In the study, Finite Element Analysis (FEA) is applied for predicting the heat transfer coefficient and thermal transmittance of the VIP under different conditions. A comparison of the insulation performance of the VIP with the

different conditions is presented, and a standard calculation model is considered as the representative reference object for comparison.

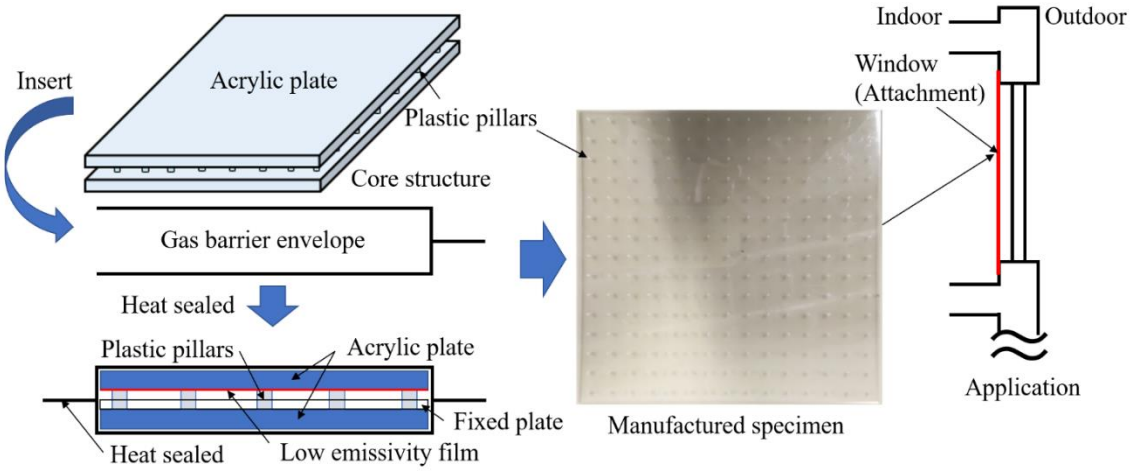

Figure 3-1 Concept diagram of the VIP application to buildings

3.2 Mechanical analysis to design the assembly of components

In this section, to determine the reasonable size of the VIP design, the authors discussed the stress analysis and the calculated maximum deflection. If the loading condition applied to the panel in the form of a distributed air compression is the same throughout as shown in Figure 3-2(A), mechanical analysis as depicted in Figure 3-2(B) [16], [17] will have to be conducted. The structural calculation model can be applied for calculating two possibilities, and Figure 3-3 shows the schematic of the calculation model.

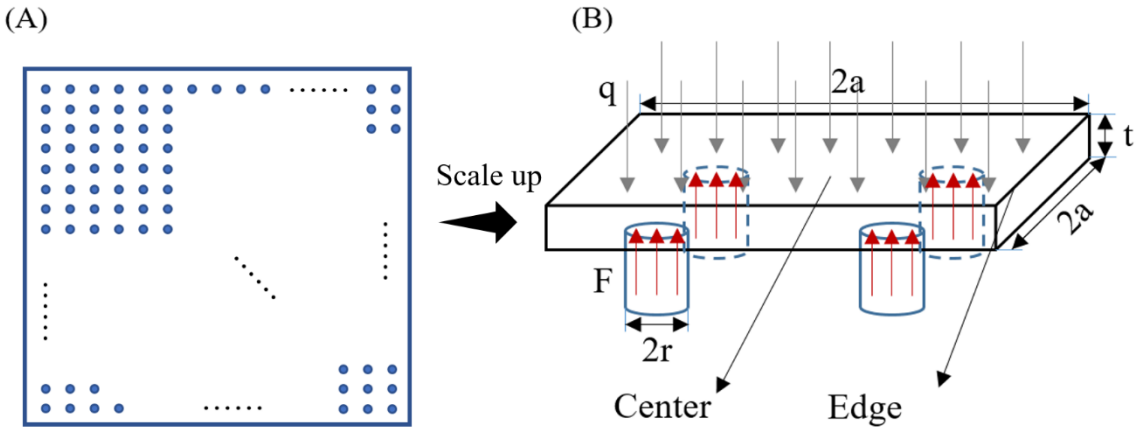

Figure 3-2 Outline of the mechanical analysis of the VIP

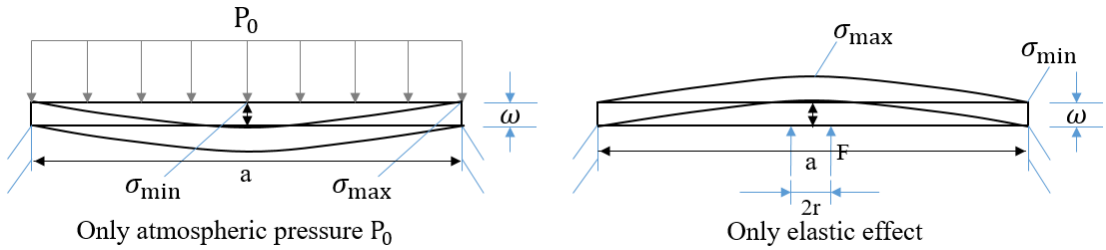

Figure 3-3 Schematic of the calculation model

In this calculation model, when the effective load is applied only through atmospheric pressure, maximum stress occurs in the center of the plate, whereas the minimum stress is on the edge. However, when only the elastic effect is present, the scenario is opposite to the above case, and hence, the stress direction is the reverse of the overall mechanical analysis. In this section, we define the relationship between the deflection and span (between the two spacer supports) by using the equations provided below.

$$\bar{\omega}_{max} = \delta \times \frac{P_0 \times a^4}{D} \tag{1}$$

$$D = \frac{E {d_p}^3}{12(1-\mu^2)} \tag{2}$$

For the acrylic plate, here, E is the elasticity modulus (= 3.2 GPa) and μ is the Poisson's ratio (= 0.35) [-]. In this model, thickness of the acrylic plate d_p = 1 mm, span a = 1 mm, δ_1 = 0.0138 [-] (coefficient when the rectangular flat plate is functioned by a uniform load, δ_2= 0.0611 [-] (coefficient when the rectangular flat plate is functioned by a uniform load) and effect in different stresses, and P_0 = 1013 [hPa]. Figure 3-4 shows the maximum deflection of the acrylic plate (both sides: the front and back) with the spacers in different spans.

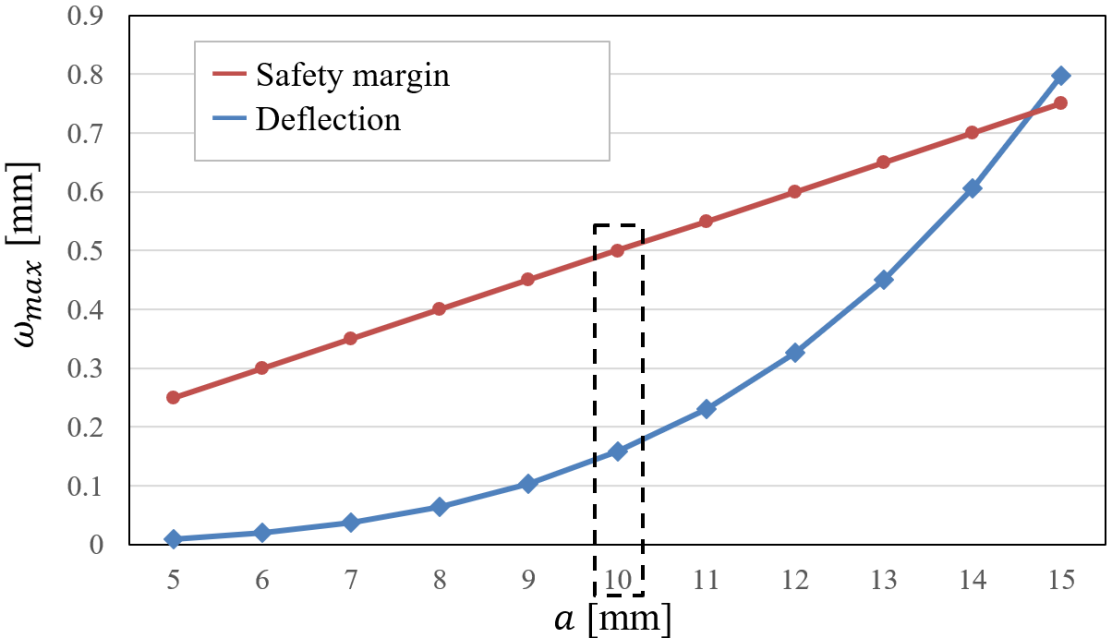

Figure 3-4 Calculation results of the maximum deflections at different spans

Figure 3-4 indicates that every designable load element can hold the vacuum layer within in the safety margin requirement for a mechanical design. To obtain and hold the vacuum layer, the authors decide the span of the spacers as 10 mm with an overall consideration of the stress affect and safety margin to ensure the application of the heat transfer model and specimen in the trial manufacture for experiment. The result ensured not only the formation of vacuum layer but also the surface can be maintained a relative flat.

Subsequently, to confirm the structural design, the authors also generate a 3-D model using the simulation software, ANSYS workbench. The distribution of the total deformation for the VIP element that is modelled in Figure 3-2 (B) is shown in Figure 3-6. The fixed boundary condition indicates the element analysis is reasonable to a full-size VIP and the meshing in Figure 3-5 shows the calculation result is pretty accuracy due to the totally 14039 nodes and 2808 elements. The result can well validate the mechanical analysis, indicating the structural design is reasonable to hold the vacuum layer and sufficiently flat for the application.

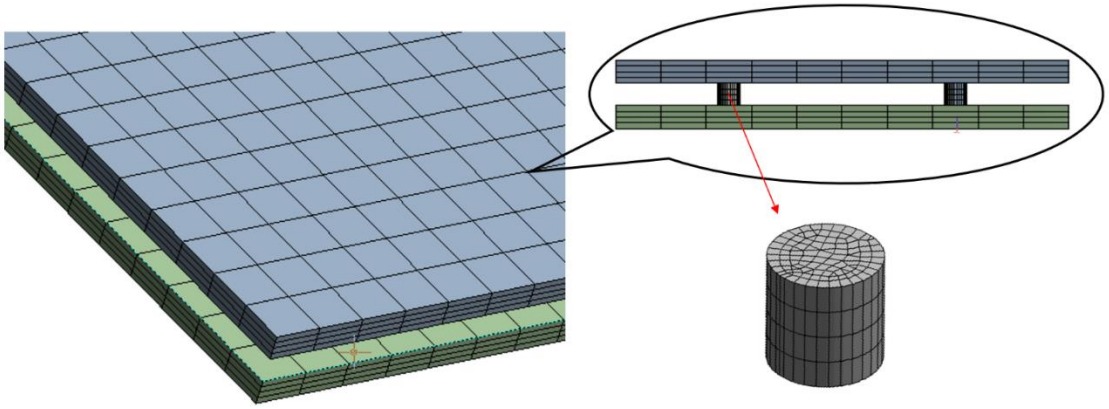

Figure 3-5 Meshing in finite element analysis (3-D)

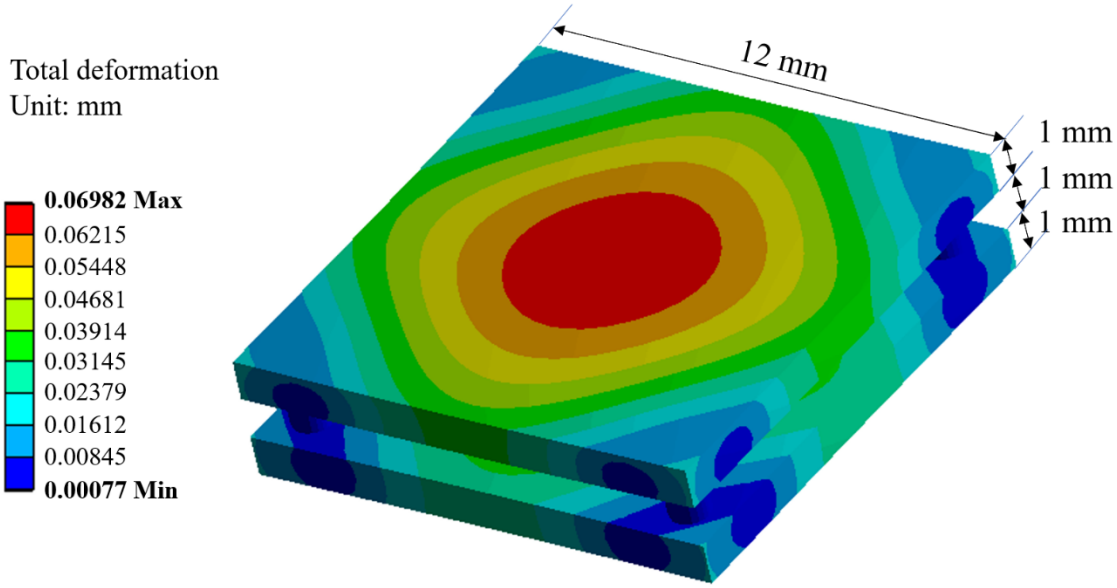

Figure 3-6 Total deformation in a VIP element (3D)

3.3 Framework of heat transfer calculation model

3.3.1 1-D heat transfer calculation model

Figure 3-7 presents the concept diagram of the 1 D calculation model. The plan (left) shows the model in 15cm×15cm, the element can be pick up as a analysis model in the Figure 3-7 (right). The calculation focus on solving the radiation and conduction through the double plate unit.

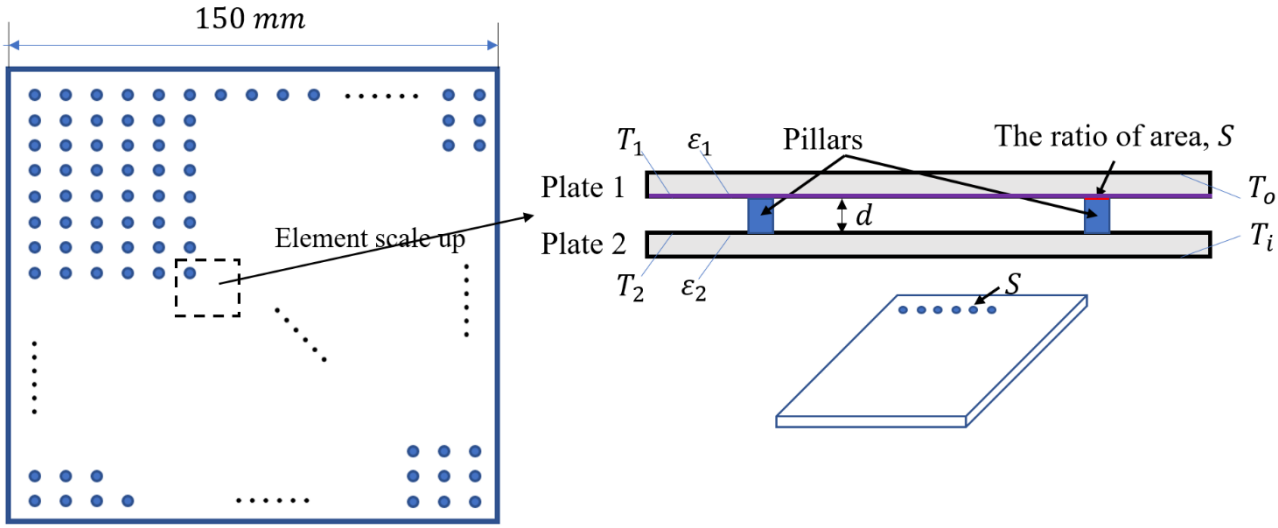

Figure 3-7 One-dimensional calculation model of VIP

The heat transmittance includes the radiant heat transfer in the vacuum space and conduction in the external surface and spacers. In this model, the heat transfer in the vacuum space is calculated as thermal resistance $R_a\,[(m^2 \cdot K)/W]$. When the spacers have ratio of area "S" between the two plates, thermal resistance $R_a\,[(m^2 \cdot K)/W]$ can be expressed as below.

$$R_a = \frac{1}{\left(\frac{\lambda_v}{d_v} + \alpha_r\right)(1-s) + \frac{\lambda_s}{d_v} s} \tag{3}$$

Radiant heat transfer α_r is calculated by the following equation:

$$\alpha_r = \varepsilon_1 \varepsilon_2 c_b \left\{ \left(\frac{T_1}{100}\right)^4 - \left(\frac{T_2}{100}\right)^4 \right\} \frac{1}{(T_1 - T_2)} \tag{4}$$

Thermal conductivity of vacuum layer λ_v is calculated by the following equations:

$$\lambda_v = 18.2 d \frac{\gamma + 1}{\gamma - 1} \frac{\beta p}{\sqrt{MT}} \tag{5}$$

$$\sqrt{\mathrm{T}} \cong \frac{2}{\sqrt{\mathrm{T}_1} + \sqrt{\mathrm{T}_2}} \tag{6}$$

The equations above can be derived by conductive heat transfer in free-molecular-state below:

$$Q_c = 18.2A\frac{\gamma+1}{\gamma-1}\frac{\beta P}{\sqrt{MT}}(T_1 - T_2) \quad (7)$$

From equations (1) – (3) and the following equation, the apparent thermal conductivity of the vacuum layer including the spacer is calculated.

$$\lambda_a = d_v / R_a \quad (8)$$

Here, λ_v is the thermal conductivity of the vacuum layer $[W/(m \cdot K)]$, λ_s is the thermal conductivity of the spacer $[W/(m \cdot K)]$, α is the radiant heat transfer $[W/(m^2 \cdot K)]$, d is the thickness of the vacuum layer $[m]$, ε_1 and ε_2 are the emittances of Plate 1 and Plate 2, respectively [-], C_b is a constant of radiance $[W/(m^2 \cdot K^4)]$, T_1 and T_2 are the surface temperatures of Plate 1 and Plate 2, respectively $[K]$, γ is the specific heat ratio c_p/c_v [-], and β is the accommodation coefficient.

3.3.2 Numerical model for heat transfer calculation

The analytical solution of the heat transfer through a VIP can be derived from a double plate unit [18]. Figure 3-8 (a) illustrates the heat transfer through a double plate unit, and Figure 3-8 (b) illustrates the schematics of thermal resistance of a double plate unit. The overall heat transfer coefficient can be obtained according this model. The heat transmittance of the VIP can ignore the convection in the vacuum space, and this will be explained in the following part.

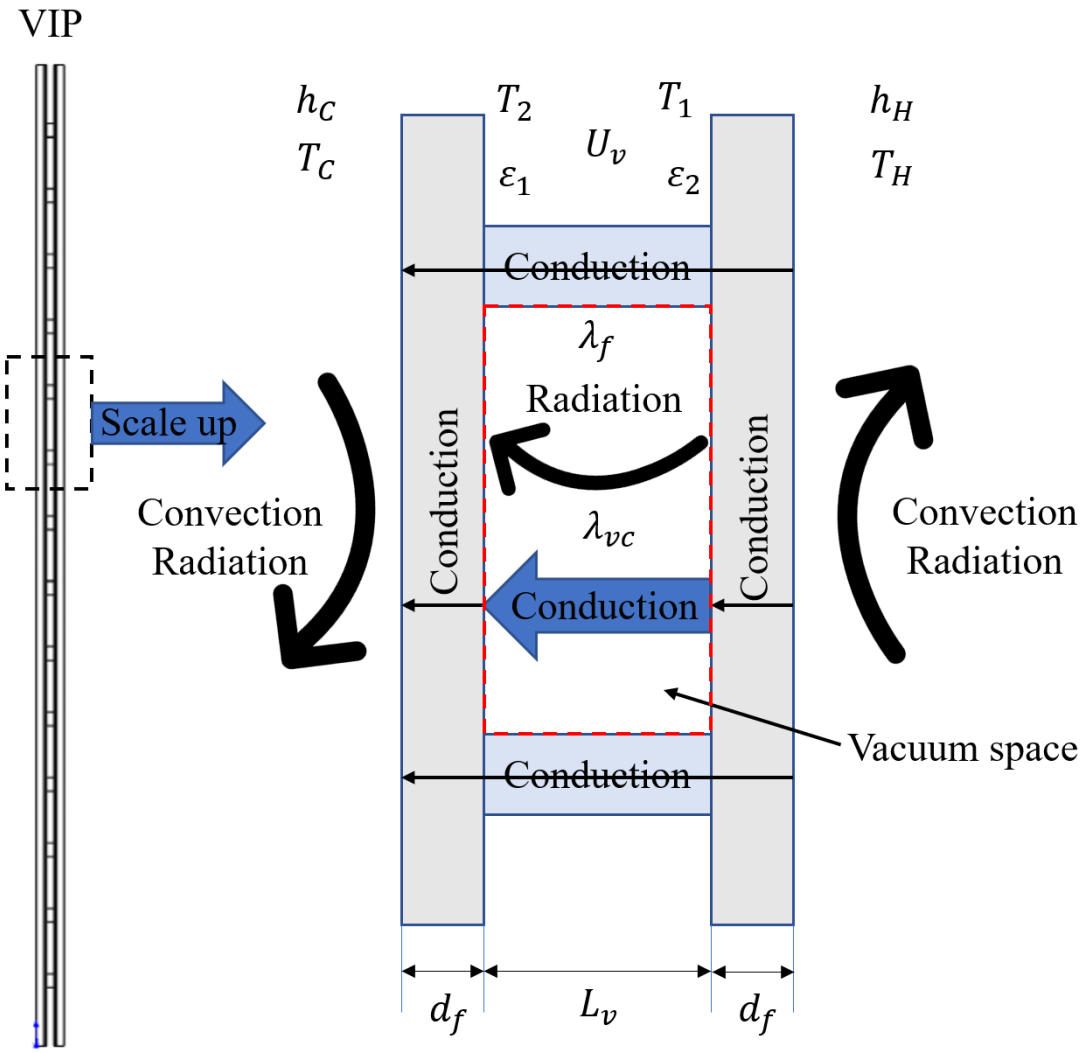

Figure 3-8 (a) Schematic of heat transfer through a double plate unit

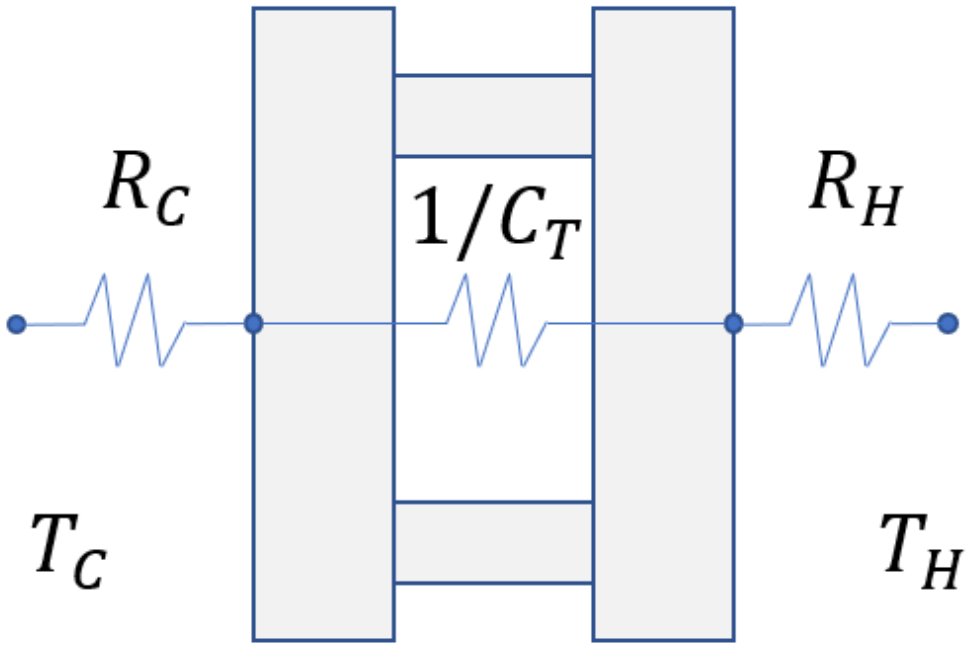

Figure 3-8 (b) Schematic of thermal resistance for a double plate unit

Calculation and design of the vacuum layer

At a constant pressure or at the vacuum state, the mass and density will be different in each part owing to the inhomogeneous temperature distribution. The density differing parts will have a relative motion affected by the same gravity, and the heat transmission occurs through the motion. Along with the different vacuums, different fluids and flow states, shapes of the heat transfer surface, and different positions of the hot and cold surface, the power of the free convective heat transfer will also be different. Numerous experimental studies show that the free convection can be converted into a pure gas heat conduction. When the equation below is established, the free convection can be converted into pure gas heat conduction.

$$G_{rm} \times P_{rm} < 10^3 \tag{9}$$

Here, P_{rm} is the Prandtl number. For air, nitrogen, and helium, P_{rm}= 0.7. G_{rm} is the Grashof number.

$$G_{rm} = \frac{g\beta\Delta T {L_v}^3}{\upsilon^2} \tag{10}$$

Here, g is the gravity acceleration [m/s^2], β is the coefficient of expansion [1/K], and β can be described by the following equation [21].

$$\beta = \frac{1}{\gamma}\left(\frac{\partial V}{\partial T}\right) P_b^2 \tag{11}$$

Here, P_b is the pressure ratio, such that $P_b = P/P_0$; P is the vacuum pressure, [Pa]; P_0 is the atmospheric pressure, [Pa]; ΔT is the temperature difference between the cold and hot surface, $[K]$ L_v is the thickness of the vacuum layer, $[m]$; and v is the kinematic viscosity, $[m^2/s]$. Here, $g = 9.8$ $[m/s^2]$, $L_v = 10^{-3}$ [m], $\Delta T = 25$ [K], $v = 1.323 \times 10^{-5}$ $[m^2/s]$, and the assumed value of vacuum pressure $P = 1000$ [Pa].

Therefore, $G_{rm} \approx 2.085 \times 10^6 \left(\frac{10^3}{10^5}\right)^2 = 2.085 \times 10^2 < 10^3$, and this result shows that convection can transform into pure gas conduction in this model if the pressure is less than 1000 Pa.

To achieve a lower thermal conductivity, the VIP with a vacuum layer between 0.1 Pa and 1 Pa will be calculated under the conditions. For a pressure of 0.1 Pa and 1 Pa, the convection can convert to pure gas conduction naturally, and therefore, the convection can be ignored in the calculation.

Generally, for the analysis of the heat conduction of gases in an adiabatic space, the evaluation behavior to separate the air flow is defined by using the *Knudsen Number* K_n. A high *Knudsen number* indicates a low pressure, and thus, a slow molecular flow; whereas a low value of the Knudsen number suggests a viscous flow. Then, the rarefied gas heat conduction in the different states can be decided by evaluating the *Knudsen number* as defined in equations (12) and (13) [19].

$$K_n = \frac{l}{L_v} \tag{12}$$

$$l = \frac{kT}{\sqrt{2}\pi d^2 P} \tag{13}$$

Here, l is the mean free path of air, [m]; L_v is the thickness of the vacuum layer, [m]; k is the Boltzmann constant, [J/K]; T is the temperature, [K]; d is the molecular diameter, [m]; and P is the pressure, [Pa].

In this paper, temperature $T = 300\,[K]$, $k = 1.38 \times 10^{-23}$ [J/K], and molecular diameter $d = 0.37\,[nm]$. Then, equation (7) can be expressed as $l = 6.8 \times 10^{-3}/P$. Assumed thickness of the vacuum layer $L_v = 1$ mm; therefore, the *Knudsen number* is 68, 6.8, and 0.68 when the pressure is 0.1 Pa, 1 Pa, and 10 Pa, respectively. Only if *Knudsen number* $K_n \geq 0.5$, the rarefied gas heat conduction is in the free molecular state.

Then, the calculation of the vacuum layer can be decided and the detailed equations will be discussed in the next section.

Establishment of heat transfer calculation model

Firstly, the calculation flow in Figure 3-9 shows the derivation of heat transmittance:

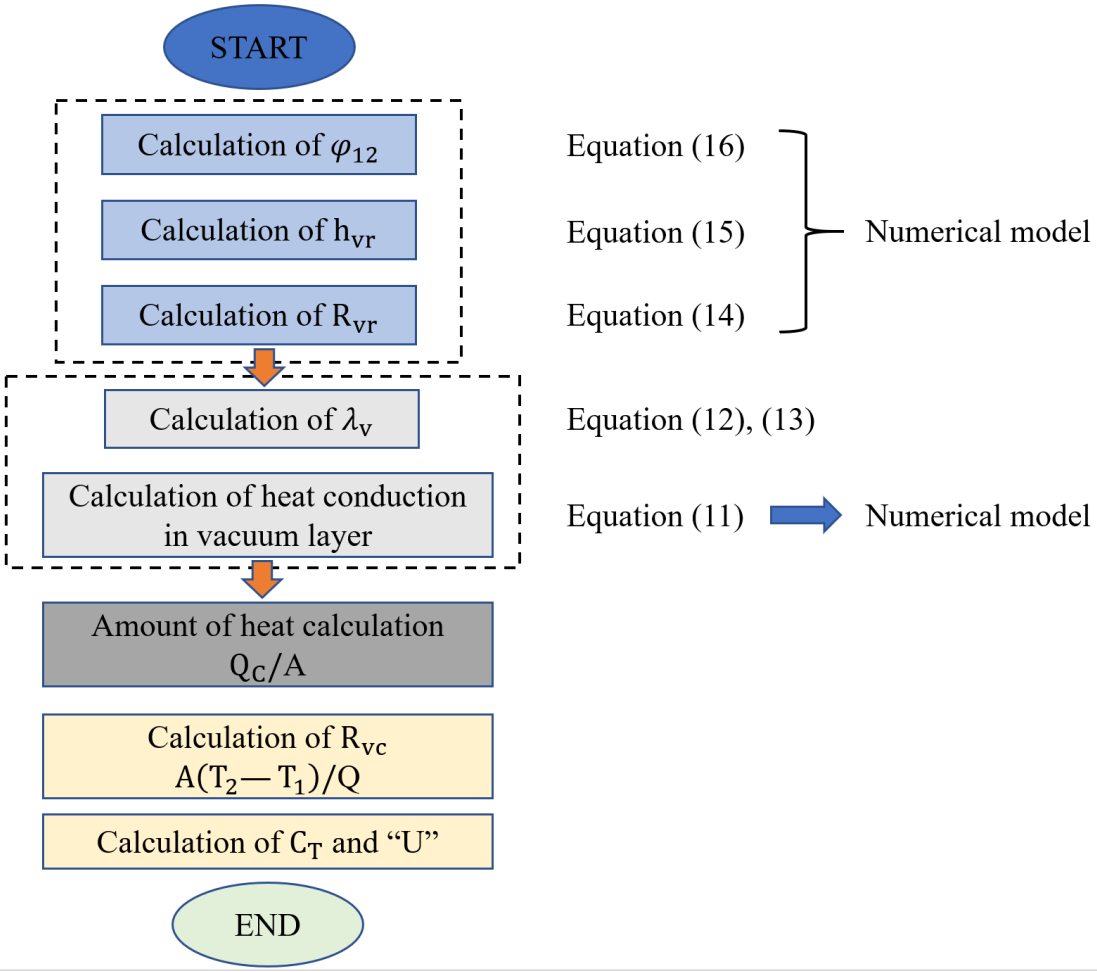

Figure 3-9 Flow of derivation for heat transmittance

The overall heat transfer coefficient of a VIP is defined by the following equations [14] [15]:

$$U = \frac{1}{R_C + 1/C_T + R_H} \tag{14}$$

Here, U is the overall heat transfer coefficient $[W/(m^2 \cdot K)]$, R_C and R_H are the thermal resistances of the cool temperature and hot temperature sides $[(m^2 \cdot K)/W]$, respectively, and C_T is the conductance of vacuum insulation panel unit $[W/(m^2 \cdot K)]$.

$$C_T = \frac{1}{U_v} + 2\frac{d_p}{\lambda_p} \tag{15}$$

Here, U_v is the overall heat transfer coefficient between a vacuum space $[W/(m^2 \cdot K)]$, d_p is the total thickness of the acrylic plate [m]; and λ_p is the thermal conductivity of the acrylic plate $[W/m \cdot K)]$. The value of U_v is calculated based on two parts, namely, the heat transfer in the vacuum space and in the spacers.

$$U_v = \frac{1}{R_{vc} + R_{vr}} \tag{16}$$

Here, R_{vc} and R_{vr} are the thermal resistances of the conduction and radiation in the vacuum space $[W/(m^2 \cdot K)]$. In the vacuum space, the total heat transfer can be calculated by conduction and radiation.

$$\frac{\partial^2 T}{\partial x^2} + \frac{\partial^2 T}{\partial y^2} + \frac{\partial^2 T}{\partial z^2} = 0 \tag{17}$$

Conduction can be calculated by the above equation, and it is considered that the heat transfer in the spacer is only the conductive heat transfer. The equation is the same as equation above. In this calculation, thermal conductivity of the vacuum space λ_v is a constant, and the thermal conductivity of the vacuum layer λ_v is calculated by the equation below: [22]

$$\lambda_v = 18.2 L_v \frac{\gamma + 1}{\gamma - 1} \frac{\beta_0 P}{\sqrt{MT}} \tag{18}$$

$$\frac{1}{\sqrt{T}} \cong \frac{2}{\sqrt{T_1} + \sqrt{T_2}} \tag{19}$$

Here, γ is the specific heat ratio, C_p/ C_v [-] is specific heat ratio, and β is the accommodation coefficient. The radiant heat transfer in the vacuum space is calculated by the equations below:

$$R_{vr} = \frac{1}{h_{vr}} \tag{20}$$

$$h_{vr} = \sigma T_m^3 (\varepsilon_1 - \varepsilon_2) \varphi_{1,2} \tag{21}$$

Here, σ is the Stefan–Boltzmann constant [$5.67 \times 10^{-8}\ W/(m^2K^4)$], ε_1 and ε_2 are the corrected emissivities of the two plates of the VIP at mean temperature T_m[K], and $\varphi_{1,2}$ is the angle factor between the two plates of the VIP and can be calculated by the following equation:

$$\varphi_{1,2} = \frac{1}{A_2}\int_{A_1}\int_{A_2} \frac{cos\,\theta_1\, cos\,\theta_2}{\pi r^2}\delta_{12}\, dA_1 dA_2 \tag{22}$$

Here, δ_{12} is determined by the visibility of dA_2 to dA_1; $\delta_{12} = 1$ if dA_2 is visible to dA_1 and 0 otherwise.

3.4 Validation of numerical model by comparing with experimental results

3.4.1 VIP production and its cost performance evaluation

The VIP test specimen is produced as per the flow in Figure 3-9. The components are installed to a core structure initially and a low-e film is covered on the surface of core structure then inserted to a transparent gas barrier envelope. In order to prevent degradation with time, calcium oxide getter is sealed together with the core material. The getter absorbs gas and effectively prevents performance degradation. For the evacuated insulation material, the air tightness is critical and the components of the gas barrier film are depicted in Figure 3-11 (a), and the airtightness for oxygen and water vapor are depicted in Figure 3-11 (b). There' re 3 reasonable transparent evacuated insulation products, silica aerogel core material VIP, vacuum glazing and the VIP we developed. For the economic considerations to retrofitting insulation to existing buildings, a reasonable product also required a good cost-performance, the Figure 3-12 shows the comparison of the industrial manufacture cost of these 3 insulation products.

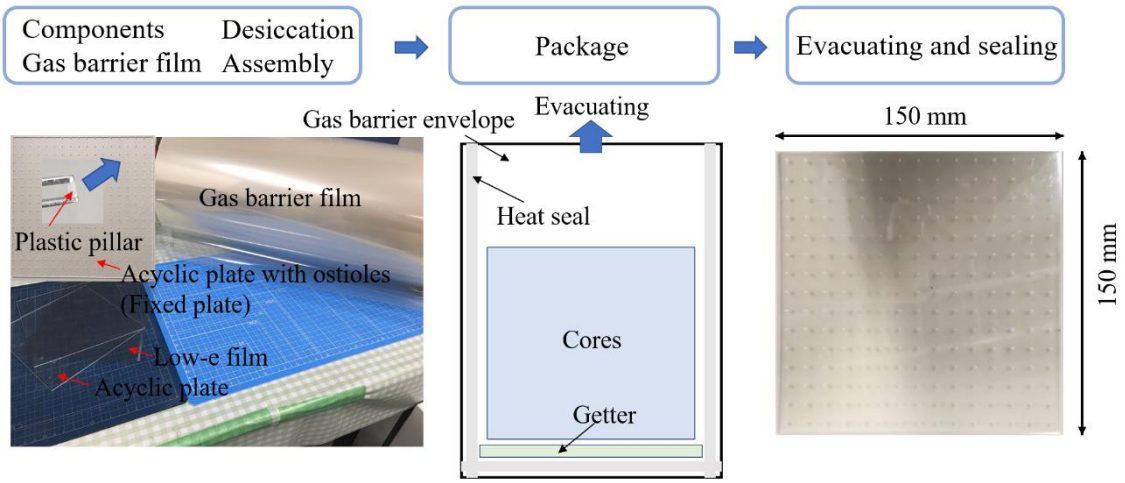

Figure 3-10 Manufacturing flow of the VIP specimens

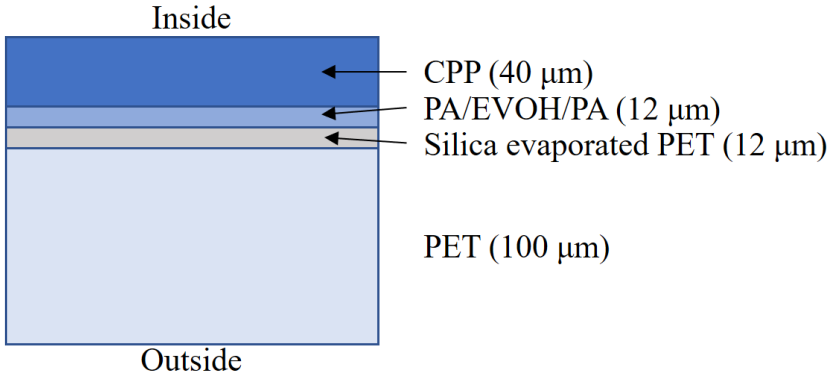

CPP: Cast Poly Polypropylene
PA: Polyamide

Figure 3-11 (a) Component diagram of the gas barrier film

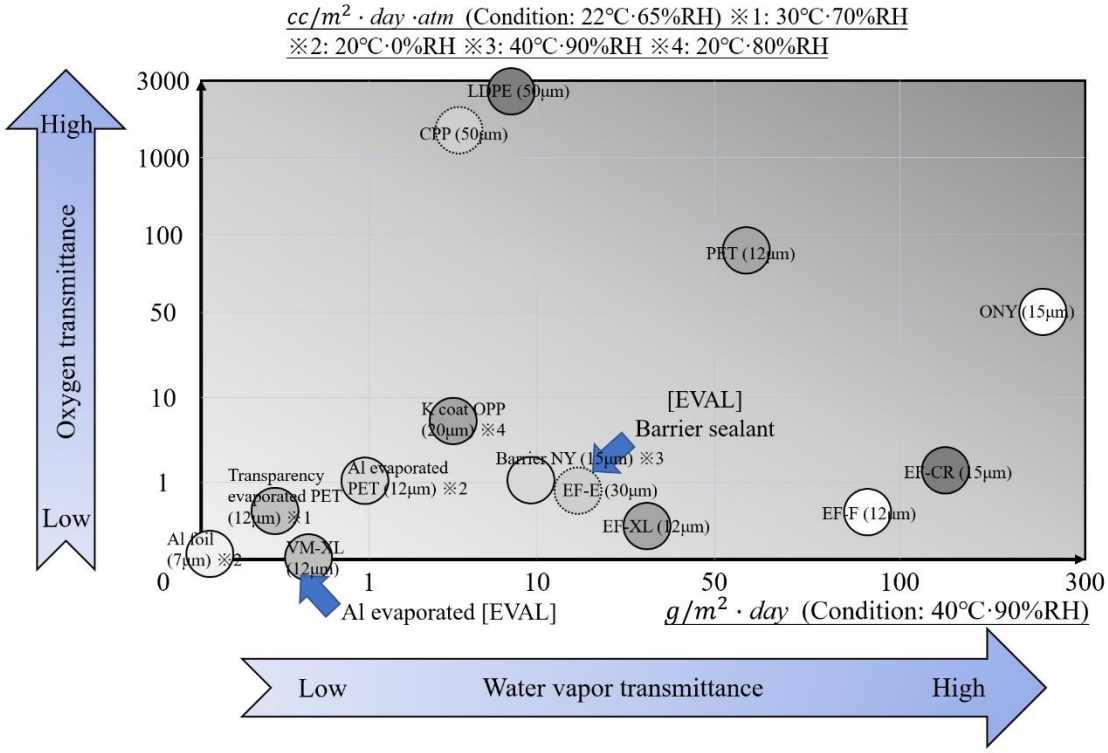

Figure 3-12 (b) Gas barrier performance of different materials

Silica aerogel core material VIP

Vacuum glazing

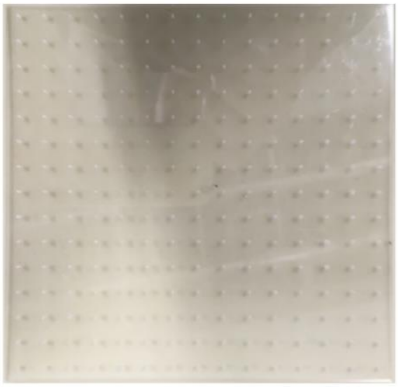

VIP in this study

Products	Industrial production Cost [JPY/㎡]
Silica aerogel core material VIP	> 500,000
Vacuum glazing	> 30,000 (+ 10,000 construction fee)
VIP in this study	< 11,000

Figure 3-13 Industrial manufacture cost of transparent evacuated insulation products

3.4.2 Framework of guarded hot plate apparatus

The measurement tools allow the determination of the thermal conductivity and thermal resistance of homogenous plates and inhomogeneous test specimens, if the specimens are plane and plate-shaped. The test specimens are installed between the heating and cooling plates. A constant heat flow flows through the test specimens in the stationary temperature state. The thermal conductivity is determined by the heat flow, mean temperature difference between the sample surfaces, and dimensions of the samples. In the steady state, the thermal conductivity of the specimen (λ) is derived by the equation as

$$\lambda = \frac{Q/2A}{\Delta T/\left(L_v + 2d_p\right)} \tag{23}$$

Here, Q [W] is the average electric power to the main hot plate, A [m^2] is area of the main hot plate, ΔT [℃] is the temperature difference of the specimen surface, and l [m] is average thickness of the specimen. Figure 3-14 shows the schematic of the GHP apparatus. The Pt-100 is applied to measuring the thermal conductivity as temperature sensors which the accuracy should be $\pm|0.15 + 0.002(t)|$. And there are 10 temperature sensors in the hot plate and 5 in the cold plate and set in different directions.

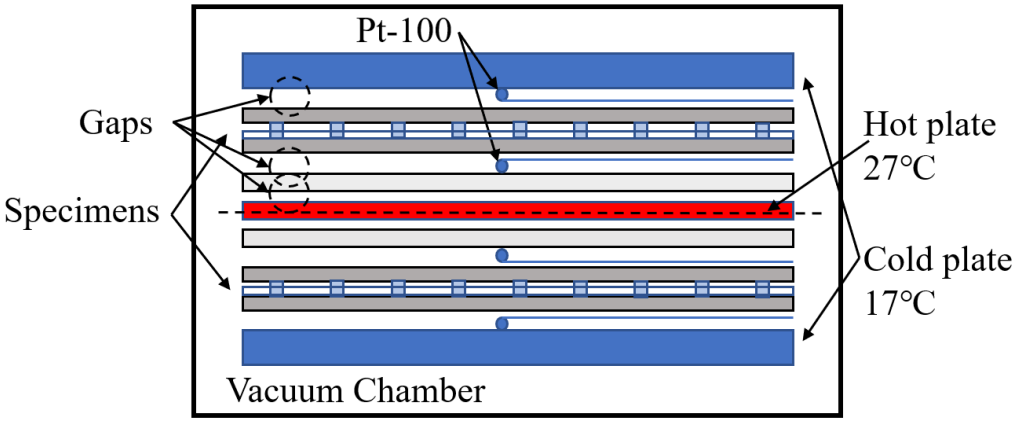

Figure 3-14 Schematic of the guarded hot plate apparatus

3.4.3 Frameworks of VIP specimen for GHP method and its calculation conditions and result

Figure 3-15 shows the concept diagram of the VIP test specimens and models of the case study. In the GHP experiment, the specimen is pressed by hot and cold plates, and the pressure in the chamber is reduced to 0.1 Pa and 1 Pa, respectively. Figure 3-14 shows

the comparison of the thermal conductivities obtained from the calculation and experimental result based on the pressure.

An element of the VIP is selected to represent the calculation conditions. The calculation conditions and specific size of the VIP for the standard model are also depicted in Figure 3-13. In this calculation, the thermal conductivities of the plastic cylinder (pillar) spacer, acrylic plate, and vacuum layer are 0.3 $[W/(m \cdot K)]$, 0.2 $[W/(m \cdot K)]$, and 0.106 $[mW/(m \cdot K)]$ (the thermal conductivity can be calculated by equation (12)) [19],[22] , respectively, and the thermal emissivities of the acrylic plate and low-e film are 0.9 and 0.3, respectively. The temperature difference for the calculation is 25 °C.

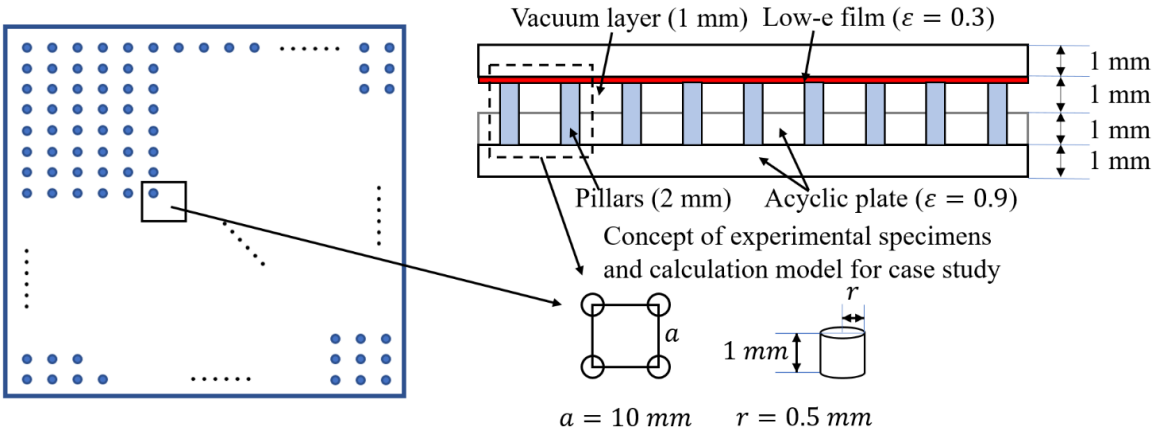

Figure 3-15 Concept diagram of the VIP specimen and model for the case study

There exist some influence factors in this experiment, particularly, the gaps between the hot and cold plates and the specimens. Therefore, the experiment result can be calculated by equation (15) to eliminate the influence of the gaps. In this experiment apparatus, the gaps are in the vacuum environment that is between the cold plate and specimen, specimen and thermocouple, and thermocouple and hot plate, respectively.

$$R_{VIP} = R_m - R_{Va1} - R_{va2} - R_{va3} \tag{24}$$

Here, R_{VIP} $[(m^2 \cdot K)/W]$ is the thermal resistance of a specimen, R_m $[(m^2 \cdot K)/W]$ is the thermal resistance of the experimental result, and R_{Va1}, R_{va2} and R_{va3} are the thermal resistances of gaps 1, 2 and 3, respectively. Here, $R_{va} = R_{vc} + R_{vr}$ and R_{vc} can be calculated by equation (12); this thermal resistance is not related to the thickness so that thermal resistance of the gaps is the same. R_{vr} is calculated by equations (14–16), and thermal emissivity $\varepsilon = 0.9$. The experimental and optimization results that can

be calculated by equation (19) is shown in Table 3-1. The simulation and experimental results are compared and illustrated in Figure 3-14.

$$\lambda_{VIP} = L_v / R_{VIP} \tag{25}$$

Table 3-1 Experimental results by GHP

Pressure [Pa]	Experimental thermal conductivity λ_m $[mW/(m \cdot K)]$	Experimental thermal resistance R_m $[(m^2 \cdot K)/W]$	Thermal resistance in the gaps R_{va} $[(m^2 \cdot K)/W]$	Thermal resistance of VIP (Calculated)R_{VIP} $[(m^2 \cdot K)/W]$	Thermal conductivity of VIP (Calculated) λ_{VIP} $[W/(m \cdot K)]$
0.1	2.9	1.45	0.21	0.83	0.005
1	3.6	1.17	0.17	0.65	0.006

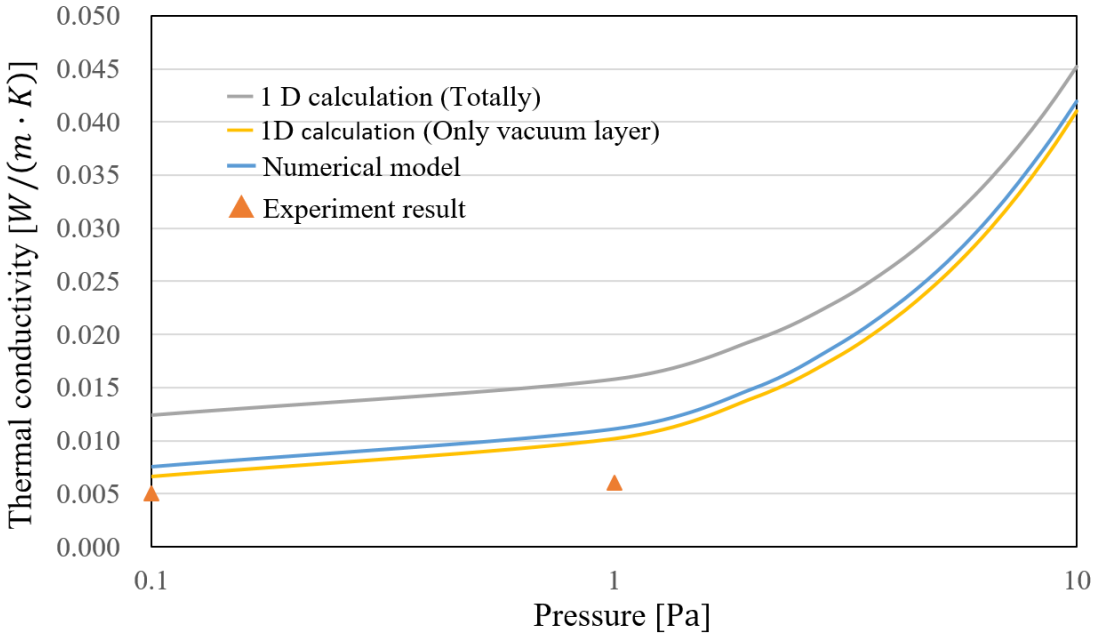

Figure 3-16 Comparison of the simulation and experimental results

According to Figure 3-16, the results of the numerical model show a good agreement with the experimental results under a high vacuum. However, in the experiment, the sockets for the spacers also have gaps owing to the difference in the diameters that decrease the thermal conductivity. Furthermore, the result of the numerical model is lower than the one-dimensional (1 D) calculation result; this is probably because the numerical model can consider the thermal resistance in different axis directions. In addition, the thermal conductivity in the absence of the effect of spacers and plates shows the high performance of the evacuated space.

3.5 Case study for vacuum layer type translucent VIP

3.5.1 Calculation conditions for case study

In this section, the vacuum layer type VIP is further considered and its performance is verified based on different design plans. By considering the cost performance, the authors determined the specification of the component of the VIP, so that the thermal conductivities of the plastic cylinder spacers and acrylic plate are 0.3 $[W/(m \cdot K)]$ and 0.2 $[W/(m \cdot K)]$, respectively. The other conditions are presented in Table 3-2.

Table 3-2 Calculation conditions in the case studies

	L_v [m]	P [Pa]	λ_v [mW/(m·K)]	ε_1	ε_2	Layers
Standard	1.0×10^{-3}	0.1	0.106	0.3	0.9	1
Case 1		1	1.06	0.9	0.9	1
Case 2		1	5.3	0.3	0.9	2
Case 3		0.5	5.3	0.3	0.9	1
Case 4		0.1	0.106	0.9	0.9	1
Case 5		1	1.06	0.3	0.9	1

3.5.2 Result and discussion

The comparison of the results from the case studies is shown in Figure 3-17. The calculated thermal conductivity in Case 1 is higher than that in the standard case owing to the higher thermal emissivity. Case 2 shows a better performance because the multiple layers cause the thermal conductivity of the vacuum layer to become half of that of a single layer. In Cases 3 and 5, the thermal conductivity of the vacuum layer decreases with the reduction in the pressure. The standard case has the lowest thermal conductivity when compared with Case 4 owing to the low-emissivity effect.

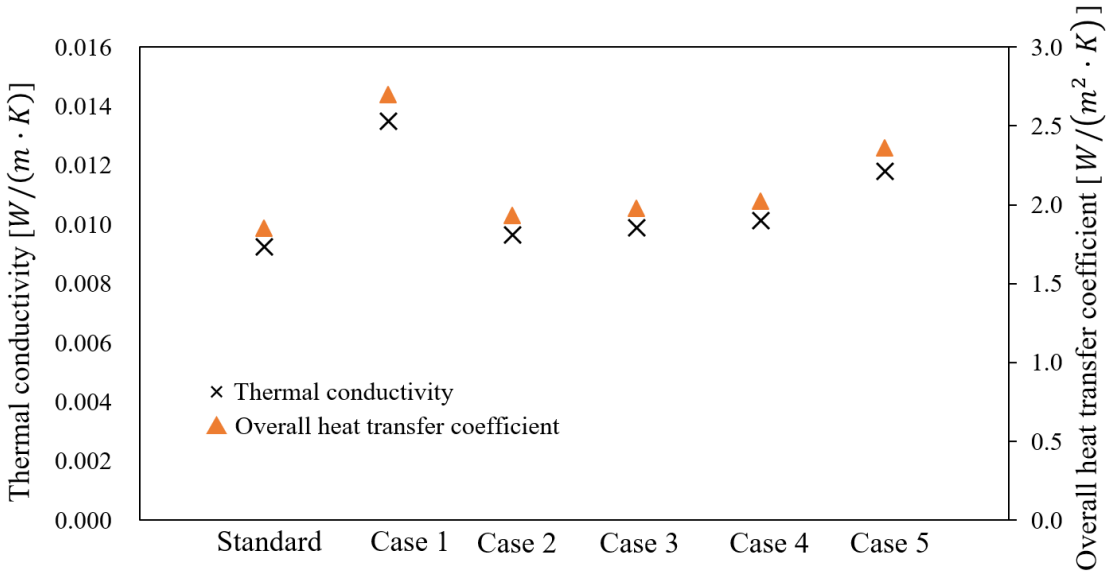

Figure 3-17 Comparison of the calculated results for the case studies

3.6 Conclusion

1) The authors proposed a vacuum layer type slim and translucent VIP with the advantages of a low manufacturing cost and easy application.
2) By using a structural calculation model, the specifications of the spacers and plastic plates that can hold the vacuum layer structurally, were investigated. The result showed that the vacuum layer could be maintained when the span between the spacers was less than 10 mm.
3) Heat transfer models were considered for the prediction of the thermal transmittance of the VIPs. The thermal conductivities of the VIPs were calculated by varying the calculation conditions of the pressure of the vacuum layer, thermal emissivity of the surface, and number of vacuum layers. The high-insulation performance was confirmed for future applications because the overall heat transfer coefficients were less than 2.0 $W/(m^2 \cdot K)$ when the pressure of the vacuum layer was reduced to less than 0.1 Pa or a double vacuum layer was produced.
4) The result showed that the thermal conductivity of a double layer VIP under a pressure of 1.0 Pa was practically similar to that of a single VIP under a pressure of 0.1 Pa.
5) The numerical results were in better agreement with the experimental results under a pressure of 1 Pa because the numerical analysis can also consider the thermal

resistance in different axis directions. Furthermore, to obtain a better insulation performance, using a multiple layer instead of a lower pressure could reduce the product cost and lead to an easy manufacture.

Reference:

[1] R.E. Collins, C.A. Davis, C.J. Dey, S.J. Robinson, J.Z. Tang, G.M. Turner, Measurement of local heat flow in flat evacuated glazing, International Journal of Heat and Mass Transfer, 36 (1993), pp. 2553–2563

[2] Nature Publishing Group, Architects of a low-energy future, Nature, 452 (2008), pp. 520–523

[3] Arto Saari, Targo Kalamees, Juha Jokisalo, Rasmus Michelsson, Kari Alanne, Jarek Kurnitski: Financial viability of energy-efficiency measures in a new detached house design in Finland, Applied Energy, 92 (2012), pp. 76–83

[4] R. E. Collins, G. M. Turner, A. C. Fisher-Cripps: Vacuum Glazing-A New Component for Insulating Windows, Building and Environment, Vol. 30, No. 4, pp. 459–492 (1995)

[5] A. C. Fisher-Cripps, R. E. Collins, G. M. Turner, E. Bezzel: Stress and Fracture Probability in Evacuated Glazing, Building and Environment, Vol. 30, No. 1, pp. 41–59 (1995)

[6] J. D. Garrison and R. E. Collins: Manufacture and cost of Vacuum Glazing, Solar Energy, Vol. 55, No. 3, pp. 151–161 (1995)

[7] G. M. Turner and R. E. Collins: Measurement of Heat flow through Vacuum Glazing at elevated Temperature, Journal of Heat Mass Transfer, Vol. 40, No. 6, pp. 1437–1446 (1997)

[8] M. Lenzen and R. E. Collins: Long-term Field Tests of Vacuum Glazing, Solar Energy, Vol. 61, No. 1, pp. 11–15 (1997)

[9] R. E. Collins and T. M. Simko: Current Status of the Science and Technology of Vacuum Glazing, Solar Energy, Vol. 62, No. 3, pp. 189–213 (1998)

[10] T. M. Simko, A. C. Fisher-Cripps and R. E. Collins: Temperature-induced in Vacuum Glazing Modelling and Experimental Validation, Solar Energy, Vol. 63, No. 1, pp. 1–21 (1998)

[11] Jongmin Kim, Choonghyo Jang, Tea-Ho Song: Combined heat transfer in multi-layer radiation shields for vacuum insulation panels: Theoretical/numerical analysis and experiment, Applied Energy, Volume 94, pp. 295–302 (2012)

[12] Jea-Sung Kwon, Choonghyo Jang, Heayong Jung, Tea-Ho Song: Vacuum maintenance in vacuum insulation panels exemplified with a staggered beam VIP, Energy and Buildings, Volume. 42, Issues 5, pp. 590–597 (2010)

[13] Mathias Bouquerel, Thierry Duforestel, Dominique Baillis, Gilles Rusaouen: Heat transfer modelling in vacuum insulation panels containing nanoporous silica-A review, Energy and Buildings, Volume 54, pp. 320–336 (2012)

[14] Jae-Sung Kwon, Choonghyo Jang, Haeyong Jung, Tae-Ho Song: Effective thermal

conductivity of various filling materials for vacuum insulation panels, International Journal of Heat and Mass Transfer, Volume 52, Issues 23–24, pp. 5525–5532 (2009)
[15] Pär Johanssonn, Bijan Adl-Zarrabi, Carl-Eric Hagentoft, Using transient plane source sensor for determination of thermal properties of vacuum insulation panels, Frontiers of Architectural Research, Volume 1, Issues 4, pp. 334–340 (2012)
[16] R.E. Collins, C.A. Davis, C.J. Dey, S.J. Robinson, J.Z. Tang, G.M. Turner, Measurement of local heat flow in flat evacuated glazing, International Journal of Heat and Mass Transfer, 36 (1993), pp. 2553–2563
[17] Timoshenko. S, Woinowsky-Krieger S. Theory of Plate and Shell. McGraw-Hill Book Company: 1959, pp.106−108.
[18] Roark R J, Warren C, Young Richard G. Budynas. Formulas for Stress and Strain (Seven Edition): pp. 508–509.
[19] Guohui Gan, Thermal transmittance of multiple glazing: computational fluid dynamics prediction. Applied Thermal Engineering: October 2001, pp. 1583–1592
[20] Handbook of Vacuum Technology (1st Edition), Edited by Karl Jousten, (2008) pp. 51–81.
[21] E. R. G. Eckert, Robert M. Drake, Heat and Mass Transfer, McGraw-Hill Inc. US; 2nd Revised Edition (1959/12)
[22] Springer G. S. Heat Transfer in Rare Field Gases. Advances in Heat Transfer, 1971, 7(2), pp. 163–218.
[23] R. E. COLLINS, G. M. TURNER, A. C. FISCHER-CRIPPS, Vacuum Glazing- A New Component for Insulating Windows, Building and Enaironmenf, Vol. 30. No. 4. pp. 459492. 1995

Chapter 4
Development of frame structural VIP

4.1 Introduction

Driven by updated building energy codes and green building initiatives across the world, vacuum insulation panel, also known as VIP, has become a desired insulation product for building envelope constructions. VIP has initial center-of-panel thermal conductivity of 0.004 $W/(m \cdot K)$ or lower, and integration of VIP in building envelopes can reduce CO_2 emissions and contribute towards 'net-zero' or 'near-net-zero' building constructions. Although VIPs have been applied in real-world constructions across the world, primarily in Asia, Europe and North America, it is still a novel building product under investigation. This overview paper is a summary of fundamentals, constituents, constructions and performances of VIPs. The paper shows there exists many advantages and challenges associated with the integration of VIPs in building envelope constructions. The speed at which VIPs will be integrated in building envelope construction in the coming years remains unclear; nevertheless, it is evident that vacuum technology is the promising way forward for sustainable building envelope constructions in the 21st century.

In recent years, a great deal of effort has been dedicated to developing new technological solutions with the aim of reducing the heating and cooling energy consumption of buildings. One of the most promising solutions for the construction sector is the use of super insulation materials, such as vacuum insulation panels (VIPs) and Areogel-containing materials, in building envelope components. They allow optimal thermal insulation levels to be achieved, while keeping the total thickness of the envelope components below a certain thickness. Nevertheless, some barriers have to be overcome in order to penetrate the building construction market and to be widely adopted by designers. In fact, although these materials show remarkable potential for reducing energy consumption, few investigations have been carried out so far to evaluate their effectiveness in real building applications. In particular, the effects of the configuration adopted for their installation, in terms of design and materials, and the procedures used to evaluate their overall performance need to be investigated in more detail.

Vacuum glazing is a new form of transparent thermal insulation that operates on the same principles as the conventional Dewar flask. It consists of two flat sheets of glass, hermetically sealed together around the edges, and separated by a narrow evacuated space. The internal surfaces of the glass sheets are kept apart under the influence of atmospheric pressure by an array of small support pillars. The pillars are made from a high strength

material, and are either metal ~stainless steel or Inconel 718, or ceramic ~alumina or zirconia. The design of vacuum glazing involves tradeoffs between the heat flow through the pillars, and the stresses in their vicinity due to atmospheric pressure. The pillars are typically 0.25–0.5 mm in diameter, and 0.1–0.2 mm high, and are spaced apart by 20–25 mm. Transparent low emittance coatings on the internal surfaces of one or both of the glass sheets are used to reduce radiative heat transport to a low level. Both pyrolytically deposited coatings ~based on tin oxide, and sputtered coatings ~multilayer stacks of silver and dielectric materials have been successfully incorporated into vacuum glazing.3 Vacuum glazing is applied in thermally insulating windows, and is therefore made in sizes up to 2 m in linear dimension, with glass sheets typically 3–4 mm thick.

4.1.1 Development of nails support VIP

To simplify the production process and make contributions to the industrial production, the authors carried out the nail support VIP which is illustrated as Figure 4-1.

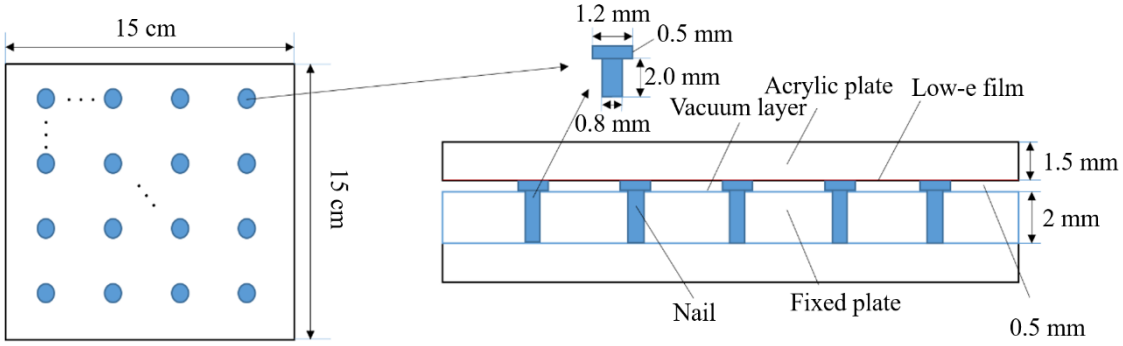

Figure 4-1 Concept diagram of nail support translucent VIP

In this model, the VIP manufacture is simplified and it's easy to make the double layer in Figure 4-2.

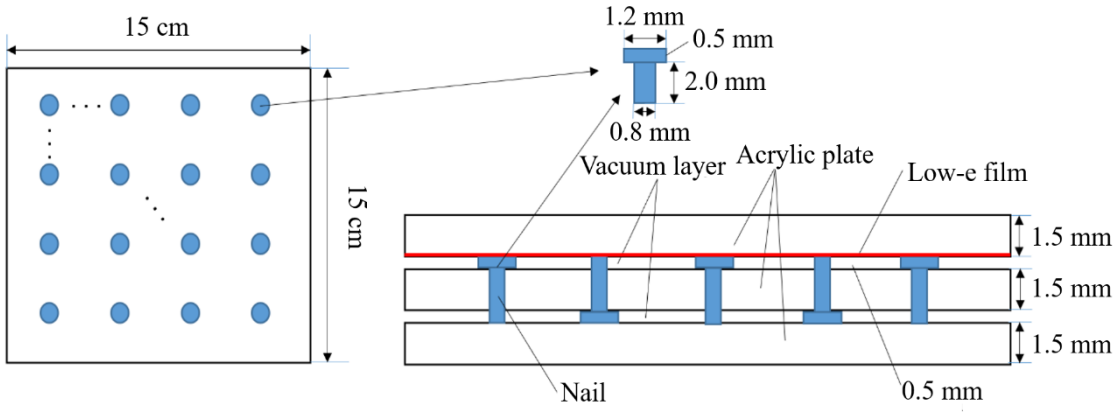

Figure 4-3 Concept diagram of double layers nail support translucent VIP

According to the result in Chapter 3, the multiple layers can increase the insulation performance which reach to a very low-pressure performance. In this case, the authors carried out the 3-D model to evaluate the insulation performance. The multiple layers' performance is shown in Figure 4-4.

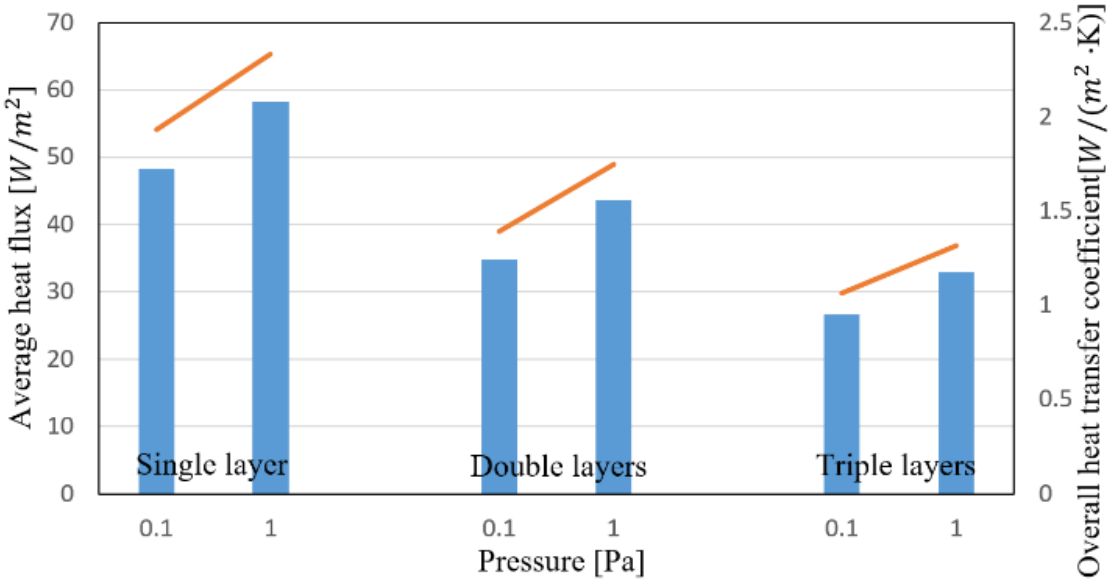

Figure 4-4 Insulation performance in different conditions

However, what about the actual performance in these models? The authors set up the heat flux meter apparatus to evaluate the real insulation performance, the specific of the heat flux meter apparatus will introduce in Chapter 5 in detail. Then, the apparent thermal conductivity is applied to evaluate the insulation performance and the result is shown in Figure 4-5.

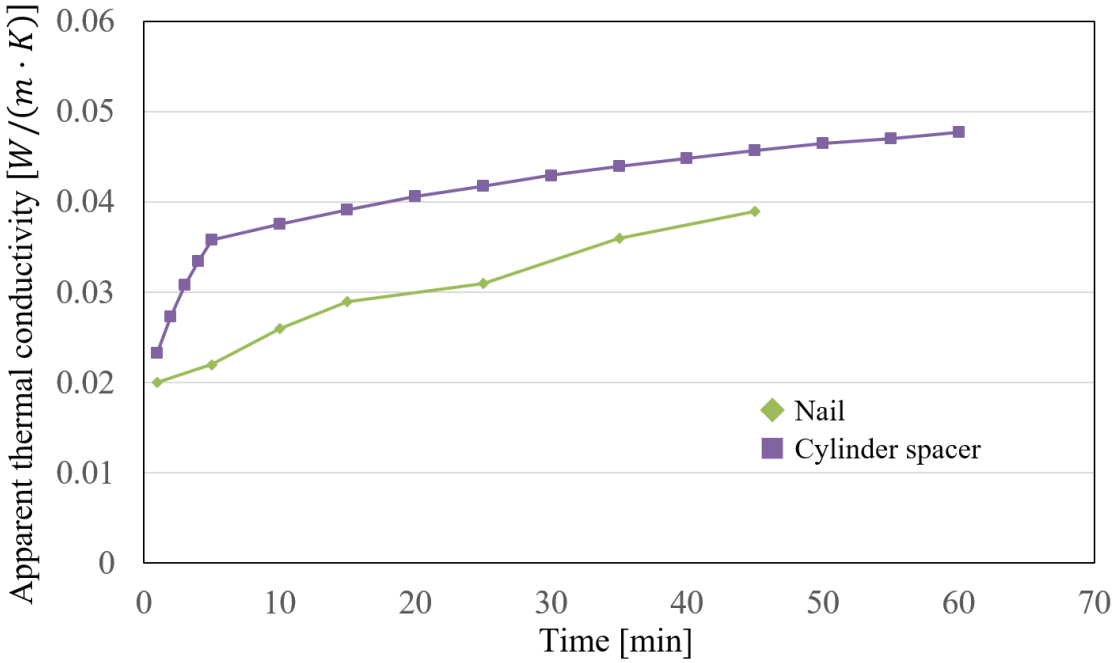

Figure 4-5 Experimental result of Nail and cylinder spacer support VIP

According to the result in Figure 4-5, the apparent thermal conductivity of nail and cylinder spacer support VIP indicate the insulation performance is much higher than prediction initially. And the performance is rapidly degraded in 1 hour. It's much higher than our objective, even though the guarded hot plate result can validate the insulation performance, however, the real performance is affect in several conditions. Such as the gas barrier performance, the internal gas generations and the gas permeation. In this study, the authors believe that the internal pressure is increased due to the gas generations, the components maintained the gas by absorption or other ways and desorption after heat sealing. Therefore, there is a good way to reduce the degradation effect that to reduce the absorption area. Then, the authors considered to another structure to hold the vacuum layer with smaller area.

4.1.2 Mesh support translucent VIP

A good way to reduce the absorption area is remove the acrylic plate. However, in this structure is difficult to have a vacuum layer. The gas barrier film is not rigid material so that the concentration of web is heavily affect the flat in the surface also affect the completeness of vacuum layer. Some studies aimed in this method and one of them is

shown as a concept diagram in Figure 4-6 [1].

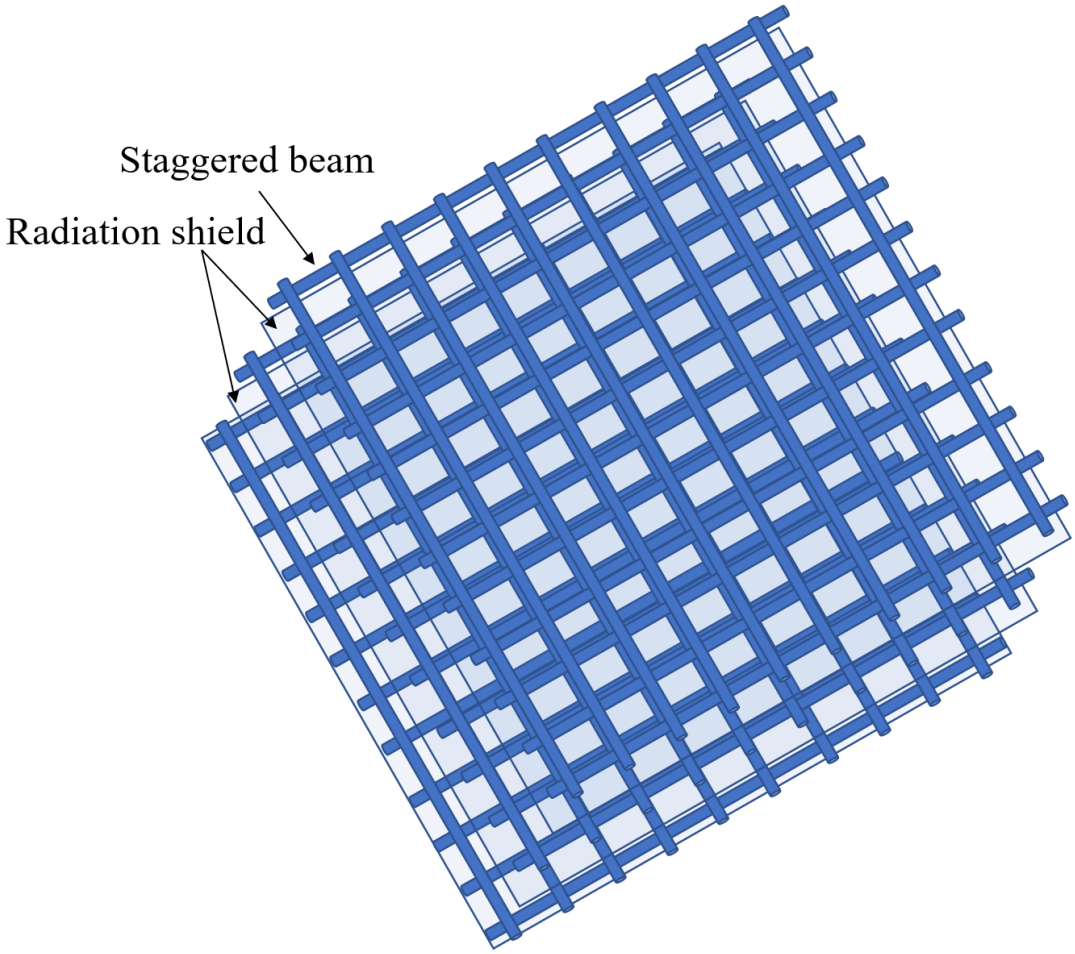

Figure 4-6 The concept diagram of staggered beam combined with radiation shields core material VIP

In this published model, the result having a good performance in a ideal state and the outgassing is also discussed, however, the multiple overlapped layers cannot give a good transparent performance, also, the slim beam may not give a good vacuum layer and flat surface. Most important is the multiple layer with multiple low-e film increased the production cost. But this calculation model is valuable to refer.

These summarized studies show us it's valuable to improve the translucent VIP with a frame structural core material.

4.2 New proposal of frame structural VIP

Of late, various energy saving techniques are being employed in new buildings; however, these techniques are difficult to apply to existing buildings. Especially, the thermal insulation performance is poor in existing buildings, hence, it's important to improve the insulation performance. The VIP has the potential to improve the insulation performance effective, however, the conventional VIPs have some issues for their applications, such as: expensive cost due to complicated manufacturing process, low durability, possibility of fatal damage due to nailing, influence of thermal bridge. Also, there's no commercial available translucent VIPs which can be applied to windows, whose insulation performances are lower. Therefore, it's effective to develop the slim and translucent vacuum insulation panel and install to the existing buildings. The authors developed a new model of a VIP that is thin and translucent and can be easily installed and contribute to retrofitting insulation to existing buildings including even the windows, as illustrated in Figure 4-7. This VIP model consisted of a frame with a low-e film coating achieved using a gas barrier film, whereas the vacuum layer was supported by frame structure. With respect to the durability, if the VIPs are easy to install, the degraded ones can be replaced by new ones, owing to the highly cost-effective core material. In terms of the cost, simplification in the production of VIPs with slim and flat core material can be expected in the preparation stage. In this paper, the heat transfer calculation model for the above VIP is described and the calculation conditions are summarized to divide how strong the condition affect the insulation performance of VIPs. The calculated results are summarized and compared with each other. Subsequently, in the study, an experiment is conducted to measure the heat flux of the VIP samples and the results are compared with the calculated results. Finally, the insulation performance of the proposed VIP is discussed. In the study, finite element analysis (FEA) is applied for predicting the heat transfer coefficient and thermal transmittance of the VIP under different conditions. A comparison of the insulation performance of the VIP with the different conditions is presented, and a standard calculation model is considered as the representative reference object for comparison.

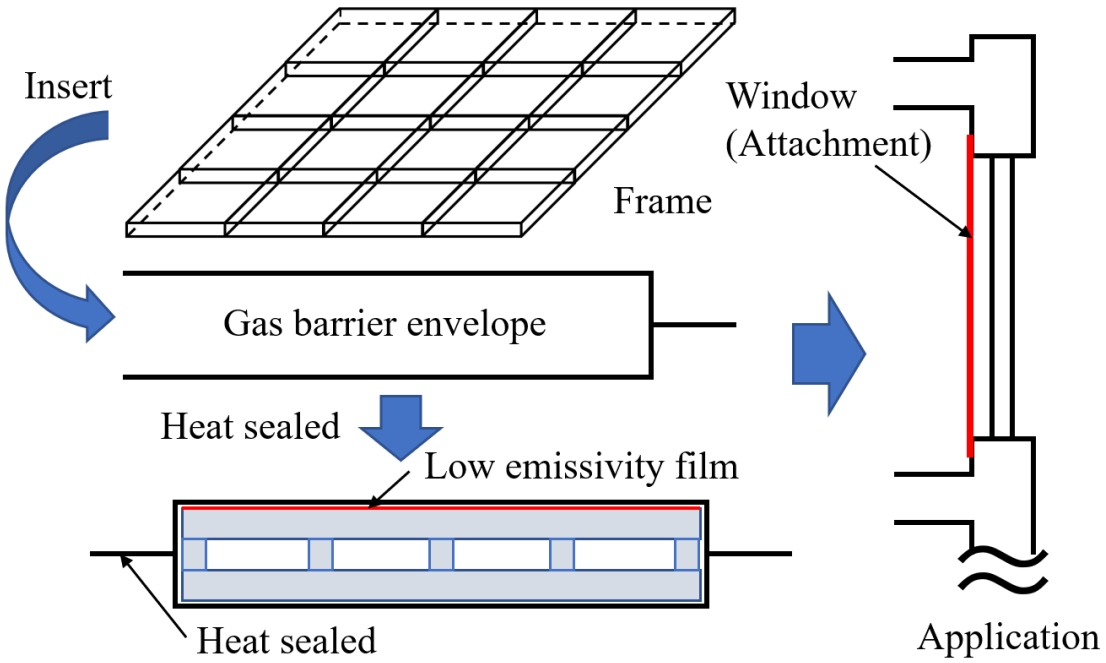

Figure 4-7 Concept diagram of the VIP application to buildings

4.3 Mechanical analysis and structural model

The same considerations as previous analysis in Chapter 3, the mechanical analysis is carry out as a simply support beam. In this section, to determine the reasonable size of the VIP design, the authors discussed the stress analysis and the calculated maximum deflection. If the loading condition applied to the frame in the form of a distributed air compression is the same throughout as shown in Figure 4-8(A), element mechanical analysis as depicted in Figure 4-8(B) [3], [4] will have to be conducted. The structural calculation model can be applied for calculating two possibilities, and Figure 4-9 shows the schematic of the calculation model. This time the distributed load is affect on the frame.

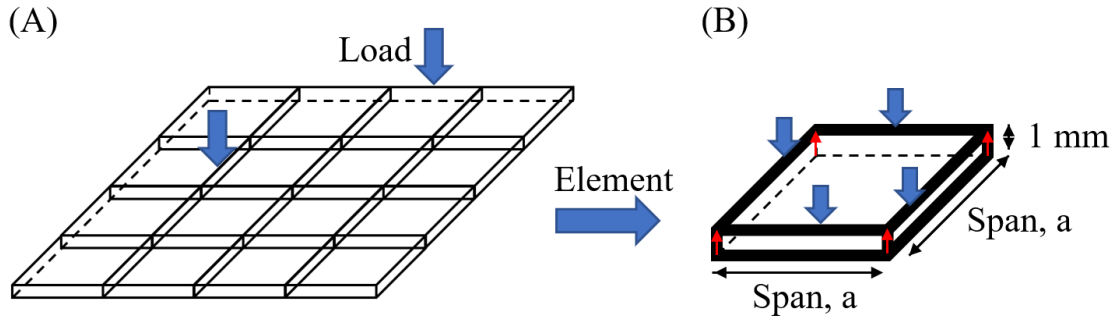

Figure 4-8 Outline of the mechanical analysis of the VIP

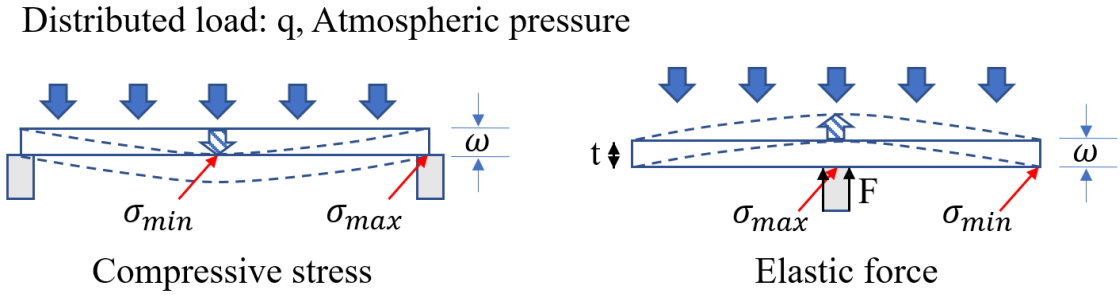

Figure 4-9 Schematic of the calculation model

In this calculation model, when the effective load is applied only through atmospheric pressure, maximum stress occurs in the center of the plate, whereas the minimum stress is on the edge. However, when only the elastic effect is present, the scenario is opposite to the above case, and hence, the stress direction is the reverse of the overall mechanical analysis. In this section, we define the relationship between the deflection and span by using the equations provided below.

$$\bar{\omega}_{max} = \delta \times \frac{P_0 \times a^4}{D} \quad (1)$$

$$D = \frac{Et^3}{12(1-\mu^2)} \quad (2)$$

For the polycarbonate frame, here, E is the elasticity modulus (= 2.32 GPa) and μ is the Poisson's ratio (= 0.39) [-]. In this model, width of the polycarbonate frame t = 1 mm, span of a = 10 mm, δ_1 = 0.0138 [-] (coefficient when the rectangular flat plate is functioned by a uniform load, δ_2= 0.0611 [-] (coefficient when the rectangular flat plate is functioned by a uniform load) and effect in different stresses, and P_0 = 1013 [hPa].

Figure 4-10 shows the maximum deflection of the frame with the different spans. In addition, the authors also carry out the structural design by changing the width of frame from 0.5 mm to 1.5 mm, and changing the spans in 5 mm, 8 mm, 10 mm, 12 mm and 15mm. And the variation of deflections is shown as Figure 4-11.

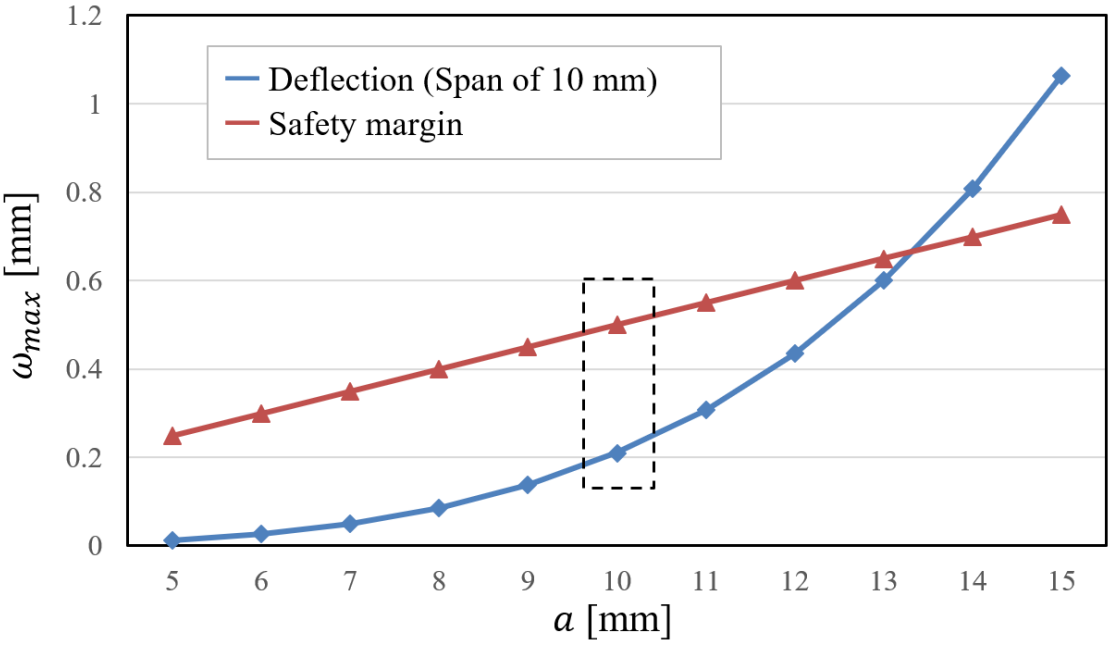

Figure 4-10 Calculation results of the maximum deflections at different spans

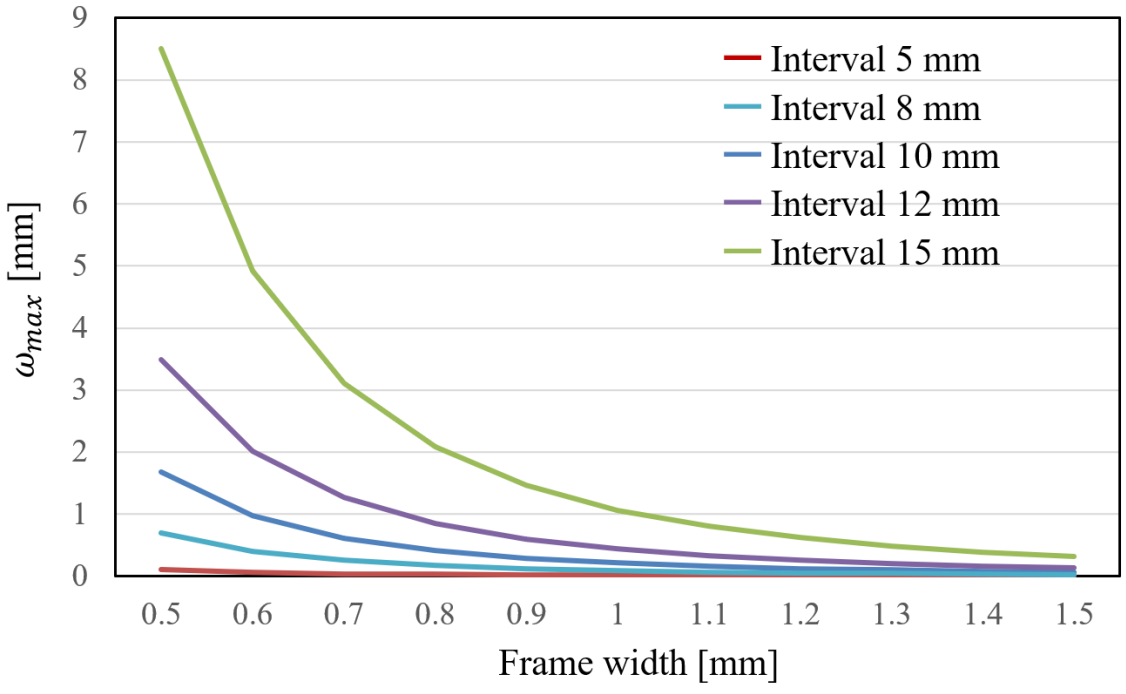

Figure 4-11 Comparison of deflections with different conditions

Figure 4-10 indicates that every designable load element can hold the vacuum layer within in the safety margin requirement for a mechanical design. To obtain and hold the vacuum layer, the authors decide the span of the frame as 10 mm with an overall consideration of the stress affect and safety margin to ensure the application of the heat transfer model and specimen in the trial manufacture for experiment. Figure 4-11 indicates the comparison of deflections based on different conditions, and the reasonable design should also consider the insulation performance and the transparency, therefore, frame width in 1 mm and span in 10 mm is suggested. Also, frame width in 1.2 mm and span in 15 mm is good for insulation performance and transparent requirement, however, this design cannot maintain a good vacuum layer in our proposal due to the gas barrier film is not a rigid material.

Subsequently, to confirm the structural design, the authors also generate a 3-D model using the simulation software, ANSYS workbench. The distribution of the total deformation for the frame VIP that is modelled in Figure 4-8 is shown in Figure 4-13 with span of 10 mm and in Figure 4-14 with span of 5 mm. The fixed boundary condition indicates the element analysis is reasonable to a full-size VIP and the meshing in Figure 4-12 shows the calculation result is pretty accuracy due to the totally 257791 nodes and 49046 elements. The result can well validate the mechanical analysis, indicating the structural design is reasonable to hold the vacuum layer and sufficiently flat for the application.

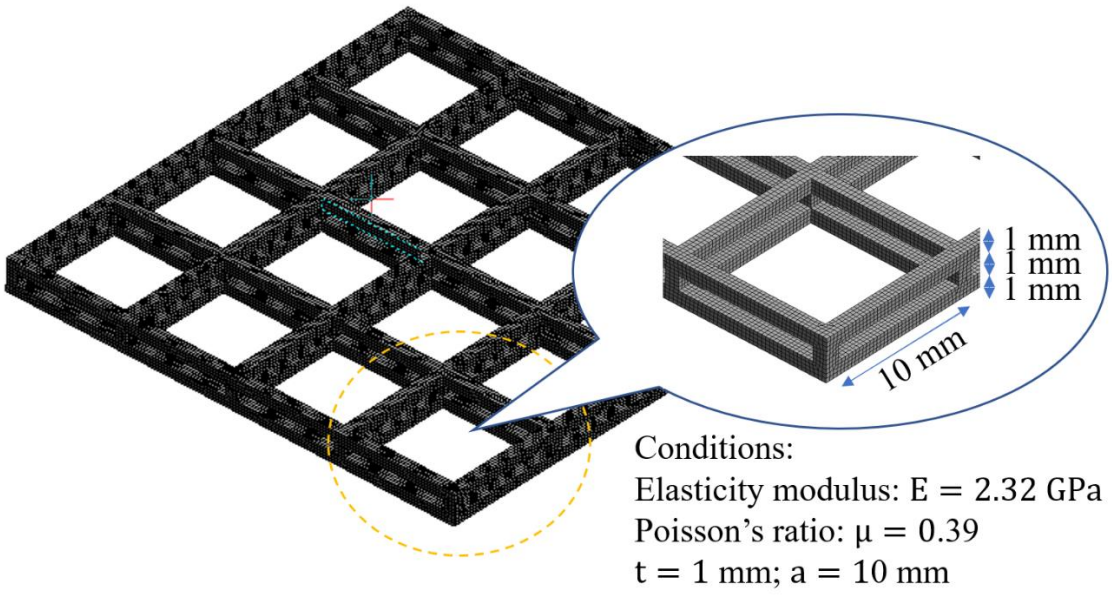

Figure 4-12 Meshing in finite element analysis (3-D)

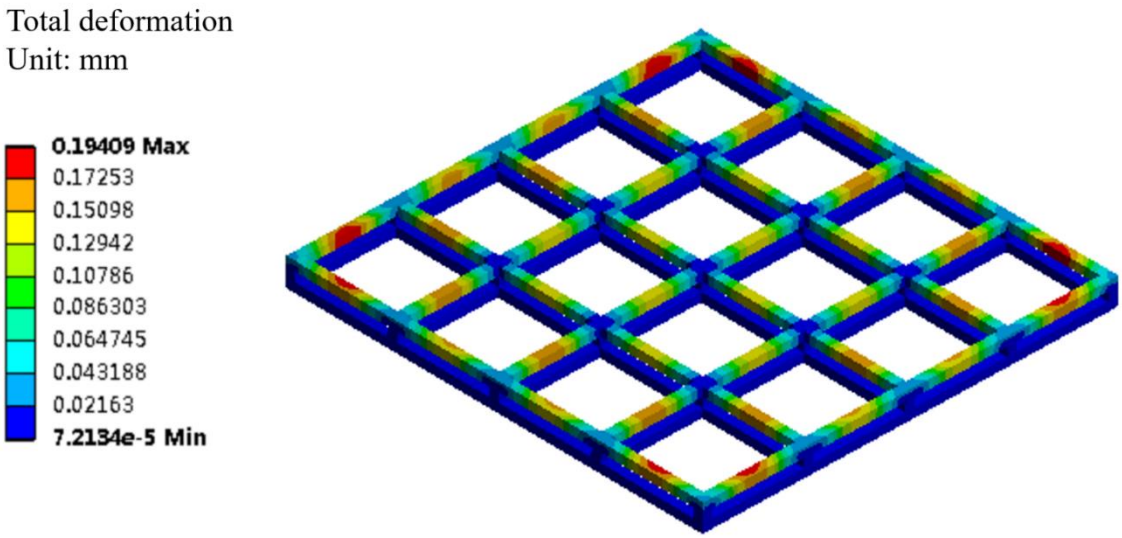

Figure 4-13 Total deformation in a VIP element (3-D)

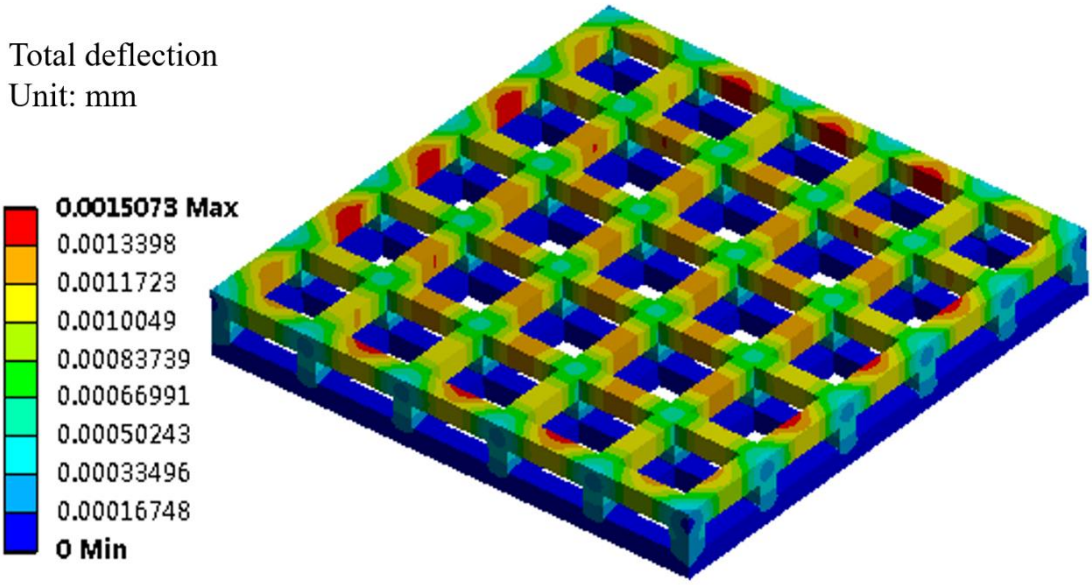

Figure 4-14 Total deformation in a VIP element (3-D)

In Figure 4-13 and Figure 4-14, it's clear that a concentrated web of a frame structure can provide a better performance to the resistance of deformation. However, a concentrated web also means the thermal bridge of the VIP will be bigger than a less concentrated web frame. Therefore, a overall consideration should support to give a reasonable design, the span in the frame element should be reasonable with the width of frame.

4.4 Numerical model and insulation performance prediction

The same as the pillars support VIP model, the frame structural VIP can also model with a FEA [5] ~ [9]. However, the area ratio for frame should be analyzed as two layers, the surface web and the support point, furthermore, the total insulation performance will predict with assume the emissivity of frame in 0.9. The 3-D calculation is carried out and the result is analyzed to compare with the experimental result. Schematic of heat transfer through a frame element is shown in Figure 4-15.

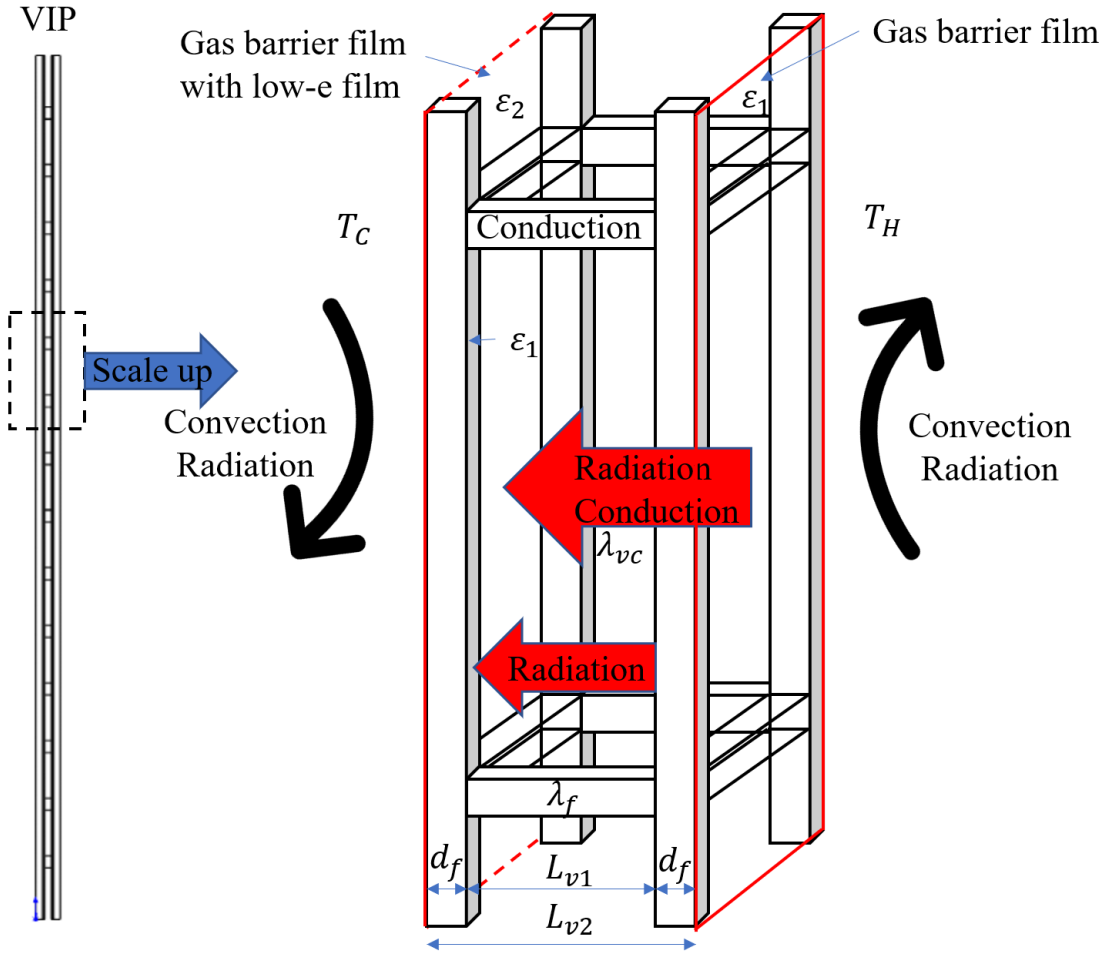

Figure 4-15 Schematic of heat transfer through a frame element

The “U” value is performed to evaluate a frame VIP element and defined by the following equations:

$$U = \frac{1}{R_C + R_V + R_H} \tag{3}$$

where U is the overall heat transfer coefficient of the VIP (W/(m2·K)); R_C is thermal resistance of low temperature surface ((m2·K)/W); R_H is the thermal resistances of high temperature surface ((m2·K)/W). R_V is the thermal resistance of evacuated space with frame ((m2·K)/W), calculation of R_V can be categorized into conductive heat transfer and radiant heat transfer, defined as Equations (4–6) and Equations (7), (8), respectively. The R_V is determined by the heat transfer model:

$$\frac{\partial^2 T}{\partial x^2} + \frac{\partial^2 T}{\partial y^2} + \frac{\partial^2 T}{\partial z^2} = 0 \tag{4}$$

Heat conduction in evacuated space can be calculated by the above equation, and the heat transfer in the frame is considered the only conductive heat transfer. The equation is the same as the equation above. Here, the thermal conductivity of the evacuated space λ_v is a constant, calculated by the equation below:

$$\lambda_v = 18.2L\frac{\gamma + 1}{\gamma - 1}\frac{\beta_0 P}{\sqrt{MT}} \tag{5}$$

$$\frac{1}{\sqrt{T}} \cong \frac{2}{\sqrt{T_1} + \sqrt{T_2}} \tag{6}$$

where γ is the specific heat ratio, defined as Cp/Cv, and β is the accommodation coefficient. L in Equation (10) is categorized into with the frame and without the frame defined as L_{v1} and L_{v2} shown in Figure 8.

The radiant heat transfer in an evacuated space is defined by the equations below:

$$h_{vr} = \sigma T_m^3(\varepsilon_1 - \varepsilon_2)\varphi_{1,2} \tag{7}$$

where σ is the Stefan-Boltzmann constant (5.67 × 10−8 W/(m2K4)), ε1 and ε2 are the optimized emissivities of the gas barrier film and low-e film at mean temperature T_m (K), and $\varphi_{1,2}$ is the angle factor between the two surfaces of the VIP that can be calculated by the following equation:

$$\varphi_{1,2} = \frac{1}{A_2}\int_{A_1}\int_{A_2}\frac{cos\,\theta_1\,cos\,\theta_2}{\pi r^2}\delta_{12}\,\mathrm{d}A_1 dA_2 \tag{8}$$

where δ_{12} is determined by the visibility of dA_2 to $\mathrm{d}A_1$, $\delta_{12} = 1$ if dA_2 is visible to $\mathrm{d}A_1$ and is 0 otherwise.

4.5 Trial production of the testing specimen

4.5.1 VIP trial production

The VIP test specimen is produced as per the flow in Figure 4-16. The frame is

manufactured by a 3-D printer (specifications in Figure 4-17) initially and a low-e film is covered on the surface of frame then inserted to a transparent gas barrier envelope. In order to prevent degradation with time, calcium oxide getter is sealed together with the core material. The getter absorbs gas and effectively prevents performance degradation. For the evacuated insulation material, the air tightness is critical and the components of the gas barrier film are depicted in Figure 4-18. There' re 3 reasonable transparent evacuated insulation products, silica aerogel core material VIP, vacuum glazing and the VIP we developed. For the economic considerations to retrofitting insulation to existing buildings, a reasonable product also required a good cost-performance, the Figure 4-19 shows the comparison of the industrial manufacture cost of these 3 insulation products.

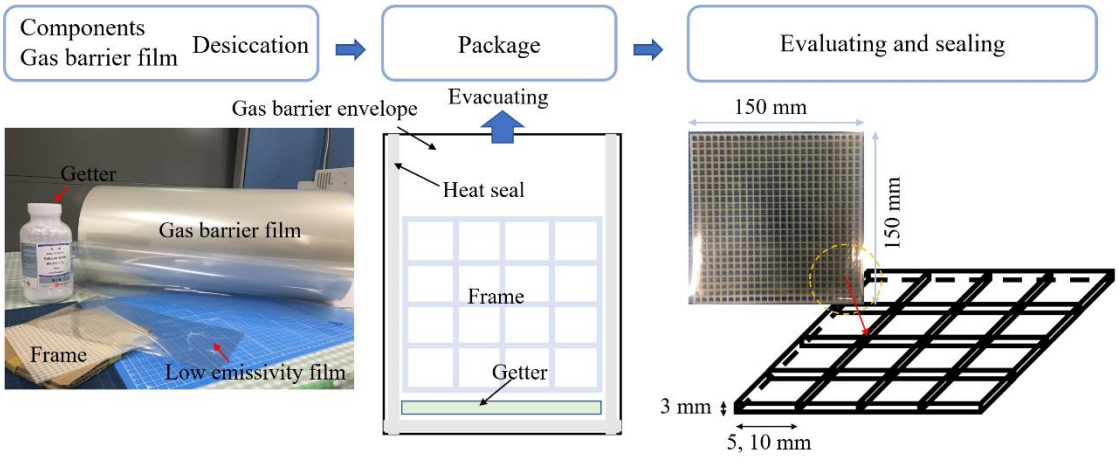

Figure 4-16 Manufacturing flow of the VIP specimens

Stratasys F370, RICOH

Specification of 3-D printer	
Scope of application	Heat resistant and durable
Shaping size (x, y, z)	355mm × 254mm × 355mm
Applicable materials	PLA*, ABS-M30™, ASA, PC-ABS
Accuracy	±0.002mm/mm
Lamination pitch	0.330mm, 0.254mm, 0.178mm, 0.127mm

Figure 4-17 Specifications of 3-D printer

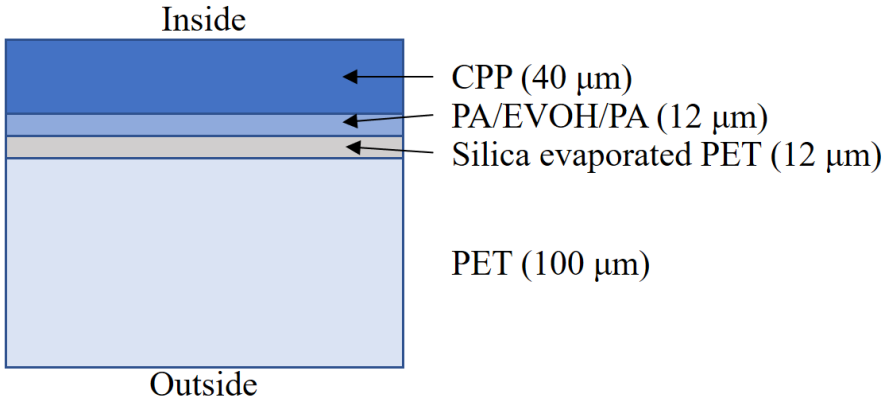

CPP: Cast Poly Polypropylene
PA: Polyamide

Figure 4-18 Component diagram of the gas barrier film

Silica aerogel core material VIP

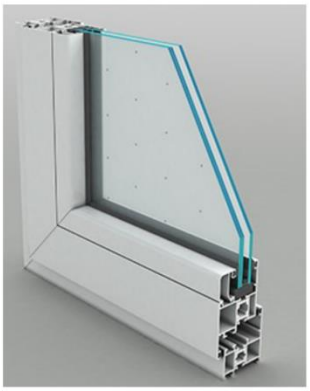

Vacuum glazing

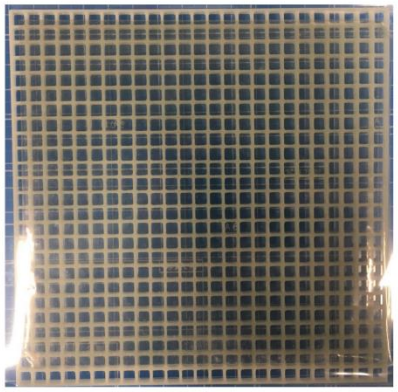

Frame structural VIP

Products	Industrial production Cost [JPY/㎡]
Silica aerogel core material VIP	> 500,000
Vacuum glazing	> 30,000 (+ 10,000 construction fee)
Frame structural VIP	< 10,000

Figure 4-19 Industrial manufacture cost of transparent evacuated insulation products

4.5.2 Framework of guarded hot plate apparatus

The measurement tools allow the determination of the thermal conductivity and thermal resistance of homogenous plates and inhomogeneous test specimens, if the specimens are plane and plate-shaped. The test specimens are installed between the heating and cooling plates. A constant heat flow flows through the test specimens in the stationary temperature state. The thermal conductivity is determined by the heat flow,

mean temperature difference between the sample surfaces, and dimensions of the samples. In the steady state, the thermal conductivity of the specimen (λ) is derived by the equation as

$$\lambda = \frac{Q/2A}{\Delta T/d} \tag{9}$$

Here, Q [W] is the average electric power to the main hot plate, A [m^2] is area of the main hot plate, ΔT [℃] is the temperature difference of the specimen surface, and d [m] is total thickness of the specimen. Figure 4-20 shows the schematic of the GHP apparatus. The Pt-100 is applied to measuring the thermal conductivity as temperature sensors which the accuracy should be $\pm|0.15 + 0.002(t)|$. And there are 10 temperature sensors in the hot plate and 5 in the cold plate and set in different directions.

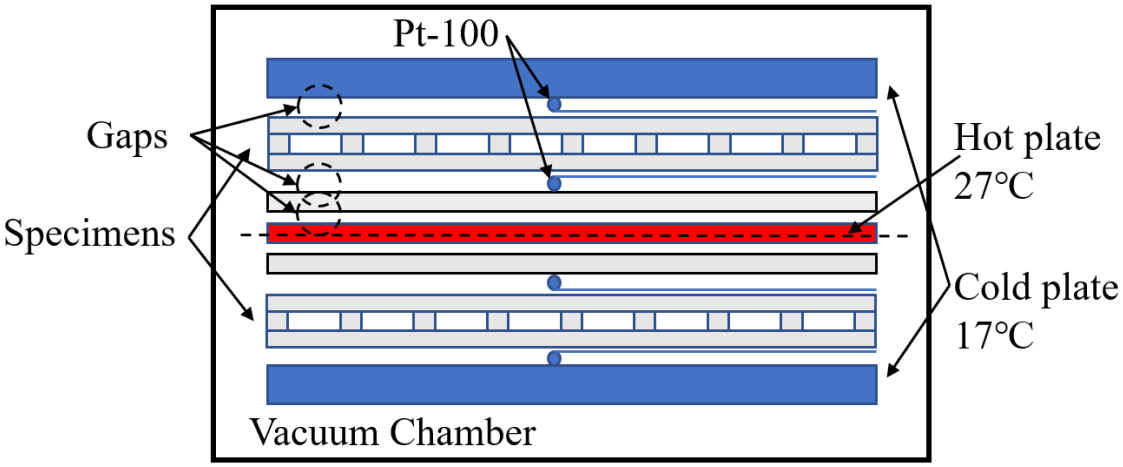

Figure 4-20 Schematic of the guarded hot plate apparatus

Figure 4-21 shows the concept diagram of the VIP test specimens and models of the case study. In the GHP experiment, the specimen is pressed by hot and cold plates, and the pressure in the chamber is reduced to 0.1 Pa and 1 Pa, respectively. Figure 4-22 shows the comparison of the thermal conductivities obtained from the calculation and experimental result based on the pressure.

An element of the VIP is selected to represent the calculation conditions. The calculation conditions and specific size of the VIP for the standard model are also depicted in Figure 4-21. In this calculation, the thermal conductivities of the polycarbonate frame is 0.2 $[W/(m \cdot K)]$, and the thermal emissivities of the polycarbonate frame and low-e

film are 0.9 and 0.3, respectively. The temperature difference for the calculation is 25 °C.

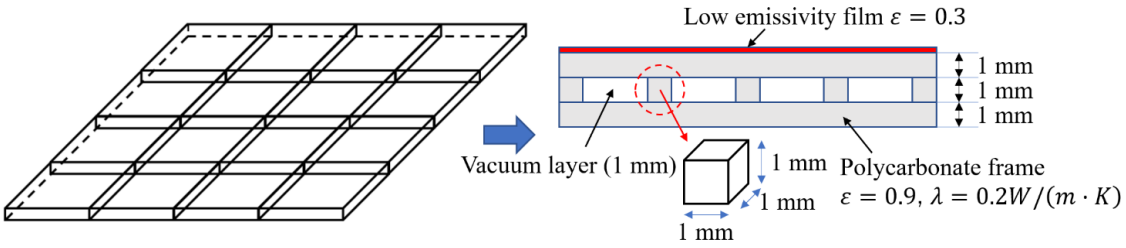

Figure 4-21 Concept diagram of the VIP specimen and model for the case study

There exist some influence factors in this experiment, particularly, the gaps between the hot and cold plates and the specimens. Therefore, the experiment result can be calculated by equation (10) to eliminate the influence of the gaps. In this experiment apparatus, the gaps are in the vacuum environment that is between the cold plate and specimen, specimen and thermocouple, and thermocouple and hot plate, respectively.

$$R_{VIP} = R_m - R_{Va1} - R_{va2} - R_{va3} \tag{10}$$

Here, R_{VIP} $[(m^2 \cdot K)/W]$ is the thermal resistance of a specimen, R_m $[(m^2 \cdot K)/W]$ is the thermal resistance of the experimental result, and R_{Va1}, R_{va2} and R_{va3} are the thermal resistances of gaps 1, 2 and 3, respectively. Here, $R_{va} = R_{vc} + R_{vr}$ and R_{vc} can be calculated by equation (12); this thermal resistance is not related to the thickness so that thermal resistance of the gaps is the same. R_{vr} is calculated by equations (14–16), and thermal emissivity $\varepsilon = 0.9$. The experimental and optimization results that can be calculated by equation (11) is shown in Table 4-1. The simulation and experimental results are compared and illustrated in Figure 4-22.

$$\lambda_{VIP} = L_v/R_{VIP} \tag{11}$$

Table 4-1 Experimental results by GHP

Pressure [Pa]	Experimental thermal conductivity λ_m $[mW/(m \cdot K)]$	Experimental thermal resistance R_m $[(m^2 \cdot K)/W]$	Thermal resistance in the gaps R_{va} $[(m^2 \cdot K)/W]$	Thermal resistance of VIP (Calculated)R_{VIP} $[(m^2 \cdot K)/W]$	Thermal conductivity of VIP (Calculated) λ_{VIP} $[W/(m \cdot K)]$
0.1	2.7	2.10	0.21	1.27	0.004
1	3.4	1.57	0.17	0.88	0.006

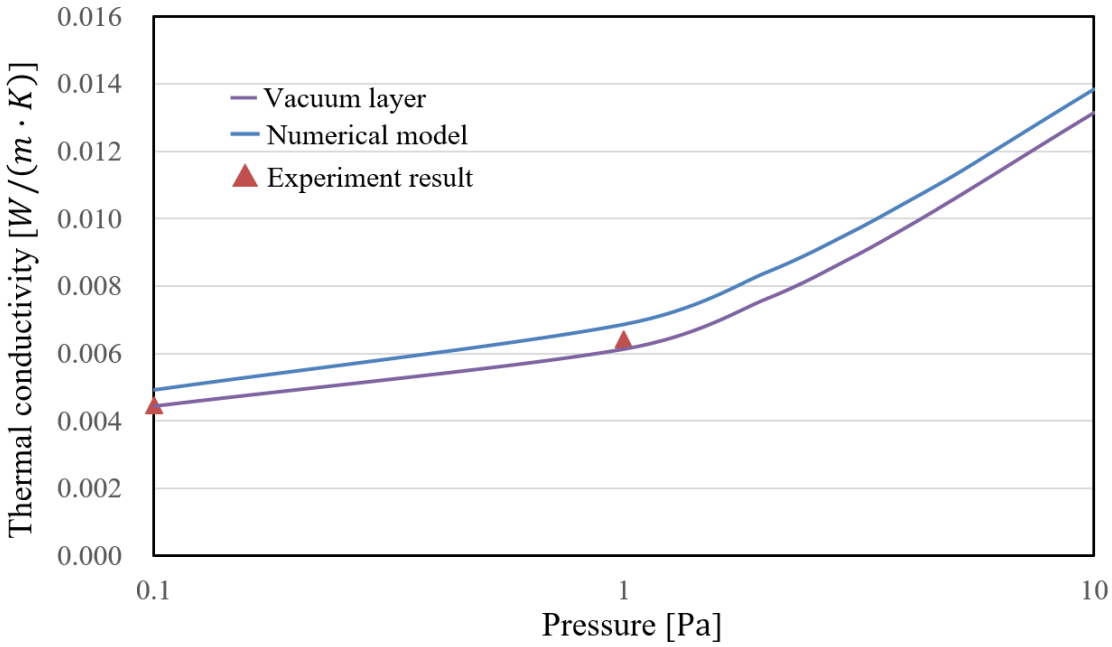

Figure 4-22 Comparison of the simulation and experimental results

According to Figure 4-22, the results of the numerical model show a good agreement with the experimental results under a high vacuum. It's valuable to predict the insulation performance in this model. Also, the frame structural VIP has very good insulation performance to retrofitting insulation in existing buildings. In addition, the thermal conductivity in the absence of the effect of supports and plates shows the high performance of the evacuated space. Then, the improvement of the design should be proposed in reasonable reducing thermal bridge of frame structure.

4.6 Case study for frame structural translucent VIP

4.6.1 Calculation conditions for case study

In this section, the vacuum layer type VIP is further considered and its performance is verified based on different design plans. By considering the stability of frame, the authors determined the specification of the VIP, so that the thermal conductivities of frame is 0.2 $[W/(m \cdot K)]$, the width of frame and span is controlled. The other conditions are presented in Table 4-2.

Table 4-2 Calculation conditions in the case studies

	L_v [m]	P [Pa]	ε_1	ε_2	Interval [mm]	Frame width [mm]	Thickness [mm]
Case 1	1.0×10^{-3}	0.1	0.3	0.9	5	0.5	2
Case 2		1	0.9	0.9	5	0.5	2
Case 3		0.1	0.3	0.9	10	0.9	2.8
Case 4		1	0.9	0.9	10	0.9	2.8
Case 5		0.1	0.3	0.9	15	1.2	3.4
Case 6		1	0.9	0.9	15	1.2	3.4

4.6.2 Result and discussion

The comparison of the results from the case studies is shown in Figure 4-23. The calculated thermal conductivity in Case 2, Case 4 and Case 6 are higher than that in the Case 1, 3 and 5 owing to the higher thermal emissivity. Case 1 and Case 2 owing the higher conduction due to the area ratio is high, and a densely frame is not good for the transparency. Case 5 and Case 6 reduce the frame area, however, it's real difficult to maintain a vacuum layer perfectly. Case 3 seems the most appropriate design with considering the structural safety, insulation performance and the transparency. The low emissivity is applied in just one side to improve the insulation performance well in a good cost performance. The small width of frame also valuable to select if the smaller thickness is required.

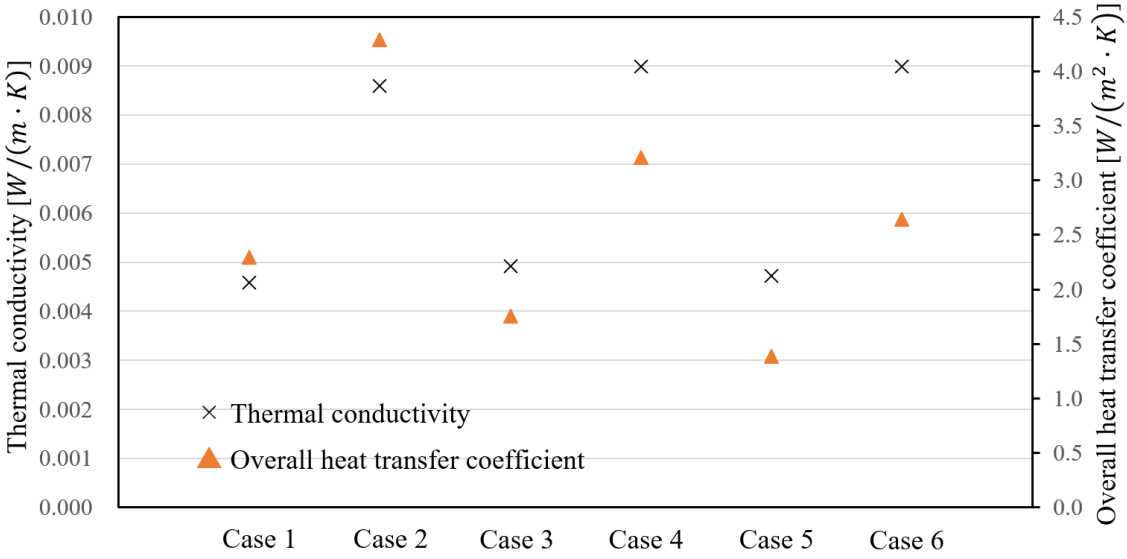

Figure 4-23 Comparison of the calculated results for the case studies

Figure 4-23 indicates that Case 3 and Case 5 should be good design due to the lower

heat transfer coefficient can make good contributions to retrofitting to existing buildings, especially, to the windows. However, the thickness of vacuum layer only 1 mm, a wilder span of frame web cannot achieve a vacuum layer very well due to the gas barrier envelope will compressed so much. To summarize, Case 3 is most valuable to produce a vacuum layer to achieve a good insulation performance, and to reduce the material area in the vacuum space is good for resistance of degradation.

4.7 Conclusion

1) The authors proposed a frame structural slim and translucent VIP with the advantages of a low manufacturing cost and easy application.
2) By using a structural calculation model, the frame can hold the vacuum layer structurally, were investigated. The result showed that the vacuum layer could be maintained when the span was 10 mm and width of frame is 1 mm.
3) Heat transfer models were considered for the prediction of the thermal transmittance of the VIPs. The thermal conductivities of the VIPs were calculated by varying the calculation conditions of the different design conditions. The high-insulation performance was confirmed for future applications because the overall heat transfer coefficients were less than 2.0 $W/(m^2 \cdot K)$.
4) The numerical results were in better agreement with the experimental results under a pressure of 1 Pa because the numerical analysis can also consider the thermal resistance in different axis directions. Furthermore, to obtain a better insulation performance, using a multiple layer instead of a lower pressure could reduce the product cost and lead to an easy manufacture

Reference:

[1] Jae-Sung Kwon, Haeyong Jung, In SeokYeo, Tae-HoSong; Outgassing characteristics of a polycarbonate core material for vacuum insulation panels; Vacuum, Volume 85, Issue 8, 1 February 2011, Pages 839-846.

[1] K. Song, P. Mukhopadhyaya; Vacuum insulation panels (VIPS) in building envelope constructions: An overview; International Review of Applied Sciences and Engineering.

[2] N. Ng, R. E. Collins; Evacuation and outgassing of vacuum glazing; Journal of Vacuum Science & Technology A: Vacuum, Surfaces, and Films 18, 2549 (2000)

[3] Timoshenko. S, Woinowsky-Krieger S. Theory of Plate and Shell. McGraw-Hill Book Company: 1959, pp.106−108.

[4] Roark R J, Warren C, Young Richard G. Budynas. Formulas for Stress and Strain (Seven Edition): pp. 508–509.

[5] Guohui Gan, Thermal transmittance of multiple glazing: computational fluid dynamics prediction. Applied Thermal Engineering: October 2001, pp. 1583–1592

[6] Handbook of Vacuum Technology (1st Edition), Edited by Karl Jousten, (2008) pp. 51–81.

[7] E. R. G. Eckert, Robert M. Drake, Heat and Mass Transfer, McGraw-Hill Inc. US; 2nd Revised Edition (1959/12)

[8] Springer G. S. Heat Transfer in Rare Field Gases. Advances in Heat Transfer, 1971, 7(2), pp. 163–218.

[9] R. E. COLLINS, G. M. TURNER, A. C. FISCHER-CRIPPS, Vacuum Glazing- A New Component for Insulating Windows, Building and Environment, Vol. 30. No. 4. pp. 459492. 1995

Chapter 5
Trial production of translucent VIP and experimental validation

5.1 Summary of previous studies

The authors proposed totally 5 VIP models: silica aerogel spacer VIP, cylinder pillars VIP, nail support VIP, mesh support VIP and the frame structural VIP. Those proposals are real reasonable design to make contribution to retrofitting insulation to existing buildings. However, those proposals are really reasonable and effective in an ideal statement only by validated with guarded hot plate apparatus. In the real situation, the insulation performance is affected by the outgassing or internal gas generation. In the Chapter 3 and Chapter 4, the authors carried out the pillars, nails and frame structural VIP, the insulation performance is evaluated with a guarded hot plate apparatus and the results is good agreement with the numerical model prediction. And in this section, the authors discuss the 5 models and give a summarized property of components of 5 models.

5.2 Introduction

This study aims at developing the vacuum insulation panels (VIPs) with a small thickness and light transmittance to contribute retrofitting insulation for existing buildings. In this paper, the authors are focus on producing the slim and translucent VIPs with vacuum layer which hold by spacers. Firstly, the outlines of vacuum layer type VIPs are introduced, the low thermal conductivity materials (transparent) to producing VIPs which have the vacuum layer hold by spacers. Next, the structural model is carried out as a mechanical analysis to determine the specific array of spacers to pillars supported type. Then, the heat transfer model is carried out by the 3-D model to predict the insulation performance of VIPs. After that, the authors set up the heat flux meter apparatus to measuring the apparent thermal conductivity to evaluate the insulation performance. Finally, the experimental result is compared and analyzed, the author summarized the properties of VIPs with different spacers. In this paper, the authors analyzed the experimental result and the outgassing and desorption issue should be the biggest affect to the VIPs production. Also, the mesh supported VIP can achieve a relative better insulation performance, however, the thermal bridge is big due to obtain and hold a vacuum layer.

The application study of VIPs to buildings as a panel and sheet is getting popular in the world. The conventional VIP consists of a highly insulating core material and a highly

conducting envelope due to the aluminum barrier layers ensuring its tightness. VIPs are considered as high-performance thermal insulation material systems. The VIPs were applied in the field of refrigeration in the USA, Japan and Europe during 1990s, then the application appeared in the field of architecture at the beginning of the 21st century, first in Europe and now spreading into East Asia and North America.

Mostly previous study focus on the insulation performance, the most of them is about: 1) study on the trial manufacture of VIPs, 2) study on the heat transfer performance of insulation materials, 3) study on the characteristics of materials' outgas and the gas invasion from the external side, 4) study on the applications in buildings, 5) study on research trends and market trends. Study on the trial manufacture of VIPs is summarized as follows: Kim use the phenolic foam as the core material for the trial manufacture [9], P. C. Tseng use the polystyrene foam to making the VIP and the measurement of thermal conductivity of general VIP is using the heat flow meter method [10], the result is $5.0 \times 10^{-3} W/(m \cdot K)$ [9],[10]. In Japan, the silica powder is usually applied to trial manufacture of VIPs, silica aerogel is applied to make the transparent VIP and there exist report when the silica powder applied, the thermal conductivity is less than $2.0 \times 10^{-3} W/(m \cdot K)$. Furthermore, aluminum vapor deposition PET film is applied as core material for analysis which called core material of metallic multilayer and fiber overlapping [11], however, it never be manufactured until now [12]. Analysis of heat transfer model for Nano porous silica vacuum insulation material is proposed by Bouquerel [13]. Kwon proposed the powder type, foam type and the fiber type then the heat transfer model of core material with staggered beam is described. Finally, the fiber type of staggered beam core material is effective as a result [14]. In addition, a method for the performance measurement of VIPs, Johansson proposed a short-term in-situ performance measurement of VIPs, and its accuracy is being verified [15]. In the topic of outgassing, the polymer fiber is applied to the experiment to analyzing the reason of outgassing which is proposed by Kwon [16]. In addition, the gas invasion form the film is described as a mass transfer model inside of the film by Bouquerel [17]. There are some examples of applicability in actual buildings which is introduced in the world, especially in Germany [18]. A trend of the topic by Baetens which reported the study about applications of VIPs in buildings which included investigations, and those elements have been summarized [19].

In this paper, the authors proposed the vacuum layer type VIPs with small thickness and light transmittance which can applied to the buildings directly with attachment installation. The VIPs is product by low thermal conductivity material with high cost performance means the application can be easily replaced. The spacers are determined and 4 vacuum layer type VIPs is carried out. The heat transfer model is carried out by the

1D calculation to predict the insulation performance. In order to produce the specimens for the experimental measurement, the authors insert the core structure (which design and analysis by the structural model) to the gas barrier film and sealed by the vacuum sealing machine. The heat flux meter apparatus is set up and the apparent thermal conductivity is measured to evaluate the insulation performance. Finally, the measurement results are compared with the prediction insulation performance, and the comparison results are summarized.

5.3 Outline and advantages of slim and translucent VIPs

The conventional VIPs have some issues for their applications, such as: expensive cost due to complicated manufacturing process, low durability, possibility of fatal damage due to nailing, influence of thermal bridge. And mostly VIPs have no commercial available which can be applied to windows, appearance of vacuum glazing solved this issue, however, it has high economic cost and less contribution to retrofitting in buildings due to the single purpose and heavy weight. Therefore, it's effective to develop the VIPs to contribute retrofitting insulation for existing buildings. The concept of the developed VIP is described as Figure 1. This study focuses on the insulation performance of VIP, pillars are applied to support the plates to ensure the vacuum layer can be held, plates and pillars with a piece of low-e film are coating by the gas barrier film. This VIP is made of transparent materials so that it has the ability of transparency which the conventional type didn't have. Therefore, this VIP can be applied as attachment insulation material to the wall, roof and window. Application of the VIP to buildings is also described in Figure 5-1.

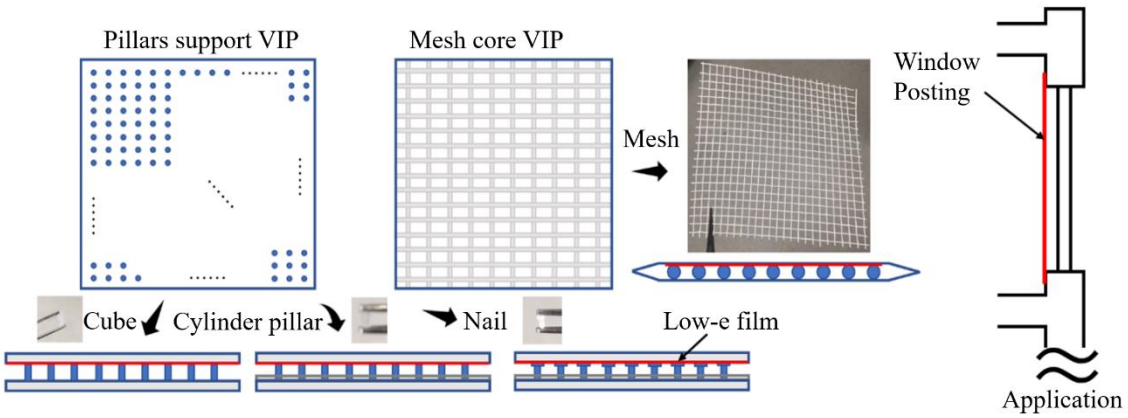

Figure 5-1 Concept diagram of translucent VIP with different spacer and its application

5.4.1 Outlines of 1-D heat transfer calculation model

Figure 5-2 shows the concept diagram of heat transfer calculation model. In this calculation, the spacers with the ratio of area "S" exist in the space which between the two plates. There is no air in the vacuum space (＜10Pa) and the convection can be ignored in the calculation. The heat transmittance included radiant heat transfer in the vacuum space, conduction in the external surface and spacers. In this model, the vacuum space is calculated as thermal resistance Ra [K・m^2/W].

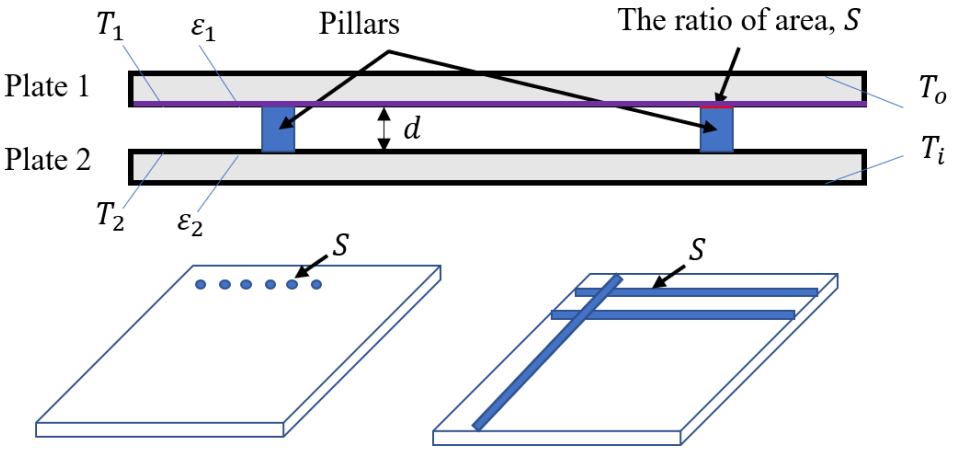

Figure 5-2 Schematic of heat transfer through a double plate unit

5.4.2 Establishment of heat transfer calculation model

The heat transmittance including radiant heat transfer in the vacuum space, conduction in the external surface and spacers. In this model, the vacuum space is calculated as thermal resistance $R_a\,[(m^2 \cdot K)/W]$. When there are the spacers with the ratio of area "S" between the two plate, thermal resistance $R_a\,[(m^2 \cdot K)/W]$ can be described as below:

$$R_a = \frac{1}{\left(\frac{\lambda_v}{d_v} + \alpha_r\right)(1-s) + \frac{\lambda_s}{d_v} s} \tag{3}$$

Radiant heat transfer α_r is calculated by the following equation:

$$\alpha_r = \varepsilon_1 \varepsilon_2 c_b \left\{ \left(\frac{T_1}{100} \right)^4 - \left(\frac{T_2}{100} \right)^4 \right\} \frac{1}{(T_1 - T_2)} \tag{4}$$

Thermal conductivity of vacuum layer λ_v is calculated by the following equation: [22] [23] [24]

$$\lambda_v = 18.2d \frac{\gamma + 1}{\gamma - 1} \frac{\beta p}{\sqrt{MT}} \tag{5}$$

$$\sqrt{\mathrm{T}} \cong \frac{2}{\sqrt{\mathrm{T}_1} + \sqrt{\mathrm{T}_2}} \tag{6}$$

From equation (1), (2), (3) and the following equation, the apparent thermal conductivity of vacuum layer including spacer is calculated.

$$\lambda_a = d_v / R_a \tag{7}$$

Here, λ_v is thermal conductivity of vacuum layer $[W/(m \cdot K)]$, λ_s is thermal conductivity of spacer $[W/(m \cdot K)]$、α is radiant heat transfer $[W/(m^2 \cdot K)]$, d is thickness of vacuum layer $[m]$, $\varepsilon_1, \varepsilon_2$ is emittance of Plata 1, Plate 2 [-], C_b is constant of radiant $[W/(m^2 \cdot K^4)]$, T_1,T_2 is surface temperature of Plata 1, Plate 2 $[K]$, γ is the specific heat ratio c_p/c_v [-], β is accommodation coefficient.

5.4.3 Modelling for vacuum layer type VIP

According to the mechanical analysis and heat transfer model, the authors decide the arrangement of spacers, thickness and properties of materials. And in this paper, the authors compared 4 vacuum layer type VIPs according to the material selection of spacers. Case 1 to Case 4 can be represented the aerogel spacer, cylinder pillars spacer, nail spacer and mesh spacer, respectively. Then the case study and experiment will be done according to these models later. The model of vacuum layer type VIPs is shown from Figure 5-3 to Figure 5-7.

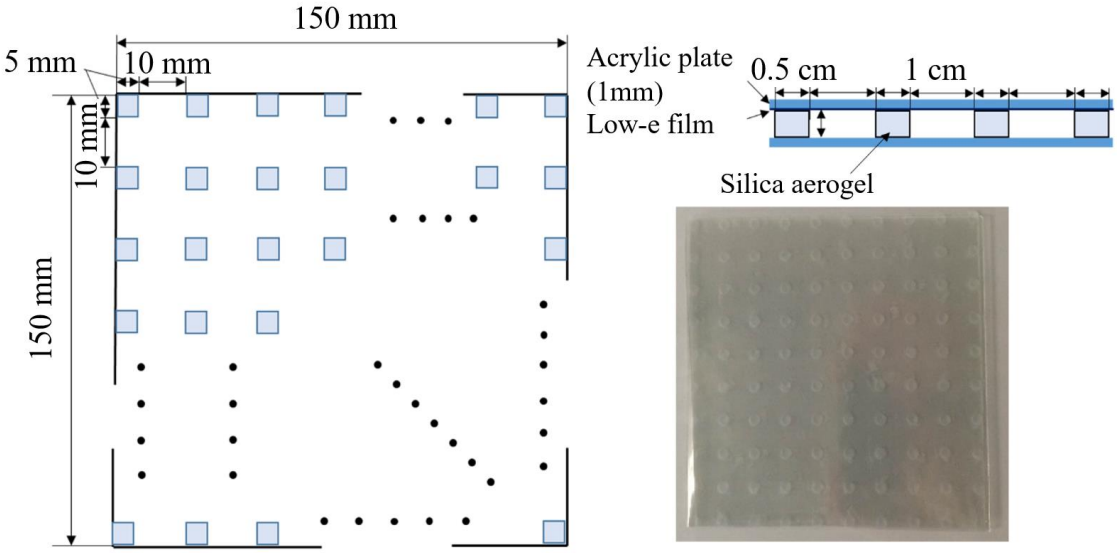

Figure 5-3 Simulation model of aerogel support VIP

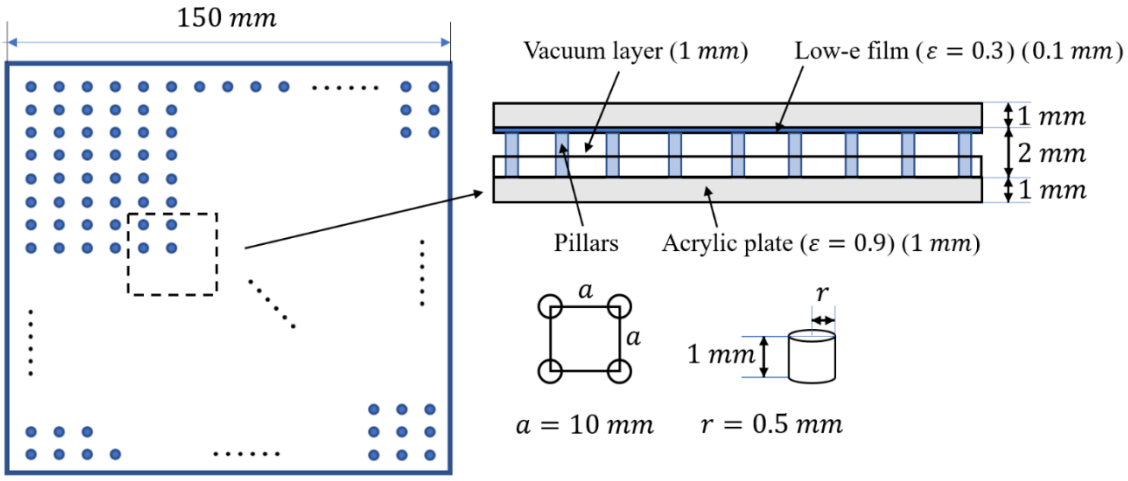

Figure 5-4 Simulation model of cylinder pillar support VIP

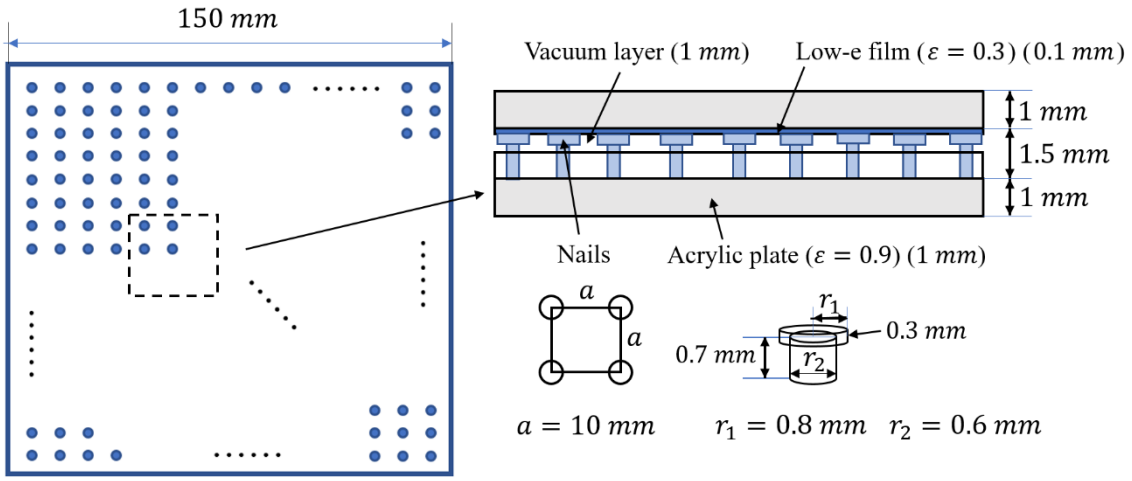

Figure 5-5 Simulation model of nail support VIP

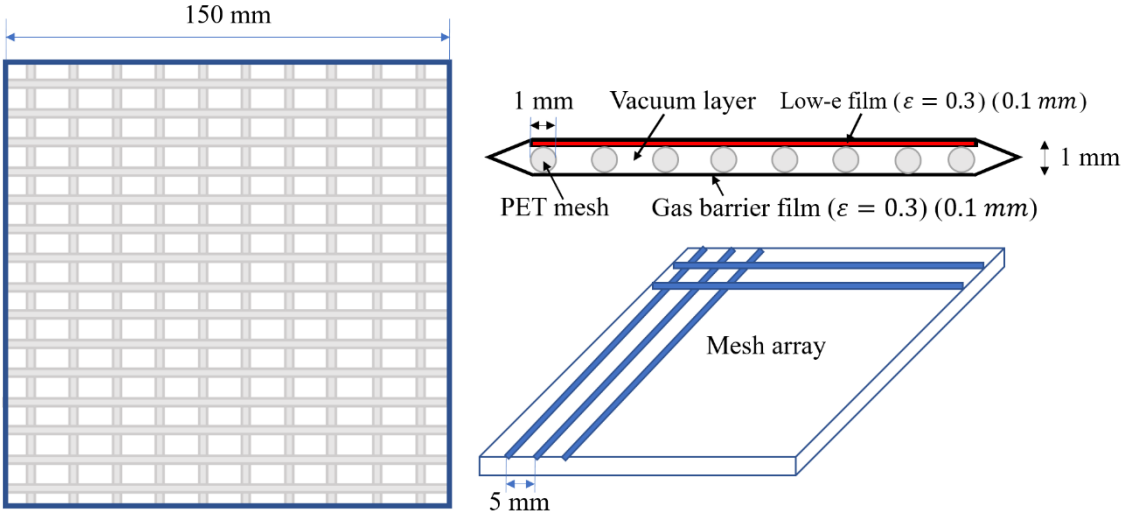

Figure 5-6 Simulation model of mesh support VIP

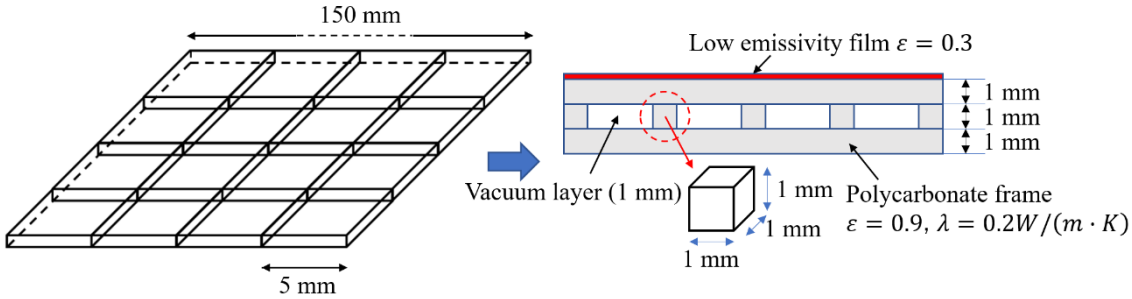

Figure 5-7 Simulation model of frame structural VIP

5.5.1 Trial manufacture of slim and translucent VIP

The size of VIP is designed by the structural model and the insulation performance can be obtained by the heat transfer model. The authors carried out the experiment to confirm the insulation performance of the designed model. The apparent thermal conductivity can be obtained by experiment which will introduced in this section.

5.5.2 Property of gas barrier film

Some of conventional VIPs are coating and sealing by the aluminum foil which applied to refrigerators mostly. Gas barrier film is applied to covering the slim and translucent VIP which is good for sealing and transparent. Table 5-1 shows the property of the gas barrier film which is applied to the trial manufacture of VIP.

Table 5-1 Property of the gas barrier film for experiment

Constitution
PET(100μm)//TEC barrier HX (12μm)【Vapor deposition surface】// Supernylon EH (15μm) // CPP (40μm)
PET(100μm)//TEC barrier LS (12μm)【Vapor deposition surface】// Supernylon EH (15μm) // CPP (40μm)

※ HX: PET vapor deposition with silica

EH: Biaxial stretching film formed by PA/EVOH/PA

◆Size · Z006: 500 mm Width × 200 m × 2R
· Z007: 500 mm Width × 200 m × 2R

5.5.3 Process of manufacture of VIPs

To prevent the dust and static electricity, the specimen should be washed by microwave washer, and desiccated by vacuum dryer. In order to make the specimen in experiment more accuracy, pressure is reduced to 0.1 Pa in the vacuum chamber and keep drying with 80℃ for 24 hours, then specimen can remove the most influence of absorbed gas, water vapor and retained moisture in the surface of materials. Figure 5-8 shows the photograph and schematic diagram of vacuum dryer and Table 5-2 shows its specifications.

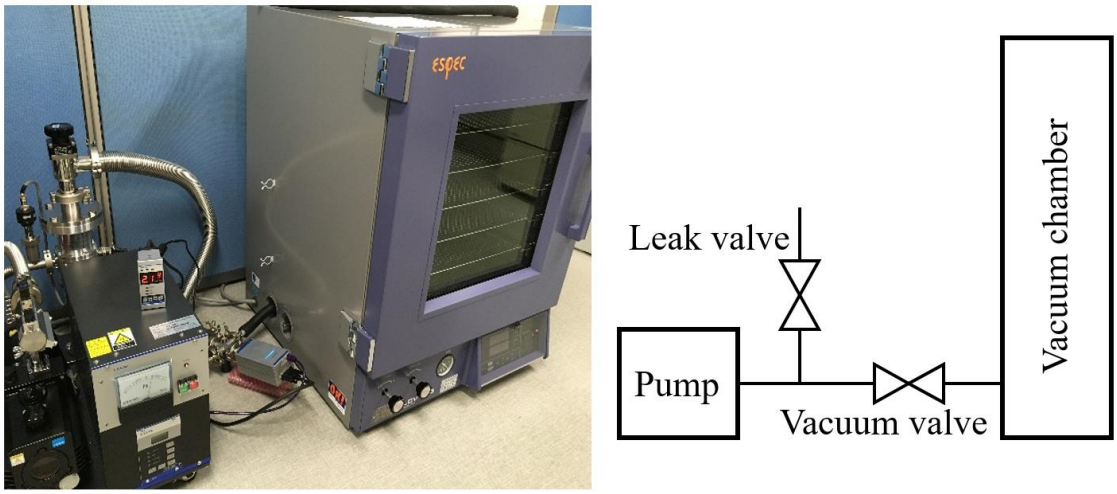

Figure 5-8 Photograph and schematic diagram of vacuum dryer

Table 5-2 Specifications of vacuum dryer

Temperature control mode	Direct heating PID control system
Temperature (˚C)	20~200
Pressure (Pa)	0~-101KPa (Gauge)
Volume (L)	90
Size (W×H×D mm)	450×450×450
Observation window	Tempered glass W400×H400
Pump	GLD-051 50Hz
Pumping speed (L/min)	50
Ultimate pressure (Pa)	0.67 G.V. Close 6.7 G.V. Open

※G.V. is an abbreviation for gas ballast valve

In this stage, core material is formed by the plates with pillars and inserted into the gas barrier film, then sealed by vacuum sealing equipment. And the process is illustrated as Figure 5-9. Figure 5-10 shows the photograph of the vacuum sealing equipment and Table 5-3 shows its specifications.

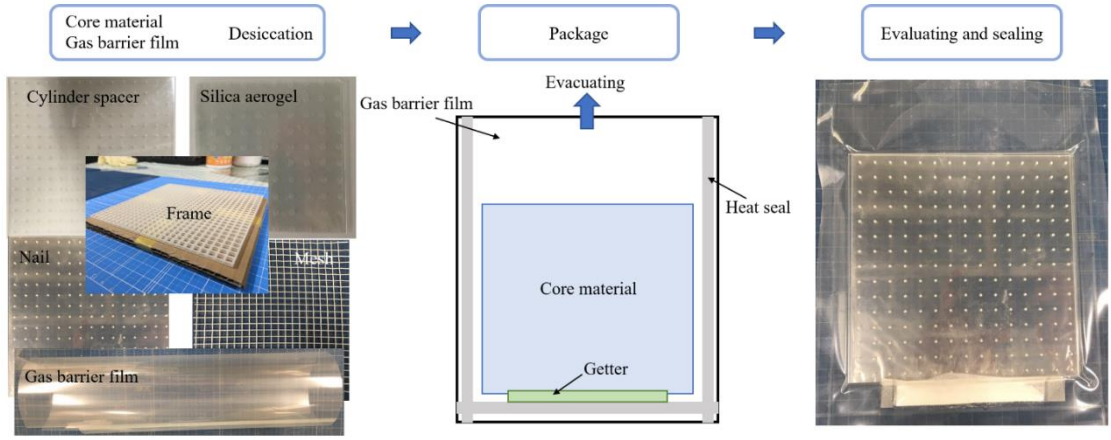

Figure 5-9 Manufacturing process of VIP specimens.

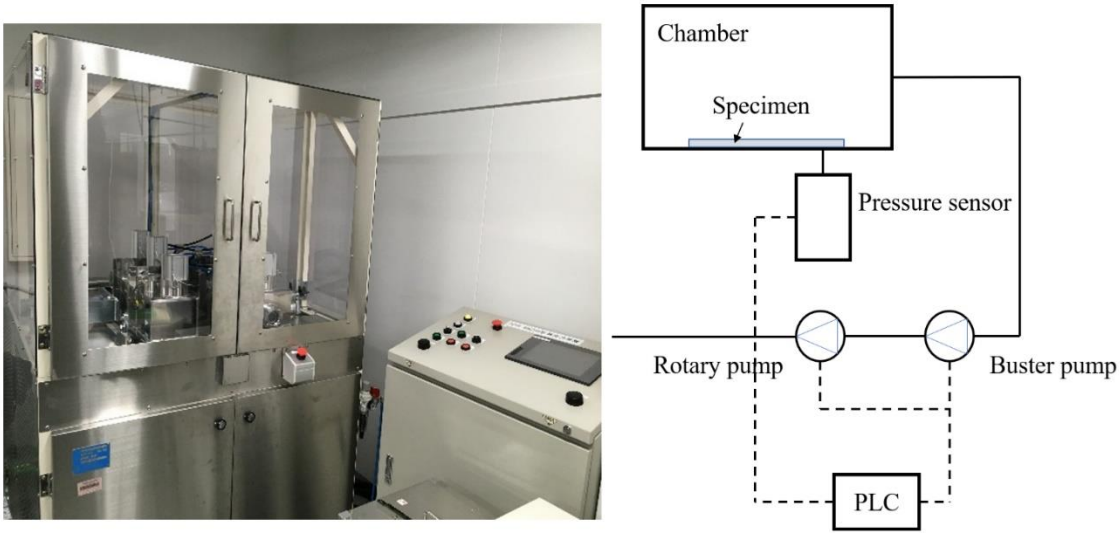

Figure 5-10 Photograph of the vacuum sealing equipment.

Table 5-3 Specifications of vacuum sealing equipment,

Buster pump			Rotary pump		
Exhaust velocity (L/s)	N_2	50	Exhaust velocity (L/s)	N_2	50
	H_2	40		H_2	40
Ultimate pressure (Pa)		10^{-7}	Ultimate pressure (Pa)		6.7×10^{-2}
Exhaust pressure (Pa)		0.13/13	Exhaust pressure (Pa)		0.13/13

For the economic considerations with respect to retrofitting insulation in existing buildings, a reasonable product also requires good cost-performance. Figure 5-11 shows the comparison of the industrial manufacturing cost of these three insulation products.


Silica aerogel core material VIP


Vacuum glazing

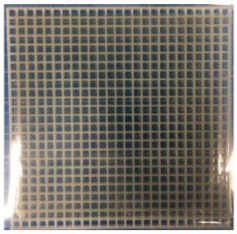
Mesh or frame structural VIP


Cylinder spacer or nail VIP

Products	Industrial production Cost [JPY/㎡]
Silica aerogel core material VIP	> 500,000
Vacuum glazing	> 30,000 (+ 10,000 construction fee)
Mesh and frame structural VIP	< 10,000
Cylinder spacer and nail support VIP	< 11,000

Figure 5-11 Comparison of industrial production cost in different transparent evacuated products.

5.6 Validation of Insulation Performance of Vacuum Layer-Type Slim and Translucent VIPs

5.6.1 Experimental Measurement with a Heat Flow Meter Apparatus

The heat flow meter apparatus is a measuring instrument for determining the steady-state heat transfer properties, thermal conductivity, and thermal resistance of flat slab specimens. It is designed for use in industrial test laboratories for quality control of thermal insulation materials of low and intermediate thermal conductivity, such as polystyrene, cork, wood wool, etc. Figure 5-12 shows the schematic diagram of the heat flow meter apparatus.

During the experiment, the setting temperature to hot and cold plate is 35.5 °C and 10.5 °C, the temperature difference is 25°C. The thermal transmission is measured by heat flux meters and data is treated by the computer. The thermal conductivity according to elapsed time after sealing is investigated by Equation (15).

$$\lambda = \frac{Q}{\Delta T \times d_s} \tag{15}$$

Here, Q is the heat flux through the testing plate (W); ΔT is the temperature difference (°C); and d_s is the thickness of specimen (m).

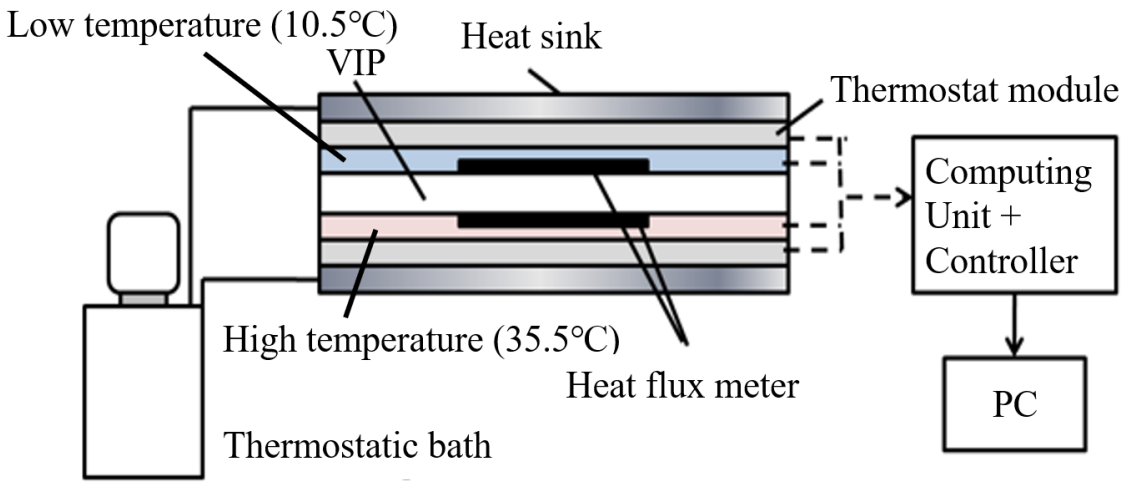

Figure 5-12 Schematic diagram of the heat flow meter apparatus.

5.6.2 Result and discussion

In this section, the authors report the experimental results from the heat flow meter apparatus. The experiment period is set as one hour (45 minutes for the nail spacer type) and shown in Figure 5-13.

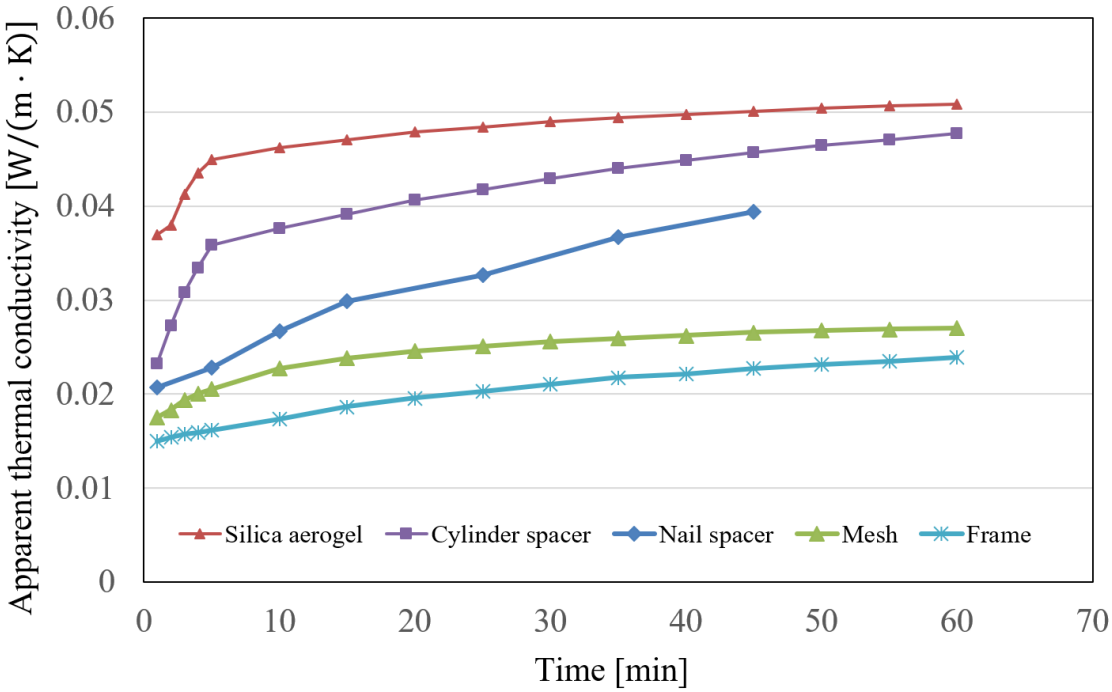

Figure 5-13 Measured apparent thermal conductivity according to elapsed time.

Also, the trial production of VIP and measurement of thermal conductivity is carried

out and repeated 3 times, and the experimental accuracy is validated. A good experimental accuracy is confirmed and obtained by error analysis in Table 2.

Table 5-4 Error analysis for experimental validation

	Minimum average thermal conductivity $(mW/m \cdot K)$)	Deviation	Maximum average thermal conductivity $(mW/m \cdot K)$)	Deviation
Case 3	20.7	1.2	39.4	0.6
Case 4	17.5	1.4	27.1	0.6
Case 5	15.0	0.4	23.9	0.8

In the experiment results from Figure 8, the apparent thermal conductivity is increasing according to the elapsed time. The apparent thermal conductivity is rapidly increasing in the first 10 minutes, and almost constant after one hour. This issue should occur due to the increased pressure, and the reason should be due to the gas generation in the vacuum space caused by the desorption of acrylic plate and the outgassing through the gas barrier film. Therefore, the mesh and frame structure can maintain a vacuum degree better than other proposals. However, the transparent effect is not good due to the tightness web on the surface. It is necessary to redesign the array of the frame structure in a reasonable analysis.

In the experiment results from Figure 8, the apparent thermal conductivity is increasing according to the elapsed time. The apparent thermal conductivity is rapidly increasing in the first 10 minutes, and almost constant after one hour. This issue should occur due to the increased pressure, and the reason should be due to the gas generation in the vacuum space caused by the desorption of acrylic plate and the outgassing through the gas barrier film. Therefore, the mesh and frame structure can maintain a vacuum degree better than other proposals. However, the transparent effect is not good due to the tightness web on the surface. It is necessary to redesign the array of the frame structure in a reasonable analysis.

The authors carried out a case study to predict the insulation performance of VIPs under different conditions. Table 5-5 shows the calculation conditions.

Table 5-5 Calculation conditions.

	Case 1	Case 2	Case 3	Case 4	Case 5
Plan view	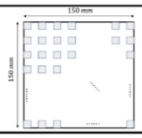	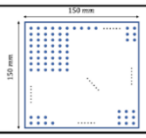	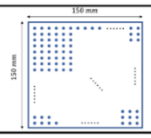	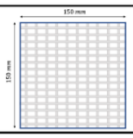	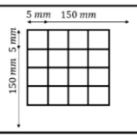
Section view (Vacuum layer)	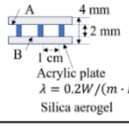	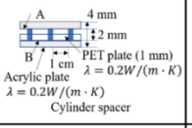	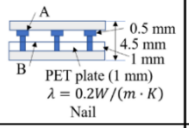	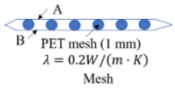	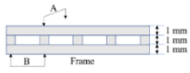
Value of "S"	0.284	0.008	0.011	0.333	a) 0.35 b) 0.03
Specification of spacers	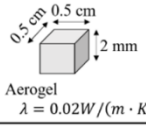	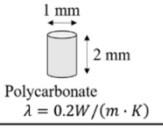	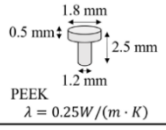	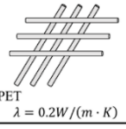	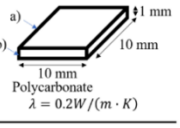
Emissivity of "A and B"	A=0.3 (Assume the low-e film) B=0.9 (Assume the common plastic surface)				

According to the calculation conditions, the insulation performance prediction can be evaluated by analyzing the thermal conductivity. Figure 5-14 shows the comparison of thermal conductivity between measurement and calculation results with internal pressure. From the comparison results, the minimum experiment result shows the experimental specimen can achieve a pressure from 2 Pa to 20 Pa in the vacuum layer. Finally, the internal pressure will reach about 10 Pa due to gas generation and outgassing.

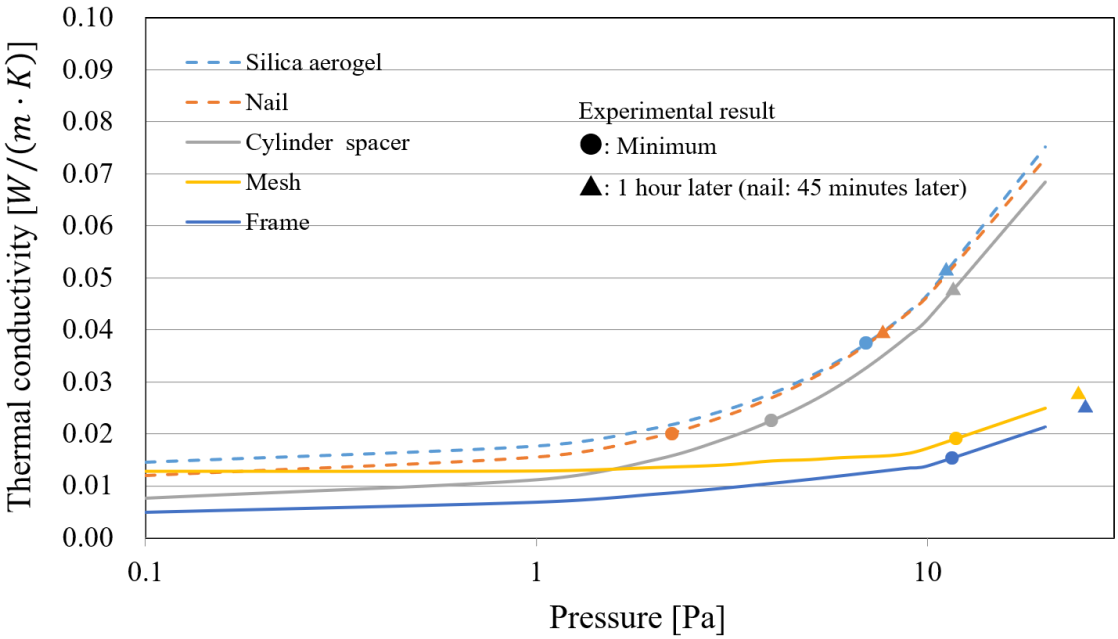

Figure 5-14 Comparison of thermal conductivity between the measurement and the calculation with internal pressure.

Figure 5-15 shows the schematic of illuminance measurement. As the Figure 5-15, the VIP specimen is put on the reflection diffuser and irradiated by incandescent light. The wave length is controlled in 800nm as visible light, and the illuminance is measured with and without VIP shading shown in Table 5-6. The concentration of spacers decided the transparency of Case 2 and Case 3. And in Case 4 and Case 5, the illuminance is decreased due to the concentrated webs.

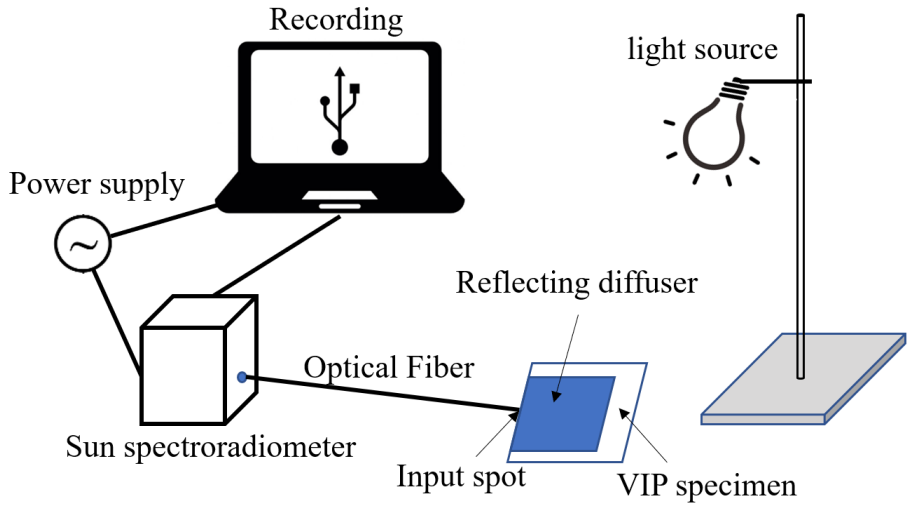

Figure 5-15 Schematic of illuminance measurement

Table 5-6 Results of illuminance measurement

Intensity of radiation at wavelength of 800 nm [$\mu W/cm^2/nm$]						
Conditions	No VIP	Case 1	Case 2	Case 3	Case 4	Case 5
Intensity	20000	14000	18000	17500	13000	15000
Ratio	1	0.70	0.90	0.88	0.65	0.75

According to Figure 5-14, the authors summarized the performance and properties of five cases, as shown in Table 5-7. In Cases 4 and 5, the mesh and frame structural VIP can achieve the most appropriate insulation performance and shows good resistance to degradation, however, it is weak in light transmittance. In Case 1, the aerogel-supported VIP required a high material cost and the performance is no better than the others. Then, in Case 2 and Case 3, the cylindrical pillar-supported VIP and nails-supported VIP achieved relatively good insulation performance and cost performance. However, the degradation of insulation performance is significant due to the acrylic plate having a large area for gas generation.

Table 5-7 Comparison of VIP with different internal structure.

Conditions	Case 1	Case 2	Case 3	Case 4	Case 5
Thickness	○	○	○	○	◎
Theoretical insulation performance	○	○	○	○	◎
Vacuum layer maintains	×	×	×	△	○
Production difficulty	△	○	○	◎	◎
Material cost	×	○	○	◎	◎
Transparency	△	◎	◎	△	○
◎ Excellent; ○ Good; △ Adequate; × Not good					

5.7 Conclusion

1) The authors proposed five structures to make the vacuum insulation panels with small thickness and light weight to apply to windows to contribute to the retrofitting of insulation in existing buildings.
2) The 3-D model is proposed to evaluate the insulation performance and the results are described.
3) The translucent VIPs are produced for experimental validation. The heat flux meter apparatus was set up to measure the thermal conductivity to validate the evaluation of insulation performance.
4) The experimental results are compared to the prediction results, and the effects of different proposals are summarized and evaluated as follows:
   a) No matter what proposal is selected, it can be observed that the apparent thermal conductivity is increasing according to the elapsed time. This is because of the outgassing of components and it is based on the total area of the components.
   b) The mesh and frame structural model can achieve better insulation performance and good resistance to degradation. The frame structure is better to hold the vacuum layer and can be easily manufactured by a 3-D printer. It is worth developing the frame structural VIP to retrofit the insulation in existing buildings.

Reference:

[1] I. M. Kirlin: United State Patent 1,370,974(1921)
[2] R. E. Collins, G. M. Turner, A. C. Fisher-Cripps: Vacuum Glazing-A New Component for Insulating Windows, Building and Environment, Vol. 30, No. 4, pp. 459-492(1995)
[3] A. C. Fisher-Cripps, R. E. Collins, G. M. Turner, E. Bezzel: Stress and Fracture Probability in Evacuated Glazing, Building and Environment, Vol. 30, No. 1, pp. 41-59(1995)
[4] J. D. Garrison and R. E. Collins: Manufacture and cost of Vacuum Glazing, Solar Energy, Vol. 55, No. 3, pp. 151-161(1995)
[5] G. M. Turner and R. E. Collins: Measurement of Heat flow through Vacuum Glazing at elevated Temperture, Journal of Heat Mass transfer, Vol. 40, No. 6, pp. 1437-1446(1997)
[6] M. Lenzen and R. E. Collins: Long-term Field Tests of Vacuum Glazing, Solar Energy, Vol. 61, No. 1, pp. 11-15(1997)
[7] R. E. Collins and T. M. Simko: Current Status of the Science and Technology of Vacuum Glazing, Solar Energy, Vol. 62, No. 3, pp. 189-213(1998)
[8] T. M. Simko, A. C. Fisher-Cripps and R. E. Collins: Temperature-induced in Vacuum Glazing Modelling and Experimental Validation, Solar Energy, Vol. 63, No. 1, pp. 1-21(1998)
[9] Jongmin Kim, Jea-Hyug Lee, Tea-Ho Song: Vacuum Insulation Properties of Phenolic Foam, International Journal of Heat and Mass Transfer, Volume 55, Issues 19-20, pp.5343-5349(2012)
[10] P. C. Tseng, H. S. Chu: The effects of PE Additive on the Performance of Polystyrene Vacuum Insulation Panels, International Journal of Heat and Mass Transfer, Volume 52, Issues 13-14, pp. 3084-3090(2009)
[11] Jongmin Kim, Choonghyo Jang, Tea-Ho Song: Combined heat transfer in multi-layer radiation shields for vacuum insulation panels: Theoretical/numerical analysis and experiment, Applied Energy, Volume 94, pp. 295-302(2012)
[12] Jea-Sung Kwon, Choonghyo Jang, Heayong Jung, Tea-Ho Song: Vacuum maintenance in vacuum insulation panels exemplified with a staggered beam VIP, Energy and Buildings, Volume. 42, Issues 5, pp. 590-597(2010)
[13] Mathias Bouquerel, Thierry Duforestel, Dominique Baillis, Gilles Rusaouen: Heat transfer modelling in vacuum insulation panels containing nanoporous silica-A review, Energy and Buildings, Volume 54, pp. 320-336(2012)
[14] Jae-Sung Kwon, Choonghyo Jang, Haeyong Jung, Tae-Ho Song: Effective thermal conductivity of various filling materials for vacuum insulation panels, International Journal of Heat and Mass Transfer, Volume 52, Issues 23-24, pp. 5525-5532(2009)

[15] Pär Johanssonn, Bijan Adl-Zarrabi, Carl-Eric Hagentoft, Using transient plane source sensor for determination of thermal properties of vacuum insulation panels, Frontiers of Architectural Research, Volume 1, Issues 4, pp. 334-340(2012)
[16] Jae-Sung Kwon, Haeyong Jung, In seok Yeo, Tae-Ho Song: Outgassing characteristics of a polycarbonate core material for vacuum insulation panels, Vacuum, Volume 85, Issues 8, pp. 839-846(2011)
[17] Mathias Bouquerel, Thierry Duforestel, Dominique Baillis, Gilles Rusaouen: Mass transfer modelling in gas barrier envelops for vacuum insulation panels: A review, Energy and Buildings, Volume 55, pp. 903-920(2012)
[18] J. Fricke, U. Heinemann, H. P. Ebert: Vacuum insulation panels-From research to market, Vacuum, Volume 82, Issues 7, pp. 680-690(2008)
[19] Ruben Baetens, Bjørn Petter Jelle, Jan Vincent Thue, Martin J. Tenpierik, Steinar Grynning, Sivert Uvsløkk, Arild Gustavsen: Vacuum insulation panels for building applications: A review and beyond, Energy and Buildings, Volume 42, Issues 2, pp. 147-172(2010)
[20] Timoshenko. S, Woinowsky-Krieger S. Theory of Plate and Shell. McGraw-Hill Book Company: 1959, PP.106−108.
[21] Roark R J, Warren C, Young Richard G. Budynas. Formulas for Stress and Strain (Seven Edition): PP. 508~509.
[22] Handbook of Vacuum Technology (1st Edition), Edited by Karl Jousten, (2008) pp. 51-81.
[23] E. R. G. Eckert, Robert M. Drake, Heat and Mass Transfer, McGraw-Hill Inc. US; 2nd Revised Edition (1959/12)
[24] Springer G. S. Heat Transfer in Rare field Gases. Advances in Heat Transfer, 1971, 7(2), PP. 163~218.

Chapter 6
Investigation on reduction of thermal bridge to existing building with installing multilayered VIP and field experiment

6.1 Introduction

Of late, various energy saving techniques are being employed in new buildings; however, these techniques are difficult to apply to existing buildings. In particular, as most of the existing buildings have poor insulation performances, it is important to improve them. Evacuated insulating material, consisting of a single slim and light weight panel, also known as a vacuum insulation panel (VIP), can be applied to architecture to render it easier to obtain a higher insulation performance. VIPs have the potential to improve the insulation performance; however, conventional VIPs have application issues such as high costs owing to a complicated manufacturing process, low durability, possibility of fatal damage due to nailing, and the thermal bridge effect [1] [2] [3] [4]. The thermal bridge, previously known as the cold bridge, has a significant negative impact on the building performance. External insulation is usually applied to reduce the effect of the thermal bridge [5] [6] [7] [8], for improving the building insulation performance. Therefore, it is crucial to improve slim and multiple layered VIPs with an overlapping installation to reduce the construction costs and enhance the insulation quality [9] [10].

There are several studies regarding VIP application for retrofitting existing buildings [7] [11] [12], including a composition board that combines VIPs with urethane foam, which can be applied to the buildings to conform to their application performance, as described in Figure 1. This can be a mainstream application method because the core material in most evacuated insulating products is glass wool [8] [13] [14] [15], also existed other materials can be filled into gas barrier envelope that we called it core material, such as silica powder, glass fiber and silica gel, etc. Glass wool, as a core material for the VIP, exhibits a good performance but the product requires complicated-manufacturing techniques to render it highly-flat and slim, during application. For VIPs with glass-wool as the core material, the only way to achieve a good insulation performance is to follow the description in **Figure 1**. However, it would be unrealistic to follow this method for the retrofit insulation of a slim wall because the combination part is very thick. In addition, the thermal bridge would also negatively impact the insulation performance.

This paper proposes the attachment of slim and light weight VIPs to internal insulation in an overlapping mode. Then, the VIPs can be applied directly to a building and the construction can be simplified. They also explore whether the overlapping mode can reduce the thermal bridge effect. With respect to the durability, if the VIPs are easy to install, the degraded ones can be replaced by new ones, owing to the highly cost-effective

core material. In terms of the cost, simplification in the production of VIPs with slim and flat core material can be expected in the preparation stage.

It's impossible to covering one insulation material to the walls and ceiling completely, Usually, insulation materials are assembled as one with enough numbers, however, this assembly produce seams where thermal bridge affect. Thickness of conventional vacuum insulation panel is about 10 mm, therefore, the overlapped combination is meaningless. The reduction performance of thermal bridge with VIP overlapped combination application is not quantified so far. In this study, total thickness of multilayered (triple layer) should be limited less than 10 mm, so that an element should less than 3.3 mm. For this objective, the authors carried out the selection of VIP core material and the specimen is product. To analyze the performance to reduce the thermal bridge, the authors carried out numerical model to predict the insulation performance in our proposal and the result is validated by hot box experiment. The proposed application (triple layer) performance in building is investigated and result is excellent. In Japan, China and other Asian countries, insulation performance in some existing buildings is poor, and this study can make contributions to retrofitting insulation to these buildings.

In this study, the apparatus is setup to analyze the “R” value to evaluate the insulation performance by a calibration hot-box measurement [16] [17] [18]. Initially, in the experiment, the insulation performance of each material is compared with the corresponding specification in order to select an appropriate core material for manufacturing the VIP test specimens. Further, a calculation model is generated to analyze the insulation performance, based on the overlapped multilayer VIPs, as illustrated in Figure 2. The width of the seam is changed to validate the experimental results, as further theoretical proof, for retrofitting existing buildings [6] [19].

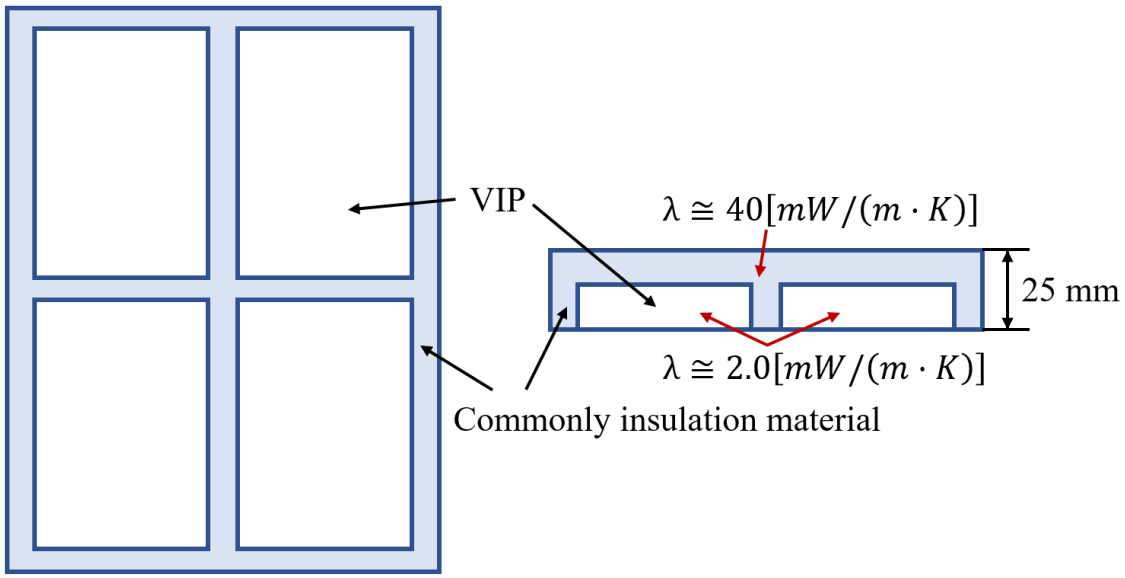

Figure 6-1 Conventional VIP application method

6.2 Methodology

6.2.1 Outline of the experiment

In this study, the insulation performance is evaluated using a calibration hot-box apparatus. Figure 6-2 shows the schematic of the calibration hot-box setup, which includes a calibration hot-box system, thermostatic chamber, measurement system, and the measurement points [20] [21] [22] [23]. The specifications of the devices in the experiment are listed in Table 6-1. In this experiment, the low temperature is set in the chamber as 5 ℃ and the high temperature is set in the hot-box as 25 ℃, respectively. This hot-box apparatus can simulate indoor and outdoor environments naturally; a heater and fan can simulate the indoor environment including the temperature control and ventilation. Figures 6-3 and 6-4 show the variation in the measured temperature and power consumption. Data is recorded every 5 min and the average data selected from the relative static measurement results is used. During the experimental period, the temperature is maintained a relative constant and the power consumption is recorded to derive the amount of heat passing through the test specimen. The overall heat transfer coefficient can be evaluated by equation (1). Here, the solution of equation (1) can be obtained by inputting the calculation results from equations (2) [24], (3), and (4). The average temperature can be adopted as the average value of the measurement points in a 10-min

period and can be used as a representative value.

$$U = \frac{Q}{A \times (\theta_{n,h} - \theta_{n,l})} \tag{1}$$

$$\theta_n = \frac{\theta_a \times {Q}/{A} + \alpha_r(\theta_a - \theta_r)\theta_s}{{Q}/{A} + \alpha_r(\theta_a - \theta_r)} \tag{2}$$

$$\alpha_r = 4\sigma E T_m{}^3 \tag{3}$$

$$T_m \cong \frac{(\theta_r + 273.15) + (\theta_s + 273.15)}{2} \tag{4}$$

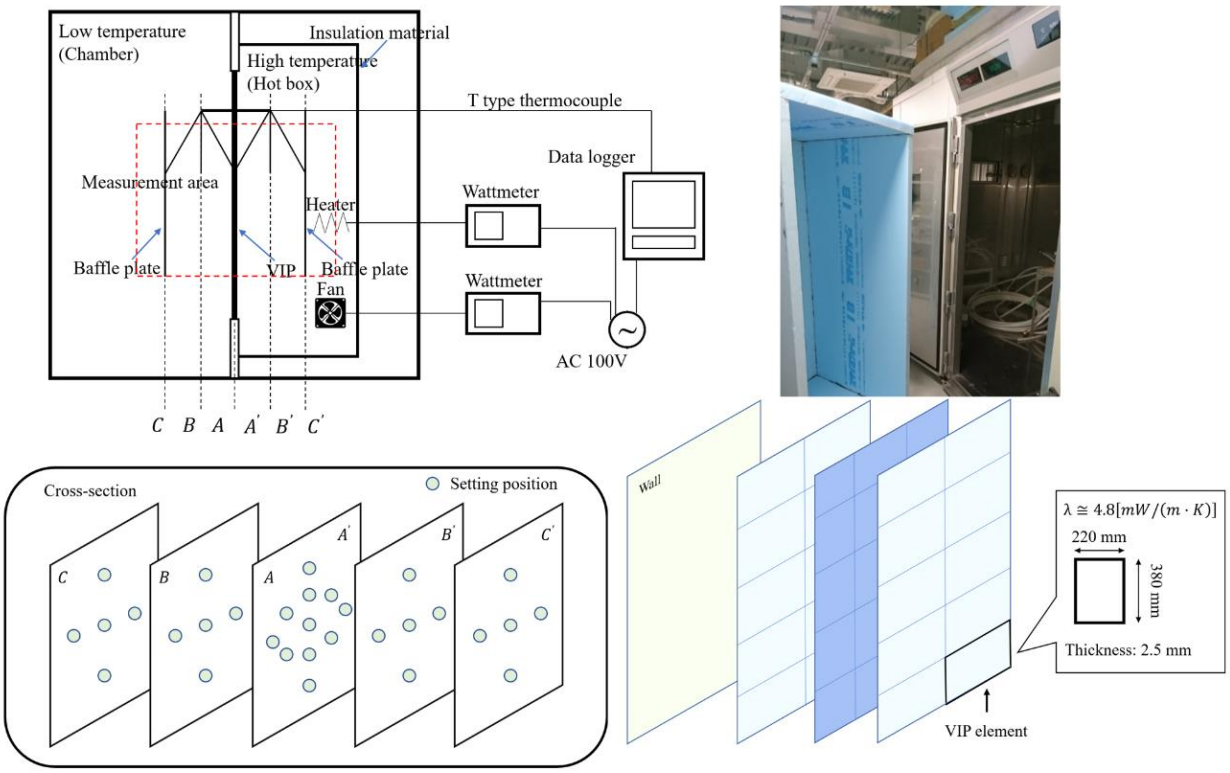

Figure 6-2 Schematic of the calibration hot-box apparatus

Table 6-1 Specifications of the devices in the experiment

Device	Specification
Heater	Length: 1.5 m Heating output: 45W (100V)
Controller	Sensor: Pt100 PID control strategy
Power meter	Clamp power meter Accuracy: Electric ±1.2%
Thermocouple	T type thermocouple Accuracy: ±0.5℃
Data logger	Measurement points: 42
Thermometer (For external temperature)	Accuracy: ±0.5℃
Thermal camera	Resolution: 120×99 Pixel Accuracy: ±2%

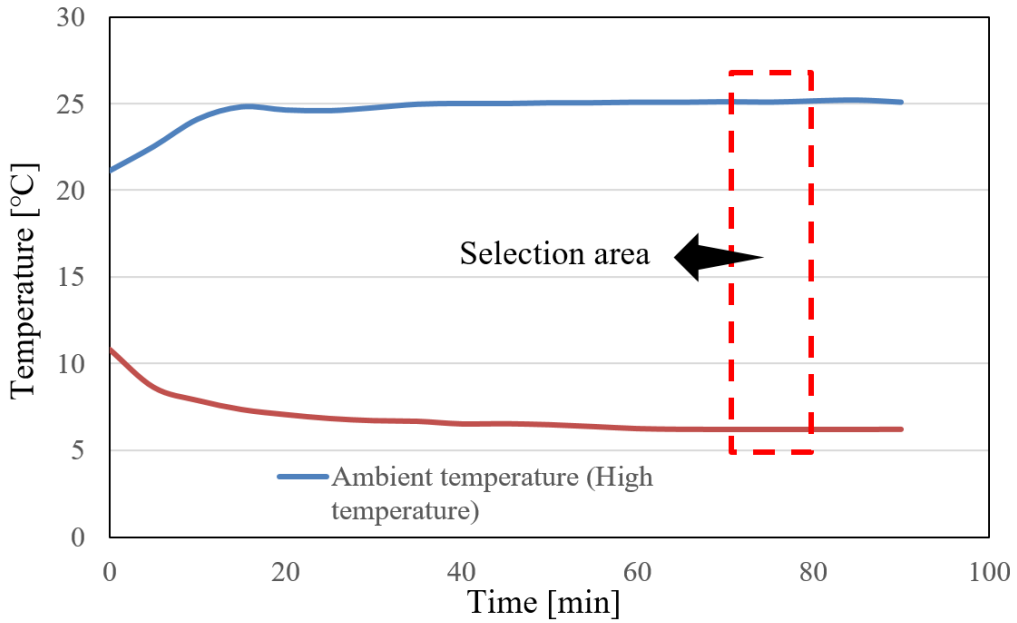

Figure 6-3 Temperature measurement results

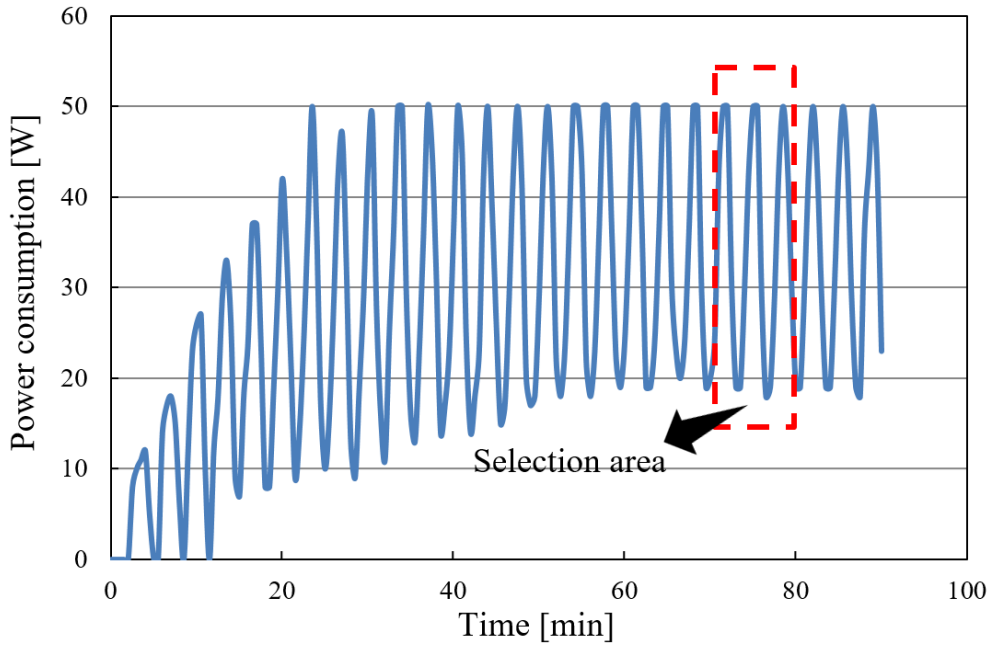

Figure 6-4 Power consumption measurement results

In this experiment, as shown in Figure 6-5, the power consumption of heater "Q" is described by equation: $Q = Q_0 + Q_1 + Q_2$, where Q_0 is the amount of heat passing through the test specimen, Q_1 is the heat loss due to the temperature difference between the high and low temperature sides, Q_2 is the heat loss due to the temperature difference between the high temperature and the indoor temperature, and d is the thickness of the VIP specimen. In this experiment, the low temperature is set in the chamber as 5 ℃ and the high temperature is set in the hot-box as 25 ℃, respectively. Therefore, Q_1 is a relative constant and Q_2 varies along with the variation in the indoor temperature. The calibrated value, Q_{0C}, can be calculated using equation (5); α_r can be calculated by equation (4). The overall heat transfer coefficient of polystyrene foam can be calculated using equations (6) and (7). Compared to Q_0 and the amount of heat, Q, which can be obtained in the experiment, the heat loss, excluding the heat transfer effect, can be solved using the equation, $Q_{loss} = Q_1 + Q_2$. $Q_{loss,}$ described as $Q_0 = Q - Q_{loss}$, can be evaluated by measuring the indoor temperature. Thus, Q_0 can be substituted for Q in equation (1). The calculation condition is shown in Table 6-2 and the calibration of the experimental results is illustrated in Figure 6-6.

$$Q_{0C} = U_0 \times A \times \Delta T_n \tag{5}$$

$$U_{0C} = \frac{1}{1/\alpha_{ti} + d_{Foam}/\lambda_{Foam} + 1/\alpha_{to}} \tag{6}$$

$$\alpha_t = \alpha_r + \alpha_c \tag{7}$$

It can be assumed that the testing surface is windless and that the convective heat transfer coefficient $\alpha_c = 4.4\ W/(m^2 \cdot K)$.

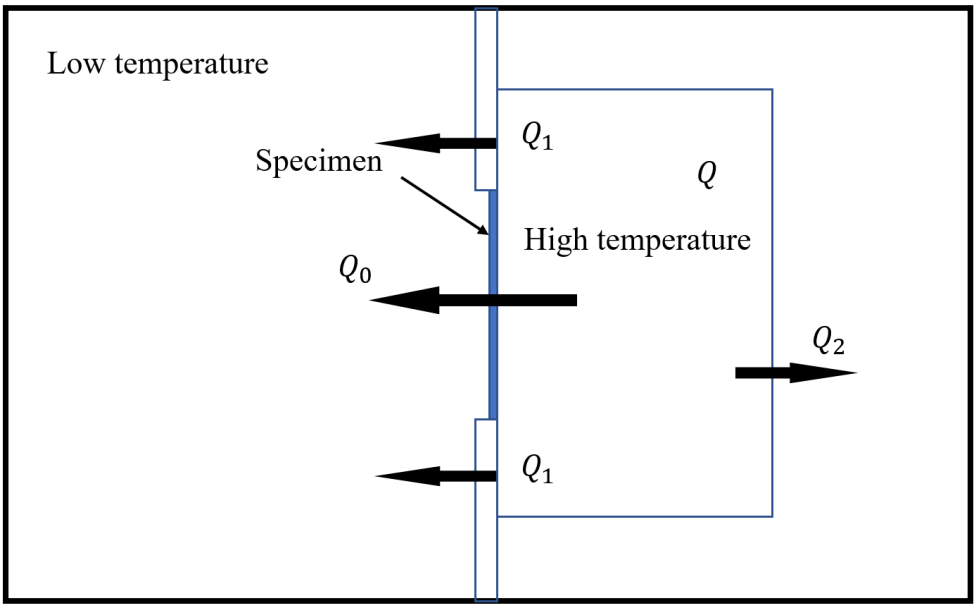

Figure 6-5 Heat loss concept diagram

Table 6-2 Calculation conditions

Area	1.564
Polystyrene foam	
Thermal conductivity [W/(m·K)]	0.04
Thickness [m]	0.025
Thermal emissivity (Hot box side)	
Specimen	0.9
Baffle plate	0.94
Thermal emissivity (Chamber side)	
Specimen	0.9
Baffle plate	0.94

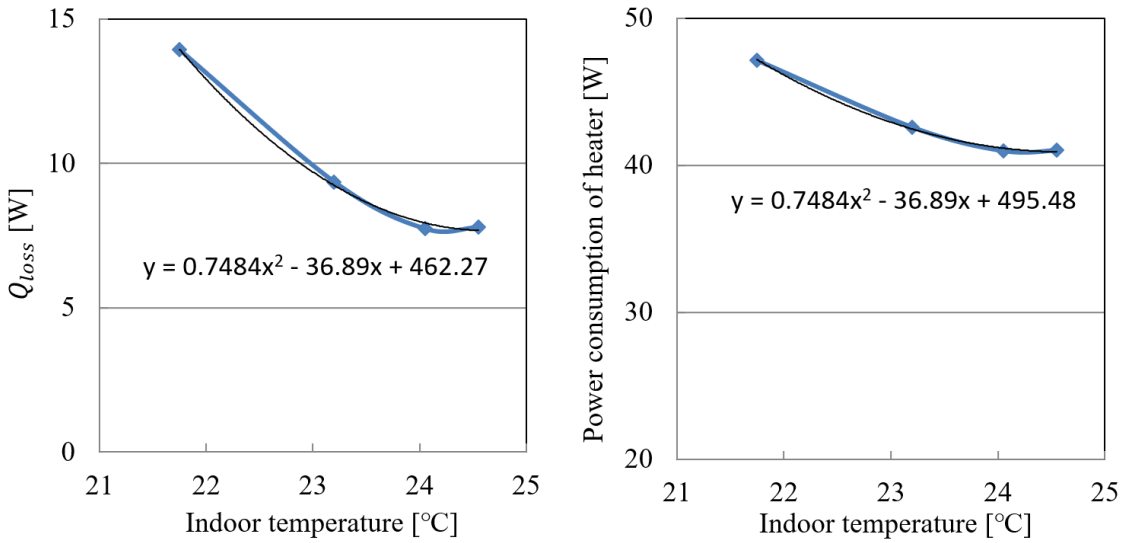

Figure 6-6 Calibration data for the measurement results

6.2.2 VIP production and performance evaluation

The VIP test specimen is produced as per the flow in Figure 6-7. The polyester fiber core material is covered by aluminum film. In order to prevent degradation with time, calcium oxide getter is sealed together with the core material. The getter absorbs gas and effectively prevents performance degradation.

This paper focuses on obtaining a core material which is slim, flat, has a low thermal conductivity, and is easy to produce. Tables 6-3 and 6-4 depict the selection method for the core material; further, the VIP is produced as per the process shown in Figure 6-7. For the evacuated insulation material, the air tightness is critical and the components of the gas barrier film are depicted in Figure 6-8.

Next, a VIP checker is applied to simplify the performance evaluation. The schematic of the VIP checker is shown in Figure 6-9. For this experiment, it is proposed that the maximum number of layers for an overlapping installation is three; it is established that the test specimens have an average thermal conductivity of $4.8mW/(m \cdot K)$, as is illustrated in Figure 6-10.

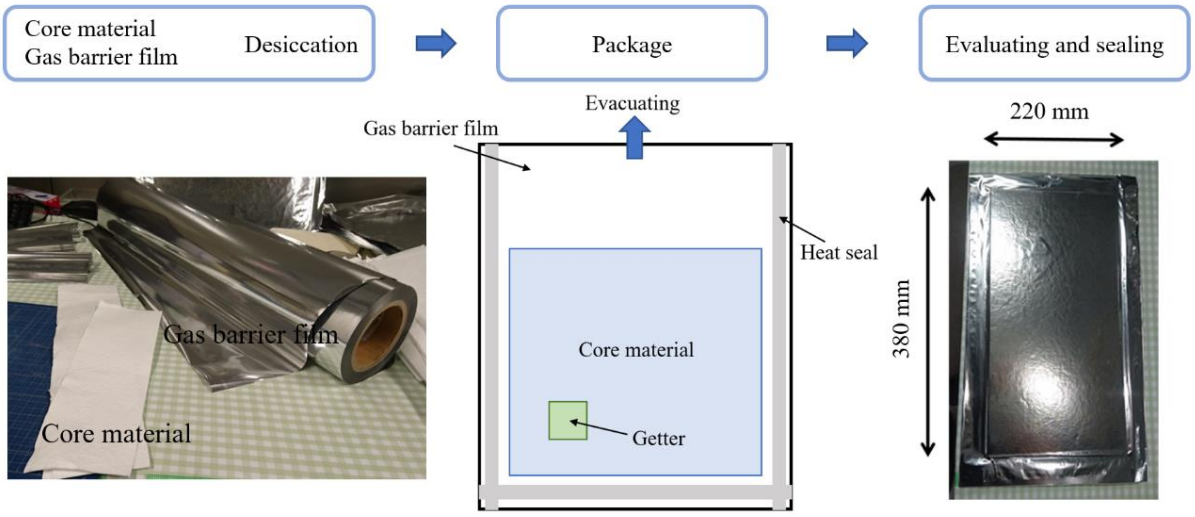

Figure 6-7 Manufacturing flow of the VIP specimens

ON 25 μm
Aluminum evaporated PET 12 μm
Aluminum 6 μm

LLDPE 50 μm

※ON: Oriented Nylon
PET: Polyethylene terephthalate
LLDPE: Linear Low Density Polyethylene

Figure 6-8 Component diagram of the gas barrier film

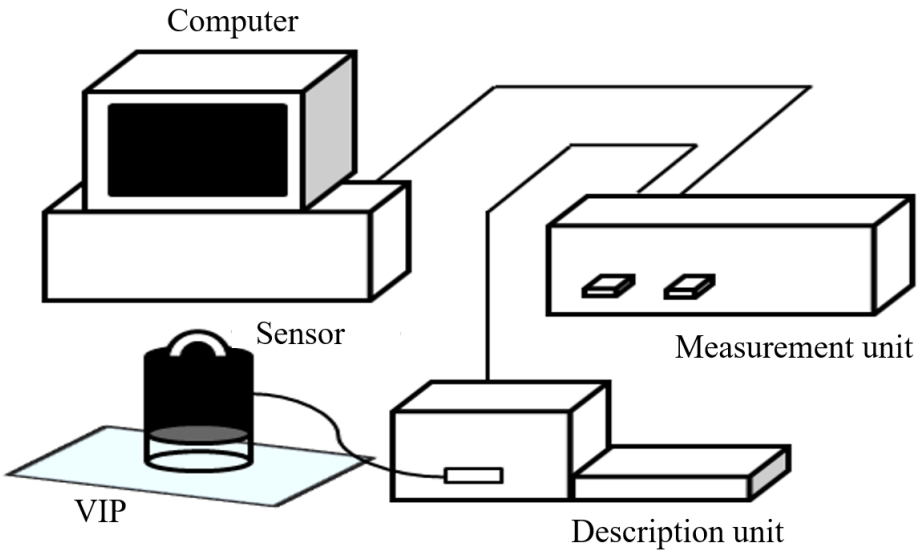

Figure 6-9 VIP checker schematic

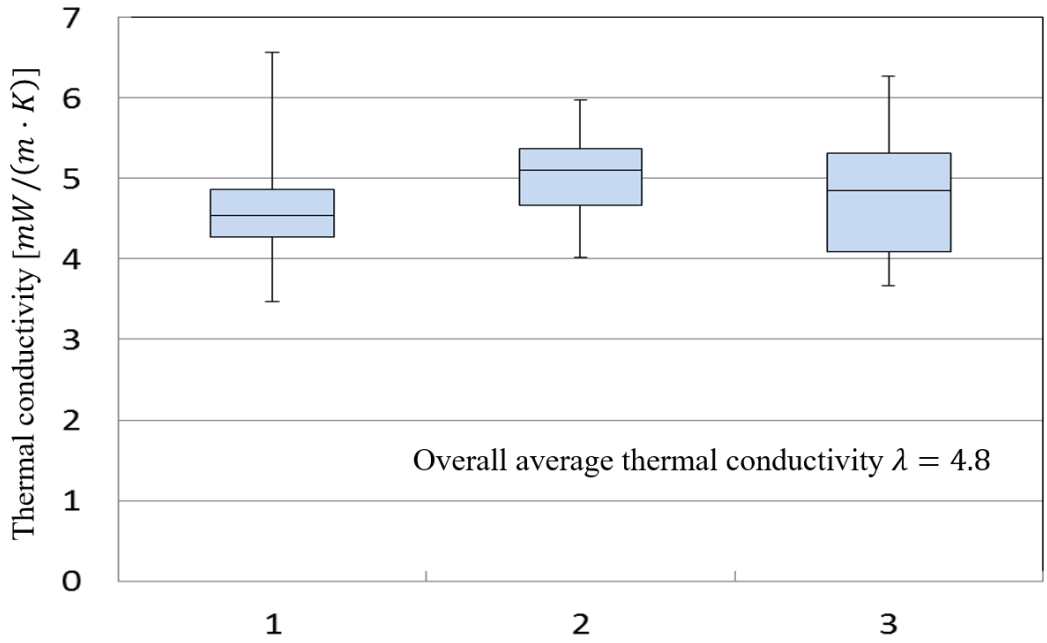

Figure 6-10 Measurement results by the VIP checker

Table 6-3 Requirement specification for the core material

Requirement of Specification for core materials	
· Thickness [m]	≤ 3 mm
· Thermal conductivity [mW/(m·K)]	≤ 7
· Flat	
· Making difficulty	

Table 6-4 Selection of the core material

	Thickness	**Thermal conductivity**	**Flat**	**Making difficulty**
①	○	○	○	○
②	×	○	×	×
③	○	×	○	×

① Polyester fibre

② Glass wool

③ Silica aerogel + Vacuum layer

6.2.3 Results of the performance evaluation and thermal bridge study

The apparent thermal conductivity, λ_a, of the VIP is calculated from the experimental results and equation (8); d_{VIP} is the thickness of the VIP specimen, d_{Foam} is the thickness of the polystyrene foam used to simulate the building envelope, and λ_{Foam} is the thermal conductivity of the polystyrene foam. Table 6-5 shows the experimental results.

$$\lambda_a = \frac{U \cdot d_{VIP}}{1 - U \cdot \left(\frac{1}{\alpha_{ti}} + \frac{d_{Foam}}{\lambda_{Foam}} + \frac{1}{\alpha_{to}}\right)} \tag{8}$$

Table 6-5 Experimental results

	Hot box			Chamber								
	θ_s	θ_a	θ_r	θ_s	θ_a	θ_r	ΔT_n	Indoor temperature	Q	Q_0	U	λ_a
	24.54	25.24	25.15	6.43	6.58	7.14	18.92	24.50	31.8095	24.3575	0.8484	0.0071
	24.85	25.31	25.33	7.56	6.18	6.26	19.17	24.45	32.1905	25.0096	0.8463	0.0071
	24.82	25.39	25.37	7.72	6.31	6.44	19.09	24.20	32.3810	24.6340	0.8370	0.0068
	24.86	25.22	25.22	7.71	6.39	6.52	18.99	24.45	30.2857	23.1248	0.7924	0.0057
	24.71	25.20	25.03	7.85	6.39	6.51	18.88	24.20	31.4762	23.7493	0.8166	0.0063
	24.83	25.33	25.22	7.80	6.44	6.55	18.83	24.50	32.0000	24.9444	0.8581	0.0074
Average							18.98	24.38	31.6905	24.3033	0.8331	0.0067
	24.67	25.15	25.08	7.23	6.25	6.41	18.96	24.15	24.0476	16.1855	0.5423	0.0051
	24.61	25.16	25.08	7.24	6.29	6.39	18.91	24.30	24.8095	17.2830	0.5819	0.0058
	24.76	25.17	25.06	7.23	6.23	6.36	19.02	24.50	23.9048	16.8591	0.5650	0.0055
	24.59	25.16	25.10	7.24	6.17	6.31	19.04	24.35	23.5714	16.1601	0.5404	0.0051
	24.82	25.14	25.01	7.24	6.14	6.25	19.04	24.45	24.4762	17.3053	0.5829	0.0058
	24.62	25.02	24.80	7.39	6.23	6.37	18.81	24.00	25.7619	17.5441	0.5940	0.0060
Average							18.96	24.29	24.4286	16.8895	0.5678	0.0056
	25.04	25.20	25.22	7.02	6.27	6.38	18.97	23.40	21.0476	11.4272	0.3915	0.0043
	25.30	25.31	25.36	7.19	6.34	6.46	19.02	24.50	20.0952	13.0596	0.4432	0.0052
	24.65	25.23	25.15	6.93	6.07	6.17	19.19	24.30	20.1429	12.7133	0.4258	0.0049
	24.80	25.18	25.10	7.32	6.37	6.45	18.87	24.15	21.4286	13.5164	0.4643	0.0057
	25.16	25.13	25.28	7.08	6.09	6.26	19.13	24.45	20.7143	13.7339	0.4650	0.0057
	24.96	25.20	25.20	7.14	6.23	6.29	19.00	24.50	21.2857	14.2301	0.4834	0.0060
Average							19.03	24.22	20.7857	13.1134	0.4455	0.0053

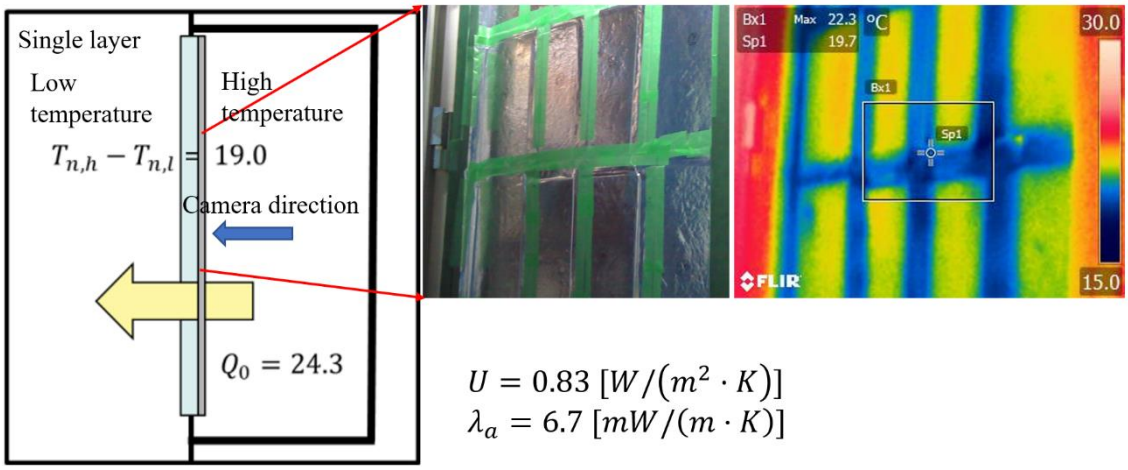

Figure 6-11 Measurement results for a single-layer VIP application

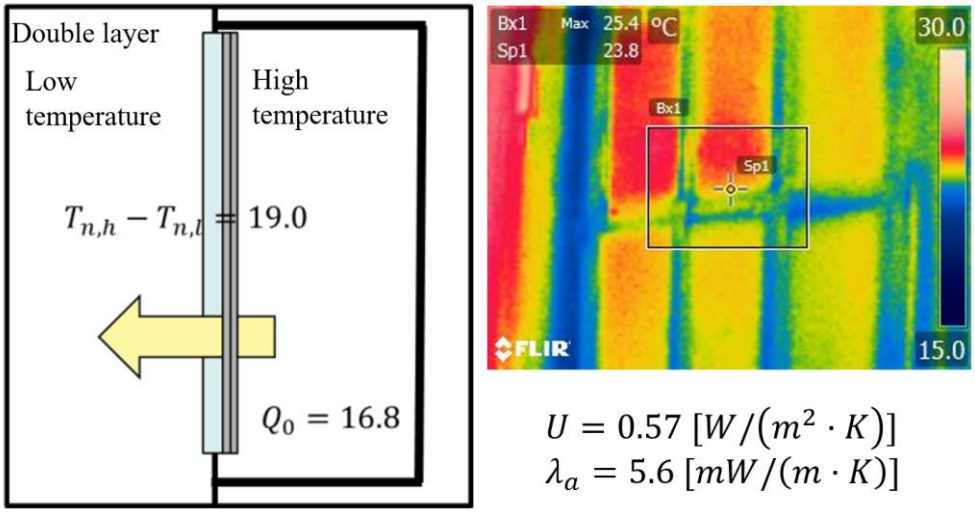

Figure 6-12 Measurement results for a double-layer VIP application

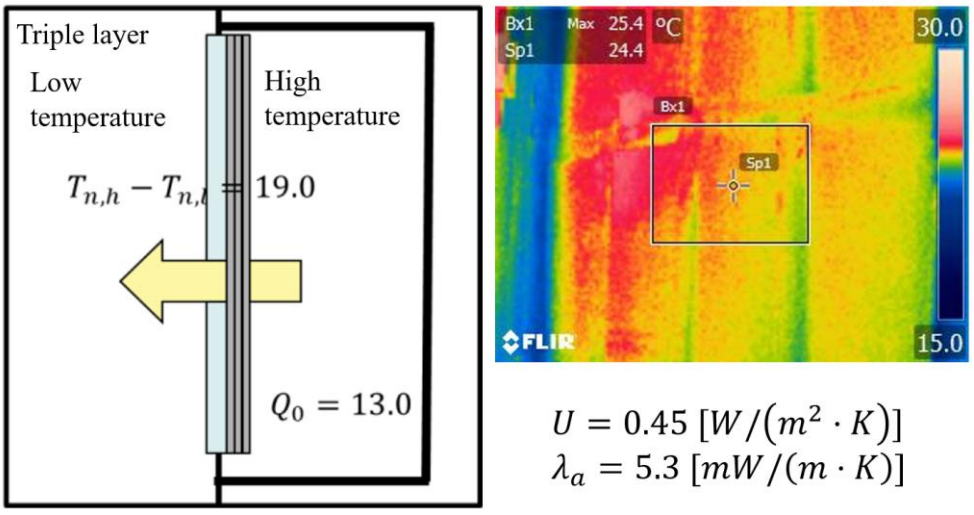

Figure 6-13 Measurement results for a triple-layer VIP application

The results and the thermal camera photograph are depicted in Figures 6-11 ~ 6-13. These results are the average values obtained from tests repeated six times. The effect of the thermal bridge can be evaluated by the apparent thermal conductivity, λ_a; the value can be 1.375, 1.125, and 1.083 times the original, with an overlapped single, double, and triple layer, respectively, insulation. The thermal camera photograph demonstrates that the temperature distribution changes, if multiple overlapping layers are applied. The results indicate that the temperature has a very small decrease, if a triple-layer VIP is installed.

6.3 Evaluation and validation of the insulation performance of multiple VIP combinations

In this section, the heat transmittance is modeled through single, double, and triple layered staggered VIPs. Finally, the simulation results are applied for validation, along with the experimental results. The width of the seam can be applied as the impact condition in which the thermal bridge is affected.

6.3.1 Derivation of the heat transmittance

The heat transmittance is modeled following the experimental specimen application proposal; the width of the seam was set to be 0.3, 0.5, and 0.8 mm. The overlapped mode is modeled as per the experiment depicted in Figure 6-2. The dynamic behavior is solved by “Finite Element Analysis” (FEA). In this study, the calculation model is generated using “ANSYS fluent” software that can provide the results of the heat flux and temperature distributions and the units can be easily changed.

In order to simulate the heat transmittance of the experimental-specimen VIP, the same size as that of the test specimen is used, for confirming the simulation result. To estimate the average heat flux in the edges of a VIP element, the VIP element is first modeled and the result is used for estimating the heat flux in the seam parts of the composed VIP layer.

6.3.2 Calculation conditions and case study

Figure 6-14 shows the calculation model and the conditions. To estimate the overall heat transfer though the application of different-layer compositions, the seams between the horizontal and vertical are assumed to be below 1 mm and the thermal resistance is

calculated as done for the layer combinations. The thermal resistance of the seam can be calculated by equation (9), where d_{seam} is the width of the seam and λ_{seam} is the thermal conductivity of the seam, which can be derived by the average heat flux calculation in the edge of a VIP element.

$$R_{seam} = \frac{d_{seam}}{\lambda_{seam}} \tag{9}$$

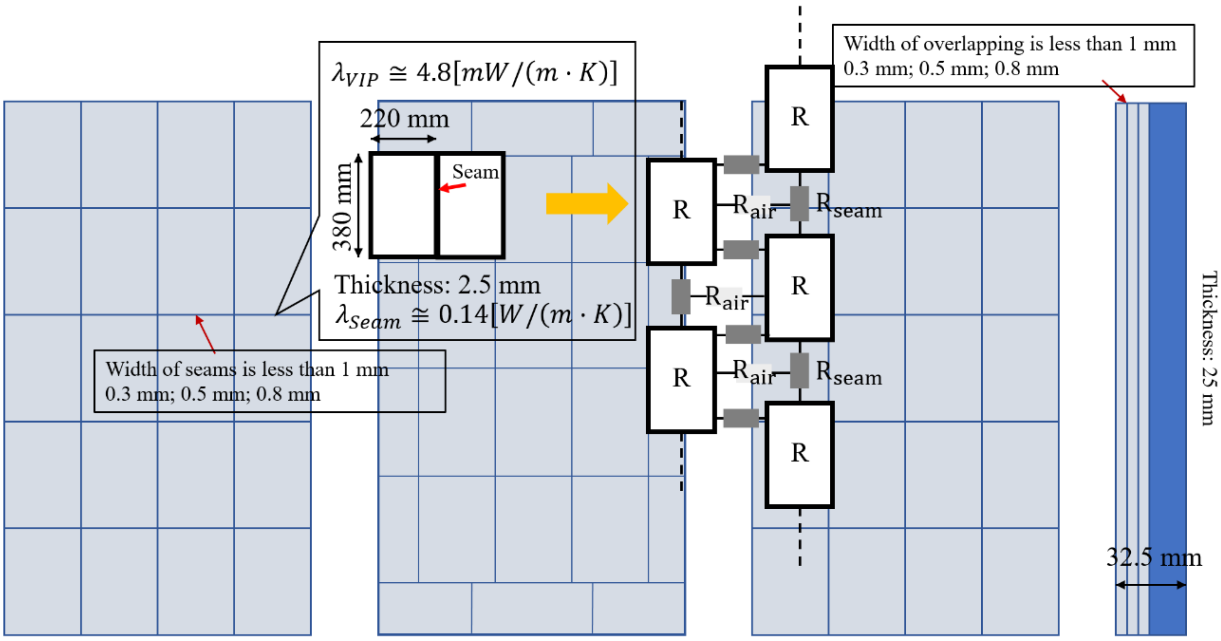

Figure 6-14 Calculation model and conditions

6.3.3 Evaluation of the insulation performance for an overlapped-VIP application

Figure 6-15 shows the comparison of the calculated and experimental results. In the calculation model, the average heat flux (for a single, double, and triple layer overlapped application) can be calculated. λ_a can be calculated using equations (1) and (8).

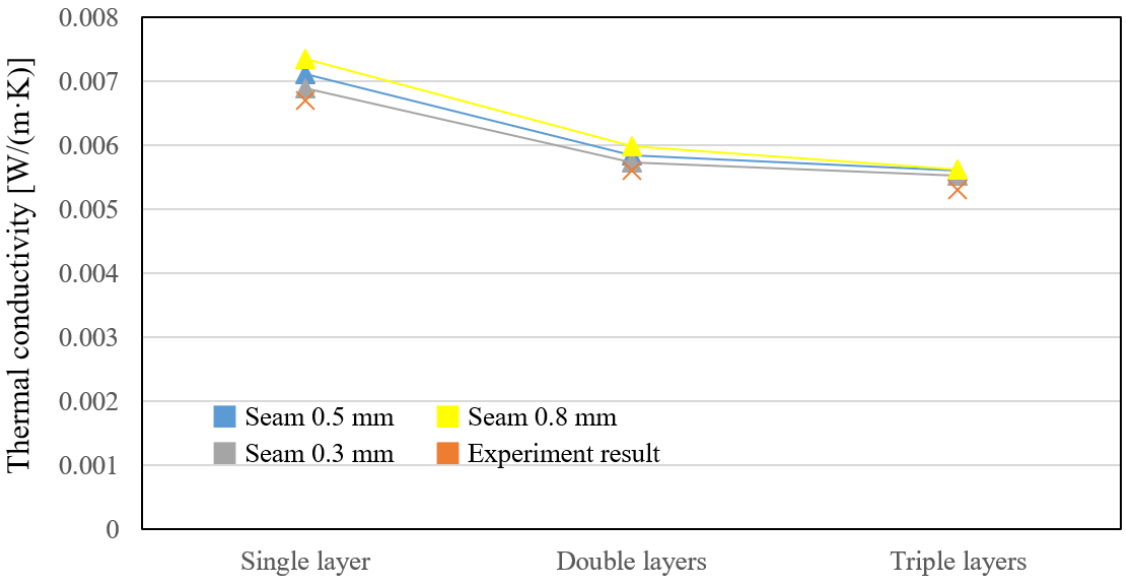

Figure 6-15 Comparison of the calculated and measured results

Figure 6-15 illustrates that the simulation results are well matched with the experimental results. A triple-layer overlapped application can reduce the thermal bridge effectively. The result also shows the advantage of using a multilayer overlapping attachment application; the apparent thermal conductivity of the triple-layer has the same insulation performance as that of the original VIP, effectively reducing the thermal bridge effect.

In this section, the large VIP is modeled to validate a real application performance; Figure 6-16 shows the concept diagram of the calculation model and Figure 6-17, the calculation results. In the calculation, the thermal conductivity is $4.0mW/(m \cdot K)$, which is the same as the setting condition in the previous calculation model.

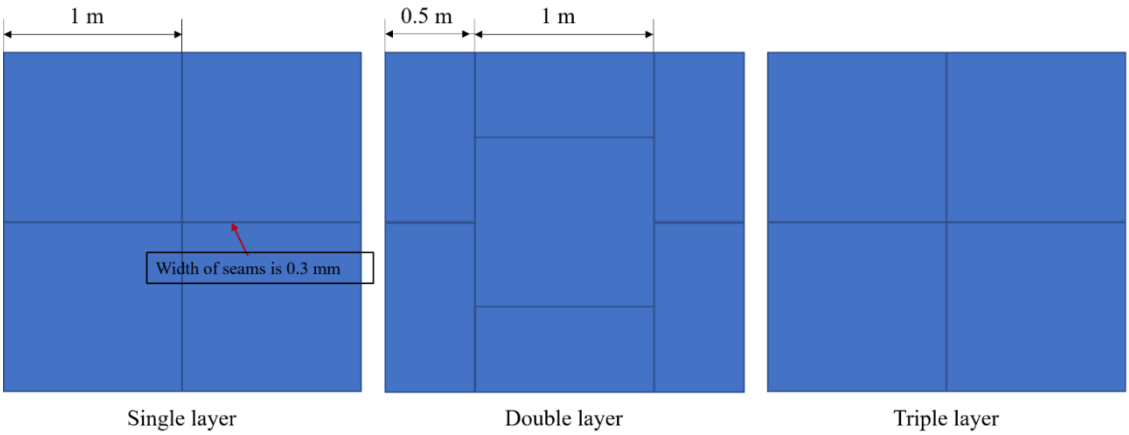

Figure 6-16 Calculation model for a large VIP application

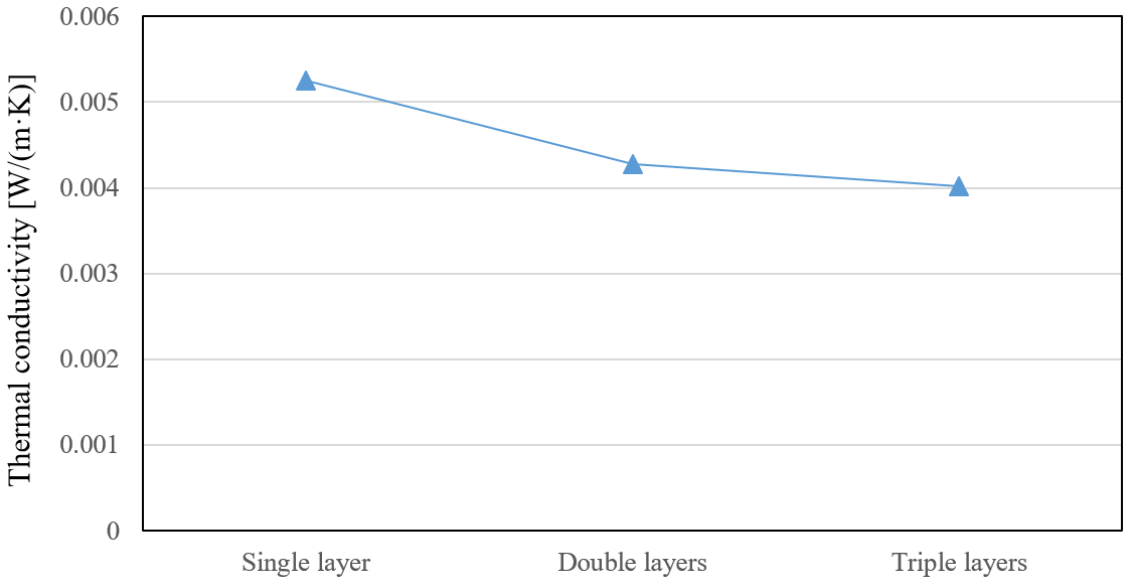

Figure 6-17 Simulation result for large-sized model

The result shows that the thermal bridge reduces on using a large model because the seam parts are reduced. The apparent thermal conductivity can be 1.31, 1.1, and 1.004 times the original, with a single, double, and triple-layered attachment application, respectively.

6.4 Case studies for VIP application to retrofit existing buildings

Case studies are carried out to determine the contribution of VIP application, in retrofitting the insulation in existing building; the conditions are as depicted in Figures 6-18 and 6-19. VIPs, as used in the experiment with triple layers, are applied and their performance is compared to that without VIPs. The thermal conductivity is as per the experimental result, $\lambda = 4.0mW/(m \cdot K)$. To confirm the insulation performance, the thermal load calculation is made using the "Businesses as Usual" (BAU); the envelope insulation conditions are varied: without VIP and with VIP, and the ventilation rate is 0.5 times per hour. The thermal load calculation is carried using the "AE-CAD" software. The result confirms that VIP application can improve the insulation performance. Also, in this section, a large VIP, as the normal manufacturing size, is modeled to prove the insulation performance. Figure 6-20 shows the simulation model for validating the insulation performance in an actual application; the calculated result is shown in Figure

6-21. The climate data of Tokyo and Fukuoka are adopted as conditions for the calculation model. Table 6-6 displays the heating schedule. The average outer shell heat transmission coefficients were $1.16W/(m^2 \cdot K)$ and $0.48W/(m^2 \cdot K)$ on installing VIPs and without installing the VIPs, respectively, in the building envelop [25].

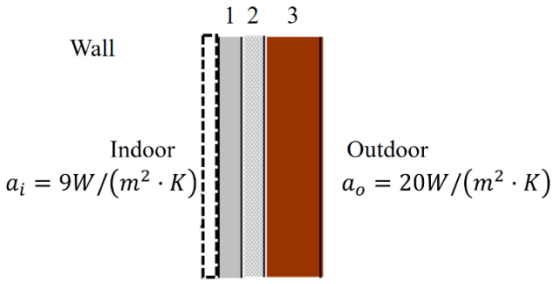

Materials	d [mm]	λ [mW/(m·K)]
Diatomite	10	690
Plywood	10	160
Wood	45	120
VIP	10	4

Figure 6-18 Wall conditions

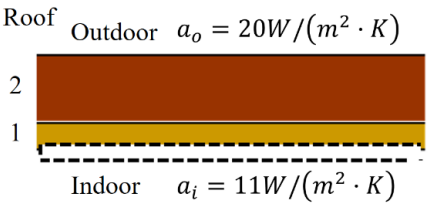

Materials	d [mm]	λ [mW/(m·K)]
Plywood	10	160
Wood	150	120
VIP	10	4

Figure 6-19 Roof conditions

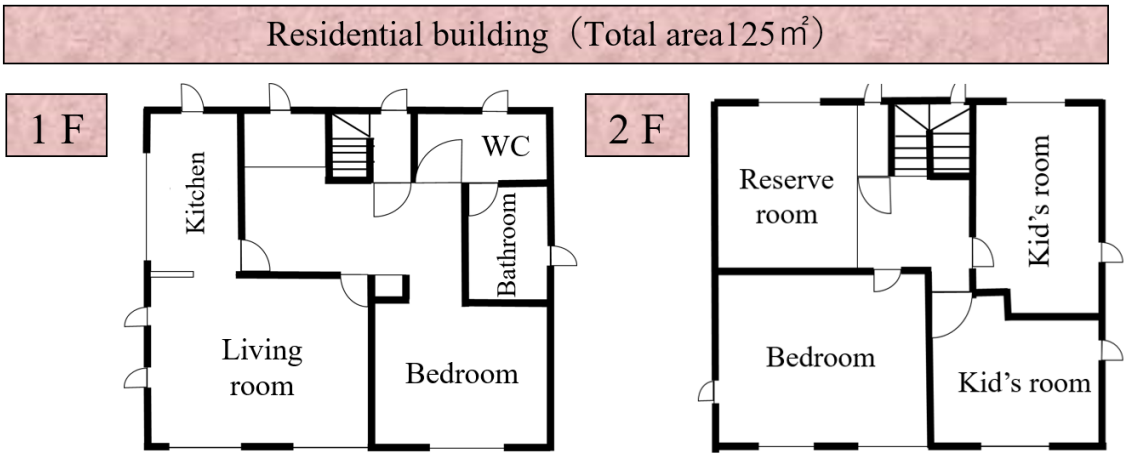

Figure 6-20 Building outline

Table 6-6 Heating schedule for a residential building model

Heating 22 ˚C			
Time	Living room	Bedroom	Kid's room
0	20	20	20
1			
2			
3			
4			
5			
6	22		
7			
8			
9	20		
10			
11			
12	22		
13			
14	20		
15			
16	22		
17			
18			
19			
20			22
21		22	
22	20		
23		20	20

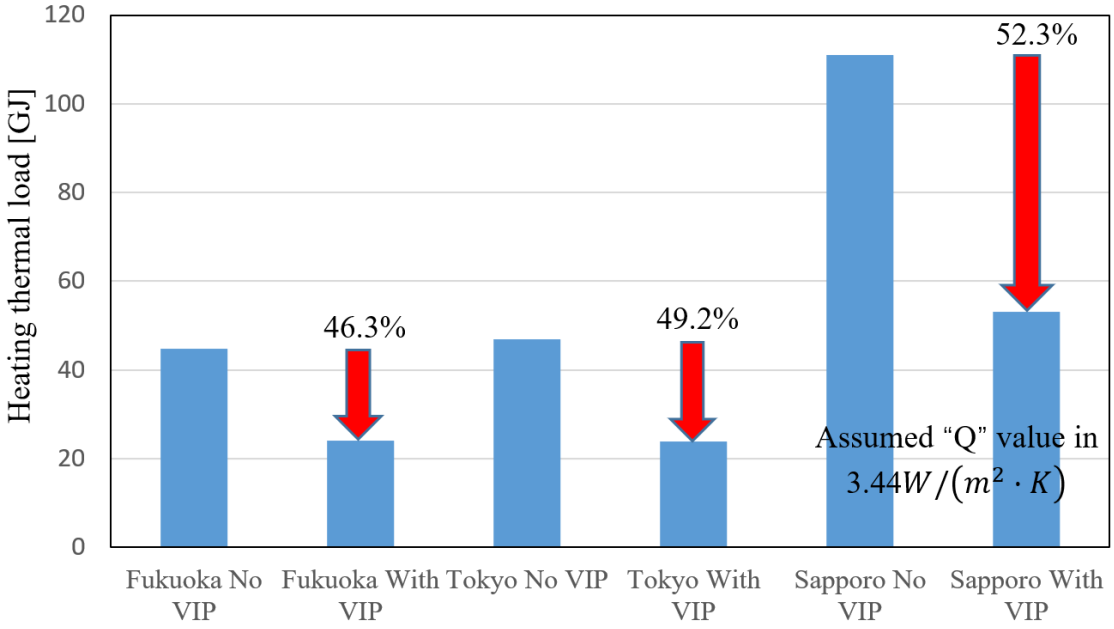

Figure 6-21 Calculated results for the total heating load

In order to discuss the insulation performance of VIP application, the authors assumed heat loss coefficient "Q" value to simulate the old buildings in Sapporo city. With these conditions, the results were obtained and are depicted in Figure 6-21. The results show that the thermal bridge reduces on using a large model because the seam parts are reduced. The heating load for the residential building can be reduced with a triple-layer attachment application; thus, the heating load can be reduced to almost half without a vacuum insulation panel application. Therefore, the proposed VIP application is an effective method for retrofitting the insulation in existing buildings.

6.6 Conclusion

1) The vacuum-insulation-panel application method is simplified, as the attachment is applied to the building surface directly. In the proposed method of overlapping the layers, the heat flow can be calibrated and experimentally evaluated.
2) A hot-box experiment was conducted and the results demonstrate the effective reduction of the thermal bridge; the apparent thermal conductivity with VIP application can be almost 1.375, 1.125, and 1.083 times the original with a single, double, and triple-layered attachment application, respectively.

3) A numerical model was generated and the result matched well with the experimental result, proving the effective reduction of the thermal bridge. A large VIP was also tested and the apparent thermal conductivity result was the 1.31, 1.1, and 1.004 times the original, with the application of a single, double, and triple layered attachment, respectively. By applying VIPs to buildings, the heating load can be reduced by half with a triple-layer attachment.

Reference:

[1] Jung-Min Oh, Jin-Hee Song, Jae-Han Lim, Seung-Yeong Song; Analysis of Building Energy Savings Potential for Metal Panel Curtain Wall Building by Reducing Thermal Bridges at Joints Between Panels; Volume 96, September 2016, Pages 696–709, Energy Procedia

[2] Jin-Hee Song, Jae-Han Lim, Yong-In Kim, Seung-Yeong Song; Thermal Insulation Performance of Metal-exterior Curtain Wall Panel Systems with Thermal Bridges in Winter; Volume 146, 2016, Pages 8–16, Procedia Engineering

[3] Chunguang Yang, Xia Gao, Xue Shao; Finite -Element Thermal Analysis of Thermal Bridge of Vacuum Insulation Panels Based on Temperature-Dependent Laminate Properties; Volume 32, 2012, Pages 658–663, Physics Procedia

[4] Alice Lorenzati, Stefano Fantucci, Alfonso Capozzoli, Marco Perino; Experimental and numerical investigation of thermal bridging effects of jointed Vacuum Insulation Panels; Volume 111, 1 January 2016, Pages 164–175, Energy and Buildings

[5] Francesco Isaia, Alfonso Capozzoli, Marco Perino; Vacuum Insulation Panels: Thermal Bridging Effects and Energy Performance in Real Building Applications; Volume 83, December 2015, Pages 269–278, Energy Procedia

[6] K. Martina, A. Campos-Celadorb, C. Escuderoa, I. Gómezb, J.M. Sala; Analysis of a thermal bridge in a calibration hot box testing facility; Volume 50, July 2012, Pages 139–149, Energy and Buildings

[7] S. Kotti, D. Teli, P.A.B. James; Quantifying Thermal Bridge Effects and Assessing Retrofit Solutions in a Greek Residential Building; Volume 38, 2017, Pages 306–313, Procedia Environmental Sciences

[8] Erdem Cucea, Pinar Mert Cuce; The impact of internal aerogel retrofitting on the thermal bridges of residential buildings: An experimental and statistical research; Volume 116, 15 March 2016, Pages 449–454, Energy and Buildings

[9] K. Ghazi Wakili,T. Stahl, S. Brunner; Effective thermal conductivity of a staggered double layer of vacuum insulation panels; Volume 43, Issue 6, June 2011, Pages 1241–1246, Energy and Buildings

[10] Francesco Isaia, Alfonso Capozzoli, Marco Perino; Vacuum Insulation Panels: Thermal Bridging Effects and Energy Performance in Real Building Applications; Volume 83, December 2015, Pages 269–278, Energy Procedia

[11] Pär Johansson, Stig Geving, Carl-Eric Hagentoft, Bjørn Petter Jelle, Egil Rognvik, Angela Sasic Kalagasidis, Berit Time; Interior insulation retrofit of a historical brick wall using vacuum insulation panels: Hygrothermal numerical simulations and laboratory investigations; Volume 79, September 2014, Pages 31–45, Building and Environment

[12] Pär Johansson, Carl-Eric Hagentoft, Angela Sasic Kalagasidis; Retrofitting of a listed brick and wood building using vacuum insulation panels on the exterior of the facade: Measurements and simulations; Volume 73, April 2014, Pages 92–104, Energy and Buildings [13] Alice Lorenzati, Stefano Fantucci, Alfonso Capozzoli, Marco Perino; Experimental and numerical investigation of thermal bridging effects of jointed Vacuum Insulation Panels; Volume 111, 1 January 2016, Pages 164–175, Energy and Buildings
[14] Ruben Baetens, Bjørn Petter Jelle, Jan Vincent Thueb, Martin J. Tenpierikd, Steinar Grynninga, Sivert Uvsløkka, Arild Gustavsen; Vacuum insulation panels for building applications: A review and beyond; Volume 42, Issue 2, February 2010, Pages 147–172, Energy and Buildings
[15] Roberto Garay, Beñat Arregi, Peru Elguezabal; Experimental Thermal Performance Assessment of a Prefabricated External Insulation System for Building Retrofitting; Volume 38, 2017, Pages 155–161, Procedia Environmental Sciences
[16] M. Harrestrup, S. Svendsen; Full-scale test of an old heritage multi-storey building undergoing energy retrofitting with focus on internal insulation and moisture; Volume 85, February 2015, Pages 123–133, Building and Environment
[17] F. Asdrubali, G. Baldinelli; Thermal transmittance measurements with the hot box method: Calibration, experimental procedures, and uncertainty analyses of three different approaches; Volume 43, Issue 7, July 2011, Pages 1618–1626, Energy and Buildings
[18] Fangzhi Chen, Stephen K. Wittkopf; Summer condition thermal transmittance measurement of fenestration systems using calorimetric hot box; Volume 53, October 2012, Pages 47–56, Energy and Buildings
[19] C. Burattia, E. Bellonia, L. Lunghia, A. Borria, G. Castoria, M. Corradi; Mechanical characterization and thermal conductivity measurements using of a new 'small hot-box' apparatus: innovative insulating reinforced coatings analysis; Volume 7, September 2016, Pages 63–70, Journal of Building Engineering
[20] ASHRAE Handbook-Fundamentals. Atlanta: American Society of Heating Refrigeration and Air Conditioning Engineers, Inc.
[21] ASTM C1058-03. 2003. Standard Practice for Selecting Temperatures for Evaluating and Reporting Thermal Properties of Thermal Insulation.
[22] ASTM C1303-07. 2007. Standard Test Method for Predicting Long-Term Thermal Resistance of Closed-Cell Foam Insulation.
[23] ASTM C1363-05. 2005. Standard Test Method for Thermal Performance of Building Materials and Envelope Assemblies by Means of a Hot Box Apparatus.
[24] ISO 8990. 1994. Thermal insulation −Determination of steady-state thermal transmission properties −Calibrated and guarded hot box

[25] Overview of the Act on the Improvement of Energy Consumption Performance of Buildings (Building Energy Efficiency Act). https://www.mlit.go.jp/common/001127790.pdf

Chapter 7
Summary and prospective

Summary

In conclusion, this study aimed at developing the slim and light-weight vacuum insulation panels with vacuum layer and assembly with transparent components. The proposed model can be applied to retrofitting insulation to existing buildings, and easy to a internal installation due to the small thickness and light weight. For this background, the authors summarized the objective to design and manufacture a reasonable translucent VIP as below:

1) A reasonable mechanical analysis to design the shape and array of the VIP to make the vacuum layer hold structurally. The structural model should be carried out for validate the mechanical analysis and give design data to the more appropriate design.

➞ The components should be analysis to assembly the core structure with the law:

a) The young's modulus should be big enough so that the stiffness will big to hold the air pressure structurally.
b) The components should be simple and low cost so that it's cost efficiency to retrofit insulation to existing buildings.
c) The shape of components should be easy to produce, also the production process of VIP should be simplified.

2) A reasonable heat transmittance should be analyzed in relative accurate simulation model, and the heat transfer model should be carried out to predict the insulation performance.

➞ The convection can be ignored in the vacuum layer so that the VIP has the good insulation performance.

➞ Then, the radiation should be controlled by a low emissivity film, and for the consideration of cost efficiency, just 1 piece of low-e film covering the core structure is totally enough.

➞ Next, the heat conduct through the surface to the core structure, local thermal bridge for VIP body is the biggest effects, and reduction of the local thermal bridge must be effective improve the insulation performance.

3) Experimental validation should be applied to evaluate the accuracy of prediction

performance, the ideal state performance can be validated by a guarded hot plate apparatus with a vacuum chamber measurement. For the real performance can be easy measure by a heat flux meter apparatus, and it can be also simplified as a VIP checker.

4) The transparent VIP can be applied to the windows with U value in 1.8. The application for the non-transparent VIP could also be improved as a overlapped installation to the wall directly.

After study about those events, the achievements should be summarized in every Chapters as follows:

Chapter 1: Introduction of the world issues and the energy problem, from the view point of carbon dioxide emission reduction effect. Then, the improvement is proposed and the significance of the VIPs is proposed.

Chapter 2: Conventional study of this field, the position and the study on the proposed VIP model previously, and our proposal as compared with the conventional conducted studies were carried out on its position, and the purpose of the present study.

Chapter 3: The authors are developing slim and light-weight vacuum insulation panels by producing vacuum layers with spacers and plastic plates. The developed VIPs have the advantages of a low cost and easy installation so that can retrofit insulation of existing buildings. In addition, one of the developed VIPs is slim and translucent so that it can be easily used for windows in an internal installation. In this Chapter, first, the authors propose a vacuum layer type slim translucent VIP and focus on a reasonable design method. Next, the authors introduce the design process in which the structural design is obtained with element mechanical analysis and a three-dimensional analysis is conducted for the VIP element. In the study, a heat transfer model is used to predict the insulation performance through finite element analysis (FEA). Subsequently, the authors perform an experiment to measure the thermal conductivity in a guarded hot plate apparatus to validate the performance prediction. Finally, case studies are performed to confirm how the different design conditions affect the insulation performance. The optimum design of the vacuum layer type slim and translucent VIP will have sufficient structural strength to hold and maintain the vacuum layer. The thermal conductivity is approximately 0.007 $W/(m \cdot K)$ that can effectively improve the insulation performance in applications.

5) The authors proposed a vacuum layer type slim and translucent VIP with the

advantages of a low manufacturing cost and easy application.

6) By using a structural calculation model, the specifications of the spacers and plastic plates that can hold the vacuum layer structurally, were investigated. The result showed that the vacuum layer could be maintained when the span between the spacers was less than 10 mm.
7) Heat transfer models were considered for the prediction of the thermal transmittance of the VIPs. The thermal conductivities of the VIPs were calculated by varying the calculation conditions of the pressure of the vacuum layer, thermal emissivity of the surface, and number of vacuum layers. The high-insulation performance was confirmed for future applications because the overall heat transfer coefficients were less than 2.0 $W/(m \cdot K)$ when the pressure of the vacuum layer was reduced to less than 0.1 Pa or a double vacuum layer was produced.
8) The result showed that the thermal conductivity of a double layer VIP under a pressure of 1.0 Pa was practically similar to that of a single VIP under a pressure of 0.1 Pa.
9) The numerical results were in better agreement with the experimental results under a pressure of 1 Pa because the numerical analysis can also consider the thermal resistance in different axis directions. Furthermore, to obtain a better insulation performance, using a multiple layer instead of a lower pressure could reduce the product cost and lead to an easy manufacture.

Chapter 4: In this Chapter, first, the authors propose a frame structural slim translucent VIP and focus on a reasonable design method. Next, the authors introduce the design process in which the structural design is obtained with element mechanical analysis and a three-dimensional analysis is conducted for the VIP element. In the study, a heat transfer model is used to predict the insulation performance through finite element analysis (FEA). Subsequently, the authors perform an experiment to measure the thermal conductivity in a guarded hot plate apparatus to validate the performance prediction. Finally, case studies are performed to confirm how the different design conditions affect the insulation performance. The optimum design of the frame structural slim and translucent VIP will have sufficient structural strength to hold and maintain the vacuum layer. The thermal conductivity is approximately 0.0049 $W/(m \cdot K)$ that can effectively improve the insulation performance in applications.

1) The authors proposed a frame structural slim and translucent VIP with the advantages of a low manufacturing cost and easy application.
2) By using a structural calculation model, the frame can hold the vacuum layer

structurally, were investigated. The result showed that the vacuum layer could be maintained when the span was 10 mm and width of frame is 1 mm.

3) Heat transfer models were considered for the prediction of the thermal transmittance of the VIPs. The thermal conductivities of the VIPs were calculated by varying the calculation conditions of the different design conditions. The high-insulation performance was confirmed for future applications because the overall heat transfer coefficients were less than 2.0 $W/(m \cdot K)$.
4) The numerical results were in better agreement with the experimental results under a pressure of 1 Pa because the numerical analysis can also consider the thermal resistance in different axis directions. Furthermore, to obtain a better insulation performance, using a multiple layer instead of a lower pressure could reduce the product cost and lead to an easy manufacture.

Chapter 5: This study aims at developing the vacuum insulation panels (VIPs) with small thickness and light transmittance to contribute to retrofitting insulation for existing buildings. In this Chapter, the authors are focused on producing the slim and translucent VIPs with a vacuum layer which is held by stable structures. Firstly, the outlines of VIPs are proposed, and the low thermal conductivity components are applied to producing VIPs which have the vacuum layer. Then, the heat transfer model is carried out by the 3-D model to predict the insulation performance of VIPs. Next, the authors report the manufactural process to make the experimental specimens. In addition, the industrial production cost is compared with other transparent evacuated products. After that, the authors set up the heat flux meter apparatus to measuring the apparent thermal conductivity to evaluate the insulation performance. Finally, the experimental result is compared and analyzed, and the authors summarize the properties of the VIPs with different components. In this paper, the authors analyzed the experimental result and the outgassing and desorption issue should be the largest effect to VIP production. Additionally, the mesh and frame structural VIPs can achieve a relatively better insulation performance, however, the thermal bridge is large and the transparency is not good due to the concentrated web.

5) The authors proposed five structures to make the vacuum insulation panels with small thickness and light weight to apply to windows to contribute to the retrofitting of insulation in existing buildings.
6) The 3-D model is proposed to evaluate the insulation performance and the results are described.

7) The translucent VIPs are produced for experimental validation. The heat flux meter apparatus was set up to measure the thermal conductivity to validate the evaluation of insulation performance.
8) The experimental results are compared to the prediction results, and the effects of different proposals are summarized and evaluated as follows:
   c) No matter what proposal is selected, it can be observed that the apparent thermal conductivity is increasing according to the elapsed time. This is because of the outgassing of components and it is based on the total area of the components.
   d) The mesh and frame structural model can achieve better insulation performance and good resistance to degradation. The frame structure is better to hold the vacuum layer and can be easily manufactured by a 3-D printer. It is worth developing the frame structural VIP to retrofit the insulation in existing buildings.

Chapter 6: Of late, various energy saving techniques are being employed in new buildings; however, these techniques are difficult to apply to existing buildings. The thermal bridge, previously known as the cold bridge, has a significant negative impact on the architectural performance. Slim and multiple layered vacuum insulation panels (VIPs) can be applied to reduce the effect of the thermal bridge, for improving the architectural insulation performance. In this study, a calibration hot-box apparatus is setup to evaluate the "U" values and the apparent thermal conductivity of a multilayered combination of VIPs. Then, a calculation model is generated for analyzing the insulation performance of full-scale VIPs, which is solved using computational fluid dynamics (CFD). Finally, the insulation performance of the VIPs and the reduction of the thermal bridge effect are evaluated by the hot-box experiment and the numerical model. As per the experimental results, the apparent thermal conductivity in a triple layer application should be 1.083 times that of the original; numerical results demonstrate that for a large VIP application with a triple layer, the apparent thermal conductivity is 1.004 times the original.

4) The vacuum-insulation-panel application method is simplified, as the attachment is applied to the building surface directly. In the proposed method of overlapping the layers, the heat flow can be calibrated and experimentally evaluated.
5) A hot-box experiment was conducted and the results demonstrate the effective reduction of the thermal bridge; the apparent thermal conductivity with VIP application can be almost 1.375, 1.125, and 1.083 times the original with a single, double, and triple-layered attachment application, respectively.
6) A numerical model was generated and the result matched well with the experimental

result, proving the effective reduction of the thermal bridge. A large VIP was also tested and the apparent thermal conductivity result was the 1.31, 1.1, and 1.004 times the original, with the application of a single, double, and triple layered attachment, respectively.

7) By applying VIPs to buildings, the heating load can be reduced by half with a triple-layer attachment.

Prospective of VIP

After studying this topic, I find that the upgrade of high insulation technique is continually needed and the way should carry on.

We already have strong frame for design and develop the VIPs, in the end, I summarized several considerations for the further study and outlook.

1) The transparent vacuum insulation panels should be continually studied due to windows is always a weak point for energy saving in buildings.
2) The frame structural VIP can be upgraded by other proposals, for example, the trusses structural VIP will enhance the structural strength meanwhile reduce the local thermal bridge of VIP body.
3) Durability of the VIP is always a big challenge, the upgrade of gas barrier film can be improved and less core structural components can make a contribution.
4) The internal gas generations should be studied to the frame structure initially. One of the significance is a validation way to the outgassing, the other significance is to make an analysis model.
5) There are so many materials can be provided to make the core structure, we already proposed to a manufactural method in 3-D printer. The stronger and cheaper material should be found to produce the core structure in the future.
6) The shape of VIP may consider again due to the edge part effects, not only to the local thermal bridge but also the installation method for actual application.